

Dailys Arronde Pérez

**Antenna Selection in the Downlink
of Precoded Multiuser MIMO
Systems**

DISSERTAÇÃO DE MESTRADO

DEPARTAMENTO DE ENGENHARIA ELÉTRICA
Programa de Pós-graduação em Engenharia
Elétrica

Rio de Janeiro
September de 2018



Dailys Arronde Pérez

Antenna Selection in the Downlink of Precoded Multiuser MIMO Systems

Dissertação de Mestrado

Dissertation presented to the Programa de Pós-graduação em Engenharia Elétrica da PUC-Rio in partial fulfillment of the requirements for the degree of Mestre em Engenharia Elétrica.

Advisor: Prof. Raimundo Sampaio Neto

Rio de Janeiro
September 2018



Dailys Arronde Pérez

Antenna Selection in the Downlink of Precoded Multiuser MIMO Systems

Dissertation presented to the Programa de Pós-graduação em Engenharia Elétrica da PUC-Rio in partial fulfillment of the requirements for the degree of Mestre em Engenharia Elétrica. Approved by the undersigned Examination Committee.

Prof. Raimundo Sampaio Neto

Advisor

Centro de Estudos em Telecomunicações – PUC-Rio

Prof. José Mauro Pedro Fortes

Centro de Estudos em Telecomunicações – PUC-Rio

Prof. Alexandre Amorim Pereira Junior

Departamento de Engenharia de Telecomunicações – IME

Prof. Márcio da Silveira Carvalho

Vice Dean of Graduate Studies

Centro Técnico Científico – PUC-Rio

Rio de Janeiro, September 14th, 2018

All rights reserved.

Dailys Arronde Pérez

Dailys Arronde Pérez graduated in Telecommunications and Electronic Engineering from the Technology University of Havana "Jose A Echeverria", Cuba, 2014

Bibliographic data

Arronde Pérez, Dailys

Antenna Selection in the Downlink of Precoded Multiuser MIMO Systems / Dailys Arronde Pérez; advisor: Raimundo Sampaio Neto. – Rio de Janeiro: PUC-Rio, Departamento de Engenharia Elétrica, 2018.

v., 82 f: il. color. ; 30 cm

Dissertação (mestrado) - Pontifícia Universidade Católica do Rio de Janeiro, Departamento de Engenharia Elétrica.

Inclui bibliografia

1. Engenharia Elétrica – Teses. 2. Sistemas MU-MIMO;. 3. Pré-codificação linear;. 4. Seleção de antenas no enlace direto;. 5. Algoritmos sub-ótimos.. I. Sampaio-Neto, Raimundo. II. Pontifícia Universidade Católica do Rio de Janeiro. Departamento de Engenharia Elétrica. III. Título.

CDD: 621.3

Acknowledgments

This work wouldn't have been possible without the continuous support of my advisor, Prof. Raimundo Sampaio Neto. I thank him for accepting my request and giving me the opportunity to work with him. His constant guidance has given me the trust and knowledge necessary to complete this work and to face future challenges.

To my mother, for her endless love and for being my constant source of inspiration. All that I am, or I hope to be, I own to her.

To my sister, for taking care of me since I was born and for her infinite confidence.

To my colleagues and friends from CETUC, for all the moments that we share together, specially to Alberth, Andres, Azucena and Yuneisy who directly contributed in the development of this work.

To my friend Bruno and his parents: Marilia and Rogerio, who opened the door of their home and made me part of their family.

To all my family and friends, who directly or indirectly contributed to this work.

I would also like to thank to PUC-Rio and CETUC for the support.

This study was financed in part by the Coordenação de Aperfeiçoamento de Pessoal de Nível Superior - Brasil (CAPES) - Finance Code 001.

Abstract

Arronde Pérez, Dailys; Sampaio-Neto, Raimundo (Advisor). **Antenna Selection in the Downlink of Precoded Multiuser MIMO Systems**. Rio de Janeiro, 2018. 82p. Dissertação de Mestrado – Departamento de Engenharia Elétrica, Pontifícia Universidade Católica do Rio de Janeiro.

This thesis focuses on the downlink of a multiuser multiple-input multiple-output (MU-MIMO) systems where the Base Station (BS) and the users' stations (UEs) transmit and receive information symbols, respectively, by selected subset of their antennas. The performance of the system is evaluated employing linear precoding techniques as Zero Forcing (ZF) and Minimum Mean Square Error (MMSE). A general model to describe the system and expressions that relate the energy spent in transmission with the energy available for detection at each user are presented. A transmit antenna selection procedure is proposed aiming at the minimization of the detection error probability. A suboptimal search algorithm, called ITES (Iterative Search), able to deliver a performance close to the one resulting from the optimal exhaustive search selection is also proposed. The receive antenna selection is also performed using a similar optimization criterion. Joint antennas selection at the transmitter and receiver contemplates the efficient combination of both strategies, leading to a complexity reduction in BS and UEs. BER performance results, obtained via simulation and semi-analytical approaches, are presented for different scenarios.

Keywords

MU-MIMO systems; Linear precoding; Downlink antenna selection; Sub-optimal selection algorithms.

Resumo

Arronde Pérez, Dailys; Sampaio-Neto, Raimundo (Orientador). **Seleção de Antenas no Enlace Direto de Sistemas MIMO Multiusuário com Pré-codificação**. Rio de Janeiro, 2018. 82p. Dissertação de Mestrado – Departamento de Engenharia Elétrica, Pontifícia Universidade Católica do Rio de Janeiro.

Esta dissertação enfoca o enlace direto de sistemas MIMO multiusuário com pré-codificação onde a estação base e os terminais dos usuários possuem múltiplas antenas mas transmitem e recebem, respectivamente, símbolos de informação através de subconjuntos selecionados de seus conjuntos de antenas. O trabalho considera sistemas que utilizam técnicas de pré-codificação linear como Zero Forcing (ZF) e Minimum Mean Square Error (MMSE). Expressões gerais que descrevem os sistemas e relacionam a energia gasta na transmissão com a energia disponível para a detecção em cada usuário são apresentadas. Com base nestas relações, um procedimento para seleção de antenas na transmissão é proposto visando a minimização da probabilidade de erro. Um algoritmo de busca não exaustiva denominado ITES (Iterative Search) foi desenvolvido e testado e mostrou-se capaz de, com apenas uma pequena fração do esforço computacional, fornecer um desempenho próximo ao da seleção ótima, que demanda uma busca exaustiva. A seleção de antenas na recepção é também efetuada usando um critério de otimização semelhante. O caso geral da seleção conjunta de antenas na transmissão e na recepção contempla a combinação de ambas estratégias, resultando na redução da complexidade tanto na estação base, quanto nos terminais dos usuários. Os resultados de desempenho em termos da taxa de erro de bit, obtidos por meio de simulações e abordagem semi-analítica, são apresentados para diferentes cenários.

Palavras-chave

Sistemas MU-MIMO; Pré-codificação linear; Seleção de antenas no enlace direto; Algoritmos sub-ótimos.

Table of contents

1	Introduction	15
2	Fundamentals of MIMO systems	18
2.1	System Model	18
2.1.1	Multiuser MIMO (MU-MIMO) Signal Model	19
2.1.1.1	Uplink	19
2.1.1.2	Downlink	20
2.2	Channel Characterization	21
2.2.1	Large-scale fading	22
2.2.2	Small-scale fading	22
2.3	Channel Estimation Techniques	24
2.3.1	Least Squares Estimation (LSE)	25
2.3.2	Minimum Mean Squares Estimation (MMSE)	25
2.4	Capacity of MIMO Systems	26
2.4.1	Capacity when Channel is Unknown to the Transmitter	27
2.4.2	Capacity when Channel is Known to the Transmitter	28
2.4.3	Ergodic Capacity	29
2.4.4	Capacity in MU-MIMO Systems	29
2.5	Detection Techniques	30
2.5.1	Linear Detectors	30
2.5.1.1	Zero-Forcing Detection	30
2.5.1.2	Minimum Mean Square Error Detector	31
2.5.2	Non-linear detection	32
2.5.2.1	Maximum Likelihood Detection	32
2.5.2.2	Successive Interference Cancellation	33
2.6	Precoding	34
2.6.1	Linear Precoding	35
2.6.2	Matched Filter (MF)	35
2.6.3	Zero Forcing (ZF)	36
2.6.4	Minimum Mean Square Error (MMSE)	36
2.6.5	Block Diagonalization (BD)	37
3	Transmit Antennas Selection	39
3.1	Energy Relations	39
3.2	Signal Model	41
3.3	Antenna Selection Approach for ZF Precoding	42
3.3.1	Proposed Sub-optimum Search Algorithm ITES	44
3.3.2	Maximum Likelihood (ML) detection	45
3.4	Antenna Selection Approach for MMSE precoding	46
3.4.1	Detection	48
3.5	Computational Complexity of ITES	48
3.6	Simulation Results	49
4	Receive Antennas Selection	57

4.1	Signal Model	57
4.2	Receive Antenna Selection Approach for ZF Precoding	59
4.2.1	Sub-optimum Receive Antenna Selection	60
4.3	Receive Antenna Selection Approach for MMSE Precoding	61
4.4	Notification	62
4.5	Simulation Results	62
5	Joint Transmit and Receive Antennas Selection	67
5.1	Joint Selection Approach	67
5.1.1	Sub-optimal Joint Selection Approaches	69
5.2	Alternative Joint Selection Approach	70
5.3	Simulation Results	71
6	Conclusions and Future Works	76
	Bibliography	78

List of figures

Figure 2.1	Point-to point MIMO system.	19
Figure 2.2	Uplink channel for MU-MIMO system.	19
Figure 2.3	Downlink channel for MU-MIMO system.	20
Figure 2.4	MU-MIMO system with Linear Precoding.	35
Figure 3.1	MU-MIMO system with antenna selector and N_{ta} RF chains.	41
Figure 3.2	BER vs. SNR(dB) for $N_T = 8$, $N_R = 4$ and $K = 2$ in ZF precoded system.	51
Figure 3.3	BER vs. SNR(dB) for transmit antenna selection considering different number of antennas and RF chains available at BS with ZF precoding, $N_R = 3$ and $K = 2$.	52
Figure 3.4	BER vs. SNR(dB) for transmit antenna selection with $N_T = 20$, $N_{ta} = 6$, $N_R = 3$ and $K = 2$ in ZF precoded system.	53
Figure 3.5	BER vs. SNR(dB) for transmit antenna selection considering different number of antennas and RF chains available at BS with MMSE precoding, $N_R = 3$ and $K = 2$.	54
Figure 3.6	BER vs. SNR(dB) for transmit antenna selection with $N_T = 20$, $N_{ta} = 6$, $N_R = 3$ and $K = 2$ in MMSE precoded system.	55
Figure 3.7	BER vs. SNR(dB) for transmit antenna selection with $N_T = 10$, $N_{ta} = 6$, $N_R = 3$ and $K = 2$.	55
Figure 3.8	Sum Rate vs. SNR(dB) for transmit antenna selection with $N_T = 10$, $N_{ta} = 6$, $N_R = 3$ and $K = 2$.	56
Figure 4.1	MU-MIMO system with N_{ra} RF chains available at each UE.	58
Figure 4.2	BER vs. SNR(dB) considering error free notification and the proposed notification scheme for $N_T = 10$, $N_R = 4$, $N_{ra} = 2$ and $K = 2$ in ZF precoded system.	64
Figure 4.3	BER vs. SNR(dB) for receive antenna selection with $N_T = 10$, $N_{ra} = 2$, $N_R = 4$ and $K = 2$ employing ZF precoding.	64
Figure 4.4	BER vs. SNR(dB) for receive antenna selection with $N_T = 10$, $N_{ra} = 2$, $N_R = 4$ and $K = 2$ employing MMSE precoding.	65
Figure 4.5	BER vs. SNR(dB) for receive antenna selection with $N_T = 20$, $N_R = 4$, $K = 5$ and differents numbers of RF chains available at the UE.	66
Figure 5.1	MU-MIMO system with N_{ta} and N_{ra} RF chains available at the BS and UE _s respectively.	67
Figure 5.2	BER vs. SNR(dB) for the joint antenna selection with $N_T = 10$, $N_{ta} = 8$, $N_R = 4$, $N_{ra} = 2$ and $K = 2$.	72

Figure 5.3 BER vs. SNR(dB) considering the suboptimal joint antenna selection with $N_T = 10$, $N_{ta} = 8$, $N_R = 4$, $N_{ra} = 2$ and $K = 2$.	73
Figure 5.4 BER vs. SNR(dB) considering the exhaustive search with $N_T = 10$, $N_{ta} = 8$, $N_R = 4$, $N_{ra} = 2$ and $K = 2$.	74
Figure 5.5 Performance comparison between joint, transmit and receive selection for $N_T = 10$, $N_{ta} = 8$, $N_R = 4$, $N_{ra} = 2$ and $K = 2$.	75

List of tables

Table 2.1	Types of wireless channels and their defining characteristics.	24
Table 3.1	Computational complexity of the transmit antenna selection approaches	56

List of abbreviations

4G	Fourth-Generation
5G	Fifth-Generation
ADC	Analog-to-Digital Converter
AOA	Angle of Arrival
AWGN	Additive White Gaussian Noise
BC	Broadcast Channel
BD	Block Diagonalization
BER	Bit-Error Rate
BS	Base Station
CSI	Channel State Information
DAC	Digital-to-Analog Converter
FDD	Frequency Division Duplexing
flops	floating point operations
GA	Genetic Algorithm
GPSM	Generalized Precoding Spatial Modulation
IB	Information Bearing
ICI	Inter Carrier Interference
ITES	Iterative Search
LNA	Low Noise Amplifier
LS	Least Square
MAC	Multiple Access Channel
MAP	Maximum a Posteriori Probability
MF	Matched Filter
MIMO	Multiple-Input Multiple-Output
ML	Maximum Likelihood
MMSE	Minimum Mean Square Error
MSE	Mean Square Error
MUI	Multiuser Interference
MU-MIMO	Multiuser MIMO
OFDM	Orthogonal Frequency Division Multiplexing
QPSK	Quadrature Phase Shift Keying
RF	Radio Frequency
SIC	Successive Interference Cancelation

SINR	Signal-to-Interference-plus-Noise Ratio
SISO	Single-Input Single Output
SNR	Signal-to-Noise Ratio
SU-MIMO	Single User MIMO
SVD	Singular Values Decomposition
TDD	Time Division Duplexing
THP	Tomlinson-Harashima Precoding
UE	User Station
ZF	Zero Forcing

*Nothing in life is to be feared, it is only to
be understood. Now is the time to understand
more, so that we may fear less.*

Marie Curie.

1

Introduction

Wireless communication systems had experienced an accelerated evolution in the last decades caused by the increasing requirements in term of data rates, latency and energy efficiency. In [1], it is predicted that between 2015 and 2021, there will be a 12X growth in mobile data traffic, that is being driven both by increased smartphone subscriptions and a continued increase in average data volume per subscription [2]. The requirements of the actual fourth-generation (4G) standards set the peak of data rate to 100 Mbps for high mobility and 1 Gbps for low mobility equipments [3,4]. As the number of smart terminals and applications are growing, research challenges arise for the implementation of the future communications systems. Under this consideration, it is expected that the fifth generation (5G) standard, which is currently being developed, achieves peak data rates of 10 Gbps for low mobility and 1 Gbps for high mobility, that represents an increase of 10 times with respect to 4G, besides the low energy consumption, reduced latency and low computational cost requirements for the signal processing [5–7].

The deployment of multiple antennas at the transmitter and receiver sides have been presented as one of the most suitable solutions to improve the capacity and reliability of wireless communication systems. Multiple-Input Multiple-Output (MIMO) makes use of multipath signal propagation to increase the spectral efficiency and data rate transmission, as well as to reduce the bit error rate. This systems are present in most wireless communication standards and for sure, will be key part of future standards, which will demand their advantages to achieve the promising transmission rates, making an efficient use of the spectrum and energy in the fifth-generation (5G) networks.

The use of a very large number of antennas at the base station (BS) to achieve more dramatic diversity gains leads to the so called Massive MIMO systems, which serves a high number of user terminals at the same time without requiring extra bandwidth resources, has been extensively studied in the last decade. An comprehensive overview from various perspectives on the topic is provided in [8,9]. The main drawback for the implementation of this technology is the cost, in terms of size, power consumption and hardware complexity, that scale with the number of antennas since there is a Radio Frequency (RF) chain

associated to each antenna element. In order to overcome this problem, it is necessary to search for strategies that can reduce the cost of implementing and operating MIMO systems, especially those with a high number of antennas, allowing to capture many of the advantages of MIMO systems.

The antenna selection strategy, at the transmitter and receiver sides, have been presented as a viable and interesting solution that reduces the hardware complexity through the use of a number of RF chains smaller than the number of available antennas in the system, i.e. the basic idea is to use a reduced number of RF chains and choose the best subset of all the antennas combinations.

The problem of antenna selection have been addressed in [10–18]. In [10] classic results on selection diversity are reviewed, followed by a discussion of antenna selection algorithm, based on the channel norm, at the transmit and receive sides. A strategy for selecting the optimal transmit antenna subset for spatial multiplexing systems when linear coherent receivers are used over slowly varying channel, is proposed in [11, 12]. The selection is carry out, using the post-processing signal-to-noise ratios of the multiplexed streams. A norm-and-correlation-based selection algorithm for energy efficiency maximization to decide the transmit RF chain configuration under the total power constraint in millimeter wave channel is proposed in [13]. An antenna selection scheme for Large-but-Finite MIMO network, using Genetic Algorithm is addressed in [14], which can be applied with different amount of channel state information (CSI), various data communication models and objective functions. In [15] an approach to receive antenna selection for capacity maximization as a convex optimization problem is presented, where an alternative approach that reaches near-optimal performance is proposed. In [16] a Generalized Pre-coding aided Spatial Modulation (GPSM) system for downlink MU-MIMO is considered. The joint transmit/receive antenna selection in single user MIMO systems is addressed in [17, 18]. In [17] a method using the real-valued genetic algorithm to improve the channel capacity of systems is proposed. In [18], a concise formula to perform the joint transmit/receive antenna selection algorithm is presented, that uses a novel partition of the channel matrix, leading to a complexity reduction of the problem.

This thesis aims to propose an antenna selection strategy for the downlink of a multiuser MIMO systems (MU-MIMO). The presence of a precoding stage in transmission, for preprocessing the signal conveyed to the different users in order to separate them in the respective receivers, make the problem of the antenna selection more challenging than in the single user case. Among the main contributions of this work, we can highlight the development of

an optimum antenna selection strategy, aiming at the minimization of the detection error probability at each user station (UE). Sub-optimal antennas selection approaches and an efficient search algorithm are also addressed, in order to relax the problem of the optimum selection, which demand an exhaustive search with computational complexity increasing with the system dimensions. The proposed antenna selection approaches are formulated for the transmit and/or receive antenna selection and extended to the more general case of joint selection.

The chapters of this thesis are organized as follows: In Chapter 2, the basic concepts for MIMO systems are studied, starting with the signal model and some propagation characteristics. Then, channel estimation techniques and channel capacity are described. Finally, the main detection and precoding techniques are presented.

In Chapter 3 we present the proposed transmit antenna selection strategy for MU-MIMO systems. The mathematical representation that describe the system and expressions that relate the energy spent in transmission with the energy available for detection at each user are derived. An efficient search algorithm is also proposed and simulation results to evaluate the performance of the addressed selection schemes, with ZF and MMSE precoding, are also presented.

In Chapter 4, the problem of receive antenna selection is addressed, describing the mathematical model of the system by considering that the BS is the one in charge to perform the selection. A frame notification scheme to inform the users the selected subset of antennas is also proposed, as well as a sub-optimum receive selection approach that significantly reduces the problem complexity. Simulation results to evaluate the performance of the proposed strategies are provided, when ZF and MMSE precoding techniques are employed.

In Chapter 5, the general case of the joint antenna selection is examined by considering the combination of the selection strategies in Chapters 3 and 4. The mathematical representation of the problem is presented and numerical results assessing the system performance, when ZF precoding is used, are also provided.

Conclusions of this work are discussed and future directions for this research topic are presented in Chapter 6.

2

Fundamentals of MIMO systems

In this Chapter, a general overview of MIMO systems is accessed. Section 2.1 describes the mathematical model for different MIMO systems, starting with point-to-point MIMO and then discussing the cases with multiple users. The MIMO channel capacity is studied in Section 2.4, where its main expressions are obtained. Due to the impact of channel characteristics on the performance of wireless communication systems, principles of radio propagation and channel estimation techniques are considered. One of the main challenges in MIMO systems is to obtain an acceptable estimation of the transmitted signal at the receiver side, for this reason some important existing detection techniques are presented in Section 2.5. Finally, some linear precoding schemes that are employed to mitigate the multiuser interference (MUI) are reviewed in section 2.6

2.1

System Model

MIMO systems were first investigated in point-to-point scenarios, also refereed as Single User MIMO (SU-MIMO), where the transmitter and the receiver are equipped with multiple transmit (N_T) and receive (N_R) antennas respectively, as depicted in Figure. 2.1. Here the wireless MIMO channel is represented by a $[N_R \times N_T]$ matrix \mathbf{H} , where the component h_{ij} represents the fading coefficients from the j th transmit antenna to the i th receive antenna. Let $\mathbf{s} \in \mathbb{C}^{N_T \times 1}$ be the vector whose components are the symbols radiated from the N_T transmit antennas, $\mathbf{s} = [s_1, s_2, \dots, s_{N_T}]^T$. The received signal vector can be expressed as $\mathbf{y} = [y_1, y_2, \dots, y_{N_R}]^T$

$$\mathbf{y} = \mathbf{H}\mathbf{s} + \mathbf{n}, \quad (2-1)$$

where $\mathbf{n} \in \mathbb{C}^{N_R \times 1}$ is the noise vector.

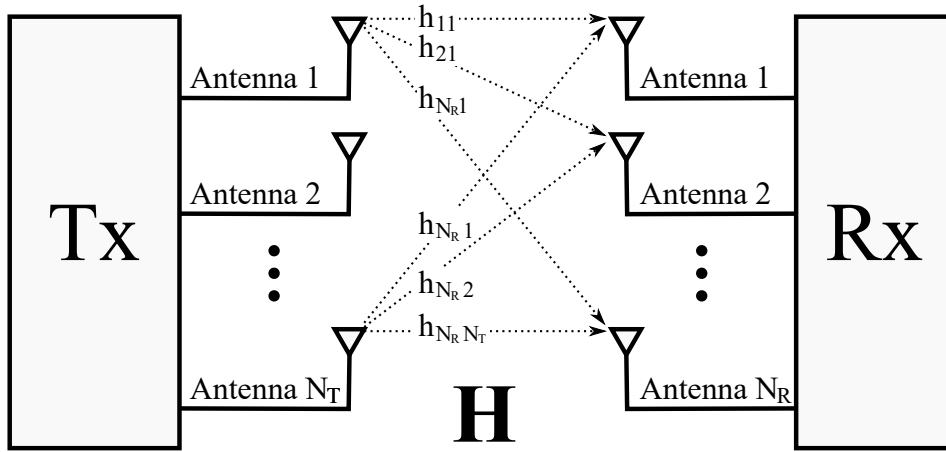


Figure 2.1: Point-to point MIMO system.

2.1.1

Multuser MIMO (MU-MIMO) Signal Model

In a cellular network there are two communication links to consider: the *uplink*, where a group of users all transmit data to the same base station, and the *downlink*, where the base station attempts to transmit signals to multiple users [19].

2.1.1.1

Uplink

In the uplink scenario, also referred as Multiple Access Channel (MAC), users transmit to the base station over the same channel. Let's consider K users, each one equipped with N_U antennas transmitting to a Base Station with N_A antennas, as shown in Figure. 2.2

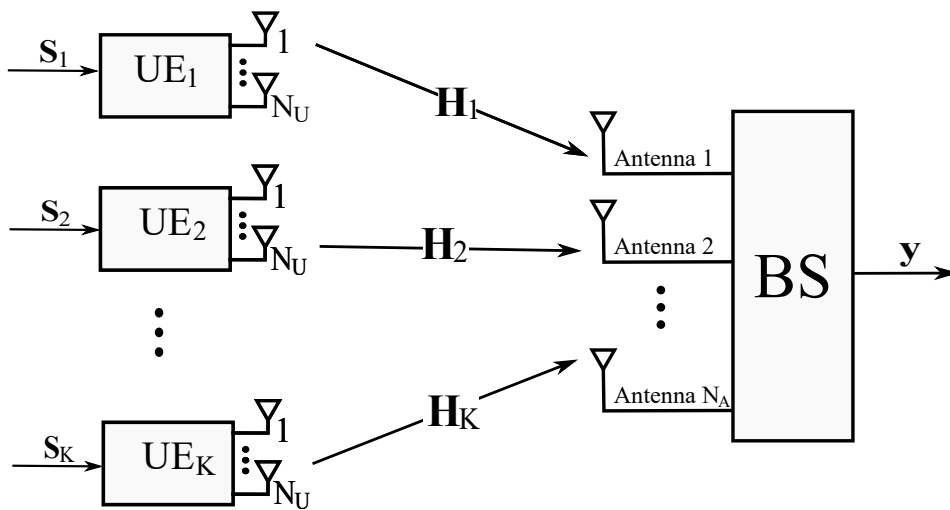


Figure 2.2: Uplink channel for MU-MIMO system.

The signal vector $[N_A \times 1]$ received at the base station can be expressed as

$$\begin{aligned} \mathbf{y} &= \mathbf{H}_1 \mathbf{s}_1 + \mathbf{H}_2 \mathbf{s}_2 + \cdots + \mathbf{H}_K \mathbf{s}_K + \mathbf{n} \\ &= \sum_{k=1}^K \mathbf{H}_k \mathbf{s}_k + \mathbf{n}, \end{aligned} \quad (2-2)$$

where \mathbf{s}_k is the $[N_U \times 1]$ signal vector transmitted by the k th user, \mathbf{H}_k is the $[N_A \times N_U]$ channel matrix and \mathbf{n} is the $[N_A \times 1]$ noise vector at the BS.

2.1.1.2

Downlink

The downlink or Broadcast Channel (BC) case is by far the most challenging one [20], where the BS is simultaneously transmitting to K users. Assuming detection in presence of additive noise, the received signal by all users is expressed in a $[KN_R \times 1]$ vector $\mathbf{y} = [\mathbf{y}_1, \mathbf{y}_2, \dots, \mathbf{y}_K]^T$

$$\mathbf{y} = \mathbf{H}\mathbf{x} + \mathbf{n}, \quad (2-3)$$

where $\mathbf{H} = [\mathbf{H}_1^T, \mathbf{H}_2^T, \dots, \mathbf{H}_K^T]^T$, $\mathbf{H} \in \mathbb{C}^{KN_R \times N_T}$ is the channel matrix for all users, with $\mathbf{H}_k \in \mathbb{C}^{N_R \times N_T}$ representing the channel matrix that connects the BS with the k th user and \mathbf{n} is a $[KN_R \times 1]$ noise vector.

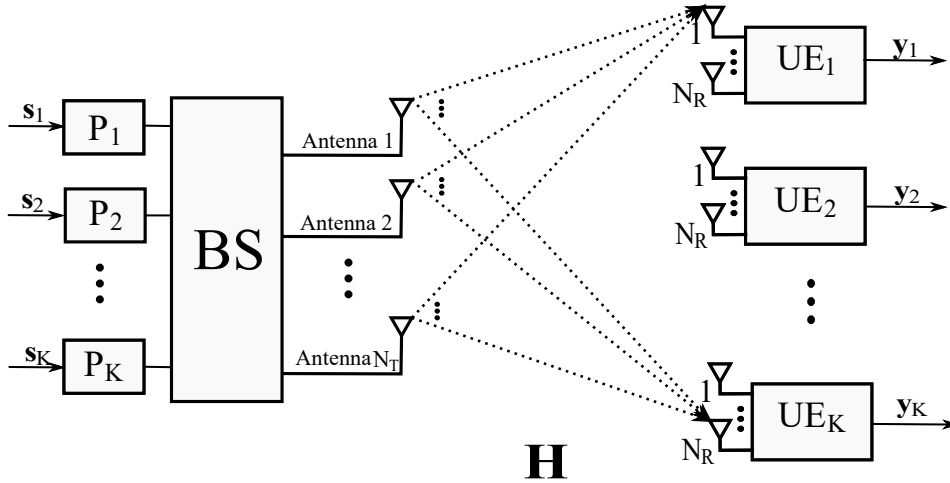


Figure 2.3: Downlink channel for MU-MIMO system.

The vector $\mathbf{x} \in \mathbb{C}^{N_T \times 1}$ contains the information transmitted by the N_T antennas at the BS. In MU-MIMO systems, it is necessary to employ a precoding technique to decouple the information conveyed to the different users and mitigate the multiuser interference (MUI), as is illustrated in Figure. 2.3. Precoding techniques will be studied in Section 2.6. The transmit vector

\mathbf{x} can be expressed as

$$\begin{aligned}\mathbf{x} &= \mathbf{P}\mathbf{s} \\ &= [\mathbf{P}_1, \mathbf{P}_2, \dots, \mathbf{P}_K] [\mathbf{s}_1^T, \mathbf{s}_2^T, \dots, \mathbf{s}_K^T]^T \\ &= \sum_{k=1}^K \mathbf{P}_k \mathbf{s}_k,\end{aligned}\tag{2-4}$$

where $\mathbf{P} = [\mathbf{P}_1, \mathbf{P}_2, \dots, \mathbf{P}_K]$, $\mathbf{P} \in \mathbb{C}^{N_T \times KN_R}$ is the precoding matrix and the information symbols for all users are organized into the $\mathbf{s} = [\mathbf{s}_1^T, \mathbf{s}_2^T, \dots, \mathbf{s}_K^T]^T$ vector. Each entry $\mathbf{s}_k \in \mathbb{C}^{N_R \times 1}$, $k = 1, 2, \dots, K$ represents the k th user information vector, to be precoded by the matrix $\mathbf{P}_k \in \mathbb{C}^{N_T \times N_R}$. For a flat fading MIMO channel, the received signal $\mathbf{y}_k \in \mathbb{C}^{N_R \times 1}$ at the k th user is given by

$$\mathbf{y}_k = \mathbf{H}_k \mathbf{P}_k \mathbf{s}_k + \mathbf{H}_k \sum_{j=1, j \neq k}^K \mathbf{P}_j \mathbf{s}_j + \mathbf{n}_k \tag{2-5}$$

where $\mathbf{x}_k = \mathbf{P}_k \mathbf{s}_k$, $\mathbf{x}_k \in \mathbb{C}^{N_T \times 1}$ is the k th user's transmit signal, the second element in (2-5) represents the interference caused by others users and $\mathbf{n}_k \in \mathbb{C}^{N_R \times 1}$ is the k th user's noise vector.

2.2

Channel Characterization

The performance of wireless communication systems is mainly governed by the wireless channel environment [21]. The study of radio channels is essential and complex due to effects of large and small scale fading that take place in the propagation of the radio waves.

The three basic propagation mechanisms for radio waves are reflection, diffraction, and scattering.

Reflection occurs when an electromagnetic signal strikes a smooth surface at an angle and is reflected toward the receiver. This happens when electromagnetic waves bounce off objects whose dimensions are large compared with the wavelength of the propagating wave [22].

Diffraction occurs when the electromagnetic signal strikes a structure that is large in terms of wavelength (the area affected by this structure is also called shadowed region). Diffraction is caused by the propagation of secondary wavelets into a shadowed region [23]. These secondary wavelets are combined to produce a new wavefront in the direction of propagation and allows radio signals to propagate around the curved surface of the earth, beyond the horizon, and behind obstructions.

Scattering occurs when the electromagnetic signal strikes objects that are much larger than a wavelength. When a radio wave impinges on a rough

surface, the reflected energy is spread out in all directions due to scattering, this causes that the received signal in a mobile radio environment is often stronger than what is predicted by reflection and diffraction models alone [22].

Scattering, reflection, and diffraction give rise to alternate propagation paths such that the received signal is a composite of numerous replicas all differing in phase, amplitude, and in time delay. The interaction between these waves causes multipath fading, because their phases are such that sometimes they add and sometimes they subtract (fade).

2.2.1

Large-scale fading

Large-scale propagation models or macroscopic fading models are based on average-received signal strength at a given distance from the transmitter i.e. large-scale fading is due to path loss of signal as a function of distance [24]. Therefore, they are characterized by a large separation between the transmitter and receiver. There exists different models that describe this phenomenon, as the Free-Space Propagation Model that is applied when the received signal is exclusively the result of direct path propagation (line-of-sight path). The free-space model allows us to compute the received power as a function of the distance from the transmitter and the path loss as the difference (in dB) between the transmitted power and the received power. In reality, we need to take into account the terrain profile for estimating path loss. Examples are the Okumura and Hata models, which are based on iterative experiments conducted over a period of time by measuring data in a specific area. With the former we can obtain the propagation path loss in an urban area and the latter supplies corrections of the first one and can be applied in suburban and rural areas.

2.2.2

Small-scale fading

Propagation models that characterize the rapid fluctuations of the amplitude, phases, or multipath delays of the received signal over very short distances or short time durations are called small-scale fading models or microscopic fading models [23]. Small-scale fading is caused by a number of signals arriving at the reception point through different paths. There are three types of microscopic fading

1. Doppler spread or time selective fading

Time selective fading results due to the motion of the transmitter or the receiver or both. When the receiver is moving, the received signal frequency will be shifted compared with its original transmitted signal. The maximum value of this additional frequency shift is known as Doppler frequency shift D_s . The coherence time is defined as

$$T_c = \frac{1}{D_s} \quad (2-6)$$

When the transmission time of the symbol is less than T_c , the state of the channel will be constant in the symbol duration, and then the pulse distortion will not occur. This is known as slow fading. Otherwise fast fading refers when the symbol time is greater than T_c and the waveform of the signal suffer distortion.

2. Delay spread-frequency selective fading

Frequency selective fading can be characterized in terms of coherence bandwidth.

$$W_c = \frac{1}{T_d} \quad (2-7)$$

where T_d is the delay spread, that express the time difference between the last and first arrived signal. When the coherence bandwidth is comparable with or less than the signal bandwidth, the channel is said to be frequency selective. Otherwise, non- frequency selective or flat fading channel refers when W_c is greater than the signal bandwidth. In other words, the frequency components in the received signal undergo the same attenuation and phase shift.

3. Angle spread-space selective fading

Angle spread at the receiver refers to the angle of arrival (AOA) of the multipath components at the receive antenna. Angle spread causes space selective fading, which means that signal amplitude depends on the spatial location of the antenna. Space selective fading is characterized by coherent distance D_c , which is the spatial separation for which the autocorrelation coefficient of the spatial fading drops to 0.7 [23].

Table 2.1 [25] shows a summary of the types of wireless channels and their defining characteristics. In this work, we focus on narrowband MIMO communication systems with frequency flat fading channels.

Table 2.1: Types of wireless channels and their defining characteristics.

Types of Channel	Defining characteristics
Fast Fading	$T_c \ll \text{symbol duration}$
Slow Fading	$T_c \gg \text{symbol duration}$
Flat Fading	$W \ll W_c$
Frequency-selective Fading	$W \gg W_c$

2.3

Channel Estimation Techniques

The deployment of MIMO systems can result in a significant capacity increase. However, this advantage is based on the assumption that the transmitter or the receiver or both have an accurate channel state information (CSI). But in real situations it is not possible to have perfect channel knowledge at both sides and it is necessary to estimate the channels parameters.

Training sequences, or pilot signals, is one of the most popular and widely used approaches to the MIMO channel estimation, that estimate the channel based on the received data and the knowledge of training symbols [26]. The principal techniques for structuring the training sequences are the preamble structure, which append a packet of strictly pilot symbols, and the pilot structure, in which the packet consists of both, pilot and information symbols [27]. The first one is effective only in slow fading channels while the other allows for tracking a fast moving channel but with less accuracy. If the training sequences from the individual antennas are orthogonal to each other, then we are dealing with a narrowband system and each subcarrier can be considered as an independent channel, free of inter carrier-interference (ICI).[21]

Let us consider a flat fading MIMO system with N_T and N_R transmit and receive antennas respectively, as described in section 2-1. In order to estimate the channel matrix \mathbf{H} , let $N \geq N_T$ training signal vectors $\boldsymbol{\pi}_1, \dots, \boldsymbol{\pi}_N$ be transmitted [26]. The corresponding $N_r \times N$ matrix $\mathbf{R} = [\mathbf{r}_1, \dots, \mathbf{r}_N]$ of the received signals can be expressed as

$$\mathbf{R} = \mathbf{H}\boldsymbol{\Pi} + \mathbf{N}, \quad (2-8)$$

where $\boldsymbol{\Pi} = [\boldsymbol{\pi}_1, \dots, \boldsymbol{\pi}_N]$ is the $N_T \times N$ training matrix and \mathbf{N} is the $N_r \times N$ noise matrix.

2.3.1

Least Squares Estimation (LSE)

Based on the knowledge of the pilot signals $\mathbf{\Pi}$ and the received data \mathbf{R} , the least-square (LS) channel estimation method finds the estimated channel $\hat{\mathbf{H}}$ as

$$\hat{\mathbf{H}}_{LS} = \mathbf{R}\mathbf{\Pi}^\dagger, \quad (2-9)$$

where $\mathbf{\Pi}^\dagger = \mathbf{\Pi}^H(\mathbf{\Pi}\mathbf{\Pi}^H)^{-1}$ is the pseudoinverse of $\mathbf{\Pi}$. The mean-square error (MSE) of this LS channel estimative is given as

$$\begin{aligned} MSE_{LS} &= \mathbb{E} \left\{ \left\| \mathbf{H} - \hat{\mathbf{H}}_{LS} \right\|_F^2 \right\} \\ &= \mathbb{E} \left\{ \left\| \mathbf{N}\mathbf{\Pi}^\dagger \right\|_F^2 \right\} \\ &= \sigma_n^2 N_R \text{Tr} \left\{ \mathbf{\Pi}^\dagger \mathbf{\Pi} \right\} \\ &= \sigma_n^2 N_R \text{Tr} \left\{ \left(\mathbf{\Pi}\mathbf{\Pi}^H \right)^{-1} \right\}, \end{aligned} \quad (2-10)$$

Where $\mathbb{E}\{\mathbf{N}^H\mathbf{N}\} = \sigma_n^2 N_R \mathbf{I}$, being σ_n^2 the receiver noise power and \mathbf{I} the identity matrix. Here $\text{Tr}\{\mathbf{\Pi}\mathbf{\Pi}^H\} = E_T$ to satisfy the transmitted training power constraint, with E_T as a given constant value. $\mathbb{E}\{\}$ and $\text{Tr}\{\}$ denote the expectation and trace operators respectively. We note that the MSE is inversely proportional to the SNR. Due to its simplicity the LS method has been widely used.

2.3.2

Minimum Mean Squares Estimation (MMSE)

Let us obtain a linear estimator that minimizes the estimate MSE of \mathbf{H} . It can be express in the following general form [26]-[28]

$$\mathbf{H}_{MMSE} = \mathbf{R}\mathbf{A}_0, \quad (2-11)$$

where \mathbf{A}_0 has to be obtained so that the MSE is minimized

$$\mathbf{A}_0 = \underset{\mathbf{A}}{\text{argmin}} \mathbb{E} \left\{ \left\| \mathbf{H} - \hat{\mathbf{H}} \right\|_F^2 \right\} = \underset{\mathbf{A}}{\text{argmin}} \mathbb{E} \left\{ \left\| \mathbf{H} - \mathbf{R}\mathbf{A} \right\|_F^2 \right\}. \quad (2-12)$$

The optimal \mathbf{A} can be found by derivating the above function and setting it to 0. Then, we have

$$\mathbf{A}_0 = \left(\mathbf{\Pi}^H \mathbf{R}_H \mathbf{\Pi} + \sigma_n^2 N_R \mathbf{I} \right)^{-1} \mathbf{\Pi}^H \mathbf{R}_H \quad (2-13)$$

Where \mathbf{R}_H is the channel correlation matrix, hence the linear estimator of \mathbf{H} can be written as

$$\hat{\mathbf{H}}_{MMSE} = \mathbf{R} \left(\mathbf{\Pi}^H \mathbf{R}_H \mathbf{\Pi} + \sigma_n^2 N_R \mathbf{I} \right)^{-1} \mathbf{\Pi}^H \mathbf{R}_H \quad (2-14)$$

The MSE of this estimator can be computed with the following expression

$$MSE_{MMSE} = \text{Tr} \left\{ \left(\mathbf{R}_H^{-1} + \frac{1}{\sigma_n^2 N_R} \mathbf{\Pi} \mathbf{\Pi}^H \right)^{-1} \right\} \quad (2-15)$$

The mean square error of MMSE technique is lower than LSE, but it requires the knowledge of the channel autocorrelation matrix and the noise autocorrelation matrix.

2.4

Capacity of MIMO Systems

The channel capacity of MIMO systems can be increased by the factor $N = \min(N_R, N_T)$ when compared to a conventional single-antenna system, for the same transmit power and spectral bandwidth.

Consider the SU-MIMO system described in section 2.1, to derive the capacity of the channel we maximize the average mutual information between the input and the output of the channel over the choice of the distribution of the input [29].

$$C = \max_{f(\mathbf{s})} I(\mathbf{s}; \mathbf{y}) \quad (2-16)$$

where $f(\mathbf{s})$ is the probability density function of the transmit vector \mathbf{s} . The mutual information between the vectors \mathbf{s} and \mathbf{y} is given by

$$I(\mathbf{s}; \mathbf{y}) = H(\mathbf{y}) - H(\mathbf{y}|\mathbf{s}) \quad (2-17)$$

where $H(\mathbf{y})$ is the differential entropy of \mathbf{y} and $H(\mathbf{y}|\mathbf{s})$ is the conditional entropy of \mathbf{y} given \mathbf{s} . The differential entropy $H(\mathbf{y})$ is maximized when \mathbf{y} is a complex circularly-symmetric Gaussian random vector with mean $\mathbf{m}_y = 0$, which consequently requires \mathbf{s} and \mathbf{n} in (2-1) to be zero-mean circularly-symmetric complex Gaussian. Since \mathbf{s} and \mathbf{n} are independent $H(\mathbf{y}|\mathbf{s}) = H(\mathbf{n})$ and

$$I(\mathbf{s}; \mathbf{y}) = H(\mathbf{y}) - H(\mathbf{n}) \quad (2-18)$$

with \mathbf{y} and \mathbf{n} being Gaussian, their entropies are given by

$$H(\mathbf{y}) = \log_2 [\det(\pi e \mathbf{R}_y)] \quad (2-19)$$

$$H(\mathbf{n}) = \log_2 [\det(\pi e \mathbf{R}_n)] \quad (2-20)$$

where \mathbf{R}_y and \mathbf{R}_n are the autocorrelation matrices of the receiver and noise

vectors respectively:

$$\mathbf{R}_n = \mathbb{E} \{ \mathbf{n} \mathbf{n}^H \} = \sigma_n^2 \mathbf{I}_{N_R} \quad (2-21)$$

$$\begin{aligned} \mathbf{R}_y &= \mathbb{E} \{ \mathbf{y} \mathbf{y}^H \} \\ &= \mathbb{E} \{ (\mathbf{H} \mathbf{s} + \mathbf{n}) (\mathbf{H} \mathbf{s} + \mathbf{n})^H \} \\ &= \mathbf{H} \mathbb{E} \{ \mathbf{s} \mathbf{s}^H \} \mathbf{H}^H + \mathbb{E} \{ \mathbf{n} \mathbf{n}^H \} \\ &= \mathbf{H} \mathbf{R}_s \mathbf{H}^H + \mathbb{E} \{ \mathbf{n} \mathbf{n}^H \} \end{aligned} \quad (2-22)$$

Substituting the above equations in (2-18) the mutual information results as

$$I(\mathbf{s}; \mathbf{y}) = \log_2 \left[\det \left(\mathbf{I}_{N_R} + \frac{1}{\sigma_n^2} \mathbf{H} \mathbf{R}_s \mathbf{H}^H \right) \right] \quad (2-23)$$

The capacity of the channel in MIMO systems is, then

$$C = \max_{\text{Tr}(\mathbf{R}_s) = E_s} \log_2 \left[\det \left(\mathbf{I}_{N_R} + \frac{1}{\sigma_n^2} \mathbf{H} \mathbf{R}_s \mathbf{H}^H \right) \right] \text{ bps/Hz} \quad (2-24)$$

2.4.1

Capacity when Channel is Unknown to the Transmitter

When the channel state information (CSI) is not available at the transmitter, it's assumed that the energy is equally distributed among the N_T transmit antennas and that the components of the information vector \mathbf{s} are uncorrelated. Then, the autocorrelation matrix of \mathbf{s} is $\mathbf{R}_s = \sigma_s^2 \mathbf{I}_{N_T}$, where σ_s^2 represents the variance of the transmit symbols. We can express the channel capacity as a function of the average energy per transmitted symbol ($\frac{E_s}{N_T}$). In this case the capacity can be expressed as

$$C = \log_2 \left[\det \left(\mathbf{I}_{N_R} + \frac{E_s}{N_T \sigma_n^2} \mathbf{H} \mathbf{H}^H \right) \right] \text{ bps/Hz} \quad (2-25)$$

Making the Eigen-decomposition of \mathbf{H} , we can rewrite $\mathbf{H} \mathbf{H}^H = \mathbf{Q} \mathbf{\Lambda} \mathbf{Q}^H$ where \mathbf{Q} is the unitary matrix whose columns are the eigenvectors of \mathbf{H} and $\mathbf{\Lambda}$ is the diagonal matrix whose diagonal elements are the corresponding eigenvalues (λ)

$$\begin{aligned} C &= \log_2 \left[\det \left(\mathbf{I}_{N_R} + \frac{E_s}{N_T \sigma_n^2} \mathbf{Q} \mathbf{\Lambda} \mathbf{Q}^H \right) \right] \text{ bps/Hz} \\ &= \log_2 \left[\det \left(\mathbf{I}_{N_R} + \frac{E_s}{N_T \sigma_n^2} \mathbf{\Lambda} \right) \right] \text{ bps/Hz} \\ &= \sum_{i=1}^N \log_2 \left(1 + \frac{E_s}{N_T \sigma_n^2} \lambda_i \right) \text{ bps/Hz} \end{aligned} \quad (2-26)$$

We can see from the results that the MIMO channel is converted into $N = \min(N_T, N_R)$ SISO channels with the same transmit energy for each transmitted signal and the capacity grows proportionally with the N .

2.4.2

Capacity when Channel is Known to the Transmitter

When the CSI is available at the transmitter using the SVD of $\mathbf{H} = \mathbf{U}\mathbf{\Sigma}\mathbf{V}^H$, the transmitted signal \mathbf{s} is pre-processed by the precoder \mathbf{V} at the transmitter side and the received signal is then post-processed with \mathbf{U}^H at the receiver side, where \mathbf{U} and \mathbf{V} are the unitary matrices with the left and right singular vectors respectively. In this case the received vector $\tilde{\mathbf{y}}$ can be expressed as

$$\begin{aligned}\tilde{\mathbf{y}} &= \sqrt{\frac{E_s}{N_T}} \mathbf{U}^H \mathbf{H} \mathbf{V} \tilde{\mathbf{s}} + \mathbf{U}^H \mathbf{n} \\ &= \sqrt{\frac{E_s}{N_T}} \mathbf{\Sigma} \tilde{\mathbf{s}} + \tilde{\mathbf{n}},\end{aligned}\quad (2-27)$$

where $\mathbb{E} \{ \|\tilde{\mathbf{s}}\|^2 \} = N_T$ and $\tilde{\mathbf{n}}$ is a complex circularly-symmetric Gaussian noise vector with zero mean and autocorrelation matrix $\mathbf{R}_n = \sigma_n^2 \mathbf{I}_{N_R}$. Equation (2-27) shows that with channel knowledge at the transmitter, \mathbf{H} can be explicitly decomposed into N_R parallel SISO channels satisfying

$$\tilde{\mathbf{y}}_i = \sum_{i=1}^{N_R} \sqrt{\frac{E_s}{N_T}} \sqrt{\lambda_i} \tilde{\mathbf{s}}_i + \tilde{\mathbf{n}}_i \quad (2-28)$$

The capacity of the MIMO channel is the sum of the individual parallel SISO channel capacities and is given by

$$C = \max_{\sum_{i=1}^{N_R} \rho_i = N_T} \sum_{i=1}^{N_R} \log_2 \left(1 + \frac{E_s \rho_i}{N_T \sigma_n^2} \lambda_i \right) \text{ bps/Hz} \quad (2-29)$$

where $\rho_i = \mathbb{E} \{ |\tilde{\mathbf{s}}_i|^2 \}$ is the energy at the i th subchannel. The values of ρ_i can be obtained making an optimal energy allocation through "the water-filling algorithm", in which more power is allocated to the channel that is in good condition and less or none at all to the bad channels.[30] It is to be expected that this method yields a capacity that is equal or better than the situation when the channel is unknown to the transmitter.

2.4.3

Ergodic Capacity

Wireless channels are not deterministic, they change randomly due to the environment conditions, mobility, etc. In general, the components of the channel matrix are modeled as complex random variables and independent realizations of the channel matrix are considered. Then if the channel is random the mutual information is also random. Assuming the randomness of the channel is an ergodic process, the ergodic capacity is defined as the expectation of the channel capacity conditioned on a given channel matrix \mathbf{H}

$$C = \mathbb{E} \{C|\mathbf{H}\} = \mathbb{E} \left\{ \max_{\text{Tr}(\mathbf{R}_s)=N_T} \log_2 \left[\det \left(\mathbf{I}_{N_R} + \frac{E_s}{N_T \sigma_n^2} \mathbf{H} \mathbf{R}_s \mathbf{H}^H \right) \right] \right\} \text{ bps/Hz} \quad (2-30)$$

When CSI is not available at the transmission, the expression above can be written using (2-26) as

$$C = \mathbb{E} \left\{ \sum_{i=1}^{\min(N_T, N_R)} \log_2 \left(1 + \frac{E_s}{N_T \sigma_n^2} \lambda_i \right) \right\} \text{ bps/Hz} \quad (2-31)$$

In this case, the eigenvalues $\lambda_1, \lambda_2, \dots, \lambda_N$ are considered random variables. On the other hand when CSI is available at the transmitted we use expression (2-29), and the ergodic Capacity is given by

$$C = \mathbb{E} \left\{ \max_{\sum_{i=1}^{N_R} \rho_i = N_T} \sum_{i=1}^{N_R} \log_2 \left(1 + \frac{E_s \rho_i}{N_T \sigma_n^2} \lambda_i \right) \right\} \text{ bps/Hz} \quad (2-32)$$

2.4.4 Capacity in MU-MIMO Systems

MU-MIMO systems have received a wide attention due to the potentiality to achieve very high data rates over wireless links. The capacity region of a general MIMO MAC was described in [31], [32] and [33]. Considering the MU-MIMO uplink scenario, described in Section 2.1.1.1, the optimum sum capacity under the condition that the sum power is constrained to \mathcal{P} is deduced in [31] and given by

$$C_{MAC} = \max_{\sum_{i=1}^K \text{Tr}(\mathbf{R}_{s_i}) \leq \mathcal{P}} \log_2 \left[\det \left(\mathbf{I} + \frac{1}{\sigma_n^2} \sum_{k=1}^K \mathbf{H}_k \mathbf{R}_{s_k} \mathbf{H}_k^H \right) \right] \text{ bps/Hz} \quad (2-33)$$

where $\mathbf{R}_{s_k} = \mathbb{E} [\mathbf{s}_k \mathbf{s}_k^H]$ is the transmit covariance matrix of user k . For the maximization of the sum-rate in (2-33), each user needs to determine its optimum covariance by using convex optimization techniques.

Considering the MU-MIMO downlink scenario, described in Section 2.1.1.2, with K non-cooperating receivers, each equipped with N_R antennas, when perfect CSI is available at the transmitting base station, equipped with

N_T antennas, the signal vector sent to the user k is precoded by the matrix \mathbf{P}_k . Under the equality power constraint $\sum_{k=1}^K \text{Tr}\{\mathbf{P}_k \mathbf{P}_k^H\} = E_T$, the achievable rate for user k is derived in [34], [35] and could be expressed as

$$R_k = \log_2 \left[\det \left(\mathbf{I}_{N_R} + \mathbf{P}_k^H \mathbf{H}_k^H \mathbf{R}_{\tilde{\mathbf{n}}_k}^{-1} \mathbf{H}_k \mathbf{P}_k \right) \right] \text{ bps/Hz} \quad (2-34)$$

where $\mathbf{R}_{\tilde{\mathbf{n}}_k}$ denotes the effective noise covariance matrix at user k , given by

$$\mathbf{R}_{\tilde{\mathbf{n}}_k} = \sigma_n^2 \mathbf{I}_{N_R} + \sum_{i=1, i \neq k}^K \mathbf{H}_i \mathbf{P}_i \mathbf{P}_i^H \mathbf{H}_i^H \quad (2-35)$$

2.5

Detection Techniques

One of the main challenges in communication systems is to obtain an as good as possible estimate of the transmitted information at the receiver side. In this section, the classic signal detection techniques for spatially multiplexed MIMO systems are accessed. We adopt the MIMO system model described in (2-1), assuming that the channel matrix $\mathbf{H} \in \mathbb{C}^{N_R \times N_T}$ is known by the receiver.

2.5.1

Linear Detectors

In linear detectors, the received signal vector \mathbf{y} , is filtered by a linear filter to reduce the channel effects [36]. The desired signal is recovered by applying a linear transformation followed by a decision on the transmitted symbol. Each symbol is estimated by a linear combination of the received signals and the filter matrix $\mathbf{W} \in \mathbb{C}^{N_R \times N_T}$. The filter matrix \mathbf{W} can be optimized by using different criteria, two of the most popular are the Zero Forcing criterion (ZF) and Minimum Mean Square Error (MMSE) criterion.

2.5.1.1

Zero-Forcing Detection

The ZF filter, that completely remove the interference between antennas in the received signal, is given by

$$\mathbf{W}_{ZF} = \left(\mathbf{H}^H \mathbf{H} \right)^{-1} \mathbf{H}^H \quad (2-36)$$

In other words, the ZF receive filter eliminates channel effects on the transmitted signal without concern about noise [37]. The estimated symbol vector

is given by

$$\begin{aligned}\hat{\mathbf{s}}_{ZF} &= \mathbf{W}_{ZF} \mathbf{y} \\ &= (\mathbf{H}^H \mathbf{H})^{-1} (\mathbf{H}^H \mathbf{H} \mathbf{s} + \mathbf{H}^H \mathbf{n}) \\ &= \mathbf{s} + \mathbf{n}_{ZF}\end{aligned}\tag{2-37}$$

With $\mathbf{n}_{ZF} = (\mathbf{H}^H \mathbf{H})^{-1} \mathbf{H}^H \mathbf{n}$. The noise power can be significantly increased by \mathbf{W}_{ZF} when the channel is ill conditioned. Thus, the BER performance of the ZF detector can be greatly reduced. The final decision on \mathbf{s} is usually made on a component-by-component basis as follows

$$\hat{\mathbf{s}} = \mathcal{Q}(\hat{\mathbf{s}}_{ZF})\tag{2-38}$$

where $\mathcal{Q}(\mathbf{x}) = [\mathcal{Q}(x_1) \mathcal{Q}(x_2) \dots \mathcal{Q}(x_n)]^T$ and $\mathcal{Q}(x)$ returns the point of the complex signal constellation closest to x .

2.5.1.2

Minimum Mean Square Error Detector

In order to reduce the effects of noise amplification caused by the ZF filter and the interference between antennas in the received signal, i.e. maximize the signal-to-interference-plus-noise ratio (SINR), the MMSE filter \mathbf{W}_{MMSE} can be computed by minimizing the mean square error (MSE) as

$$\begin{aligned}W_{MMSE} &= \arg \max_{\mathbf{W}} \mathbb{E} \{ \|\mathbf{s} - \mathbf{W} \mathbf{y}\|^2 \} \\ &= \mathbb{E} \{ \mathbf{s} \mathbf{y}^H \} (\mathbb{E} \{ \mathbf{y} \mathbf{y}^H \})^{-1} \\ &= \mathbf{H}^H \left(\mathbf{H} \mathbf{H}^H + \frac{\sigma_n^2}{\sigma_s^2} \mathbf{I} \right)^{-1} \\ &= \left(\mathbf{H}^H \mathbf{H} + \frac{\sigma_n^2}{\sigma_s^2} \mathbf{I} \right)^{-1} \mathbf{H}^H\end{aligned}\tag{2-39}$$

Then the estimated symbol vector is given by

$$\begin{aligned}\hat{\mathbf{s}}_{MMSE} &= \mathbf{W}_{MMSE} \mathbf{y} \\ &= \mathbf{W}_{MMSE} \mathbf{H} \mathbf{s} + \mathbf{W}_{MMSE} \mathbf{n},\end{aligned}\tag{2-40}$$

And the usual suboptimal decision of $\hat{\mathbf{s}}$ is given by

$$\hat{\mathbf{s}} = \mathcal{Q} \left(\mathbf{D}^{-1} (\mathbf{W}_{MMSE} \mathbf{H}) \hat{\mathbf{s}}_{MMSE} \right),\tag{2-41}$$

where $\mathbf{D}(\mathbf{W}_{\text{MMSE}} \mathbf{H})$ represents a diagonal matrix, containing the real non-negative main diagonal elements of $\mathbf{W}_{\text{MMSE}} \mathbf{H}$. In the case of PSK modulation

$$\hat{\mathbf{s}} = \mathcal{Q}(\hat{\mathbf{s}}_{\text{MMSE}}), \quad (2-42)$$

Linear Detectors are more feasible due to their lower complexity compared to non-linear detectors, however they offer a limited performance, due to the impact of interference and noise.

2.5.2

Non-linear detection

2.5.2.1

Maximum Likelihood Detection

The Maximum Likelihood (ML) Detection is equivalent to the maximum a posteriori probability (MAP) detection when the transmitted vectors are equally likely. The ML detector minimizes the error probability by estimating the transmitted signal vector $\hat{\mathbf{s}}_{ML}$ based on the knowledge of the received vector \mathbf{y} and the channel matrix \mathbf{H} . The estimate of the transmitted signal vector with the highest a posteriori probability is given by

$$\begin{aligned} \hat{\mathbf{s}}_{MAP} &= \arg \max_{\hat{\mathbf{s}} \in \mathcal{C}^{N_T}} P(\mathbf{s} = \hat{\mathbf{s}} | \mathbf{y}) \\ &= \arg \max_{\hat{\mathbf{s}} \in \mathcal{C}^{N_T}} \frac{P(\mathbf{s} = \hat{\mathbf{s}}) p_{\mathbf{y}|\mathbf{s}}(\mathbf{y} | \mathbf{s} = \hat{\mathbf{s}})}{p_{\mathbf{y}}(\mathbf{y})}, \end{aligned} \quad (2-43)$$

where \mathcal{C} denotes the modulation constellation with order M , $p_{\mathbf{y}}(\mathbf{y})$ is the probability density function of the observation \mathbf{y} and $p_{\mathbf{y}|\mathbf{s}}(\mathbf{y} | \mathbf{s} = \hat{\mathbf{s}})$ is the conditional probability density function of \mathbf{y} when the transmitted signal is $\hat{\mathbf{s}}$. Since $p_{\mathbf{y}}(\mathbf{y})$ does not depend on $\hat{\mathbf{s}}$ and all the transmitted signals have the same a priori probability, then (2-43) reduces to

$$\hat{\mathbf{s}}_{ML} = \arg \max_{\hat{\mathbf{s}} \in \mathcal{C}^{N_T}} p_{\mathbf{y}|\mathbf{s}}(\mathbf{y} | \mathbf{s} = \hat{\mathbf{s}}) \quad (2-44)$$

Considering (2-1) we know that $p_{\mathbf{y}|\mathbf{s}}(\mathbf{y} | \mathbf{s} = \hat{\mathbf{s}}) = p_{\mathbf{n}}(\mathbf{y} - \mathbf{H}\hat{\mathbf{s}})$ and the probability density function of \mathbf{y} , which is complex Gaussian with i.i.d. circularly symmetric component, given \mathbf{s} is

$$p_{\mathbf{y}|\mathbf{s}}(\mathbf{y} | \mathbf{s} = \hat{\mathbf{s}}) = \frac{1}{(\pi\sigma_n^2)^{N_R}} \exp\left(-\frac{\|\mathbf{y} - \mathbf{H}\hat{\mathbf{s}}\|^2}{\sigma_n^2}\right). \quad (2-45)$$

Note that (2-45) is maximized by minimizing $\|\mathbf{y} - \mathbf{H}\hat{\mathbf{s}}\|^2$. Then the optimal detector determines the estimate of the symbol vector $\hat{\mathbf{s}}_{ML}$ selecting the

message with the smallest Euclidean distance between the received signal vector \mathbf{y} and the hypothesis message $\mathbf{H}\hat{\mathbf{s}}$.

$$\hat{\mathbf{s}}_{ML} = \arg \min_{\hat{\mathbf{s}} \in \mathcal{C}^{N_T}} \|\mathbf{y} - \mathbf{H}\hat{\mathbf{s}}\|^2 \quad (2-46)$$

The ML detection achieves an optimal performance and its BER performance can be used as the lower bound to measure the performance of other detection algorithms, however, its computational complexity increases exponentially as the number of dimensions increases, such as modulation order (M) and the number of transmit antennas (N_T) [38], since the algorithm requires an exhaustive search of the M^{N_T} possible symbols.

2.5.2.2

Successive Interference Cancellation

The Successive Interference Cancellation (SIC) detection finds a good trade-off between the ML and the Linear detection, in view of the BER performance and computational complexity [39]. As opposed to linear detection, SIC detector don't detect the N_T data symbols simultaneously, it makes the detection in a sequential form. The successively detected symbol in each stage is then subtracted from the received signal and the remaining received signal, with the reduced interference, is used of performing the estimation for the following symbols [38]. The SIC detector uses a bank of linear detectors and each detects a selected component s_i of \mathbf{s} . The successively interference canceled received vector in the i th stage is

$$\begin{cases} \tilde{\mathbf{y}}^i = \mathbf{y} & ; i = 1 \\ \tilde{\mathbf{y}}^i = \mathbf{y} - \sum_{j=1}^{i-1} \mathbf{h}_j \hat{s}_j & ; i \geq 2 \end{cases} \quad (2-47)$$

with \mathbf{h}_j representing the j th column vector of the channel matrix \mathbf{H} .

After subtracting the detected symbols from the received signal vector, the remaining signal is processed either by an MMSE or a ZF filter for the symbol estimation in the following stage. The detected signal is subtracted through a feedback loop that performs an interference cancellation and improves the overall bit error rate in MIMO systems [38].

If $\hat{s}_i = s_i$ the interference is successfully cancelled but in the case that $\hat{s}_i \neq s_i$ the subtraction with the erroneous detected symbol will produce an error burst and overall performance degradation. To avoid this ordering mechanisms to detect reliable signals in the early stages are implemented.

These methods can be SINR based ordering, SNR based ordering and Norm based ordering. In the first one, signals with higher SINR are detected first and the linear MMSE detection is used. In the second one, the first

detected signals are the ones that have higher SNR and the linear ZF detection is considered. The last one is proposed to reduce the complexity of the previous, and the norm of the column vectors in the channel matrix is used for ordering, therefore the signals can be detected in decreasing order of the norms $\|\mathbf{h}_i\|$.

2.6

Precoding

MU-MIMO systems are highly sensitive to multiuser interference (MUI). In order to mitigate this effect, precoding methods are used at the transmitter side, which are designed to optimize the signal transmission form. Precoding is implemented at the base station (BS) due to its higher processing capacity and normally the power supply is not a problem.

The idea of precoding is to eliminate the MUI and/or to simplify the detection procedures based on the knowledge of the channel. In general, a transmitter does not have direct access to the channel state information. The CSI necessary for precoding is obtained from the users through estimation techniques, refereed in Section 2.3, using feedback channel in Frequency Division Duplexing (FDD) or reciprocity in Time Division Duplexing (TDD).

In FDD system, uplink and downlink use different frequency bands, allowing full duplex transmission. FDD usually does not have channel reciprocity between opposite directions, the BS relies on the channel feedback information from the receiver [21]. Its main disadvantage is that additional resource is necessary for transmit the feedback information. On the other hand, in TDD system, the information is allocated at different time intervals and the same frequency band is used for both downlink and uplink. Here the channel reciprocity is exploited, based on this assumption, only CSI for the uplink needs to be estimated. As long as the channel gains in both directions are highly correlated, channel condition in one direction can be implicitly known from the other direction.

Precoding techniques can be linear or non-linear. In linear techniques, we find the widely used Zero-Forcing and MMSE precoding, whereas in non-linear, we have Tomlinson-Harashima Precoding (THP), Vector perturbation and Dirty-Paper Coding. Compared with linear precoding methods, non-linear have better performance albeit with higher implementation complexity. However, with an increase in the number of antennas at the BS, linear precoders, such as MF and ZF, are shown to be near-optimal [8]. Thus, we focus our study mainly on linear precoding techniques since it is more practical to use this low-complexity schemes.

2.6.1

Linear Precoding

Consider the downlink channel model in MU-MIMO, described in Section 2.1.1.2, at the BS the information vector $\mathbf{s} = [\mathbf{s}_1, \mathbf{s}_2, \dots, \mathbf{s}_{KN_R}]$ is precoded applying a linear transformation to obtain the transmit vector $\mathbf{x} \in \mathbb{C}^{N_T \times 1}$

$$\mathbf{x} = \mathbf{P}\mathbf{s} \quad (2-48)$$

where \mathbf{P} is the $[N_T \times KN_R]$ precoding matrix. Figure 2.4 shows a block diagram of the system, where the receiver signal $\mathbf{y} = [\mathbf{y}_1, \mathbf{y}_2, \dots, \mathbf{y}_K]$ can be expressed then as

$$\mathbf{y} = \mathbf{H}\mathbf{P}\mathbf{s} + \mathbf{n} \quad (2-49)$$

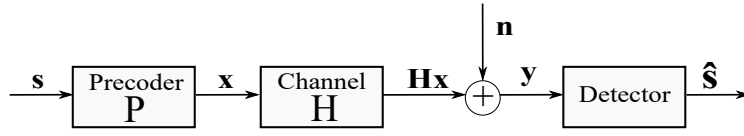


Figure 2.4: MU-MIMO system with Linear Precoding.

The received signal at the k th user, defined in (2-5), is

$$\mathbf{y}_k = \mathbf{H}_k \mathbf{P}_k \mathbf{s}_k + \sum_{j=1, j \neq k}^K \mathbf{H}_k \mathbf{P}_j \mathbf{s}_j + \mathbf{n}_k. \quad (2-50)$$

The second term represents the interference caused by the other users. The matrix \mathbf{P} is designed in such a way that the terms in the summation are minimized or eliminated. The linear precoding is also known as channel inversion, because eliminates the effect of the channel and interferences caused by other users. $N_T \geq KN_R$ is considered for transmit processing.

2.6.2

Matched Filter (MF)

Considering that the transmitter has perfect knowledge of the channel matrix, a transmit filter that maximize the desired signal at the receiver was introduced in [40] by moving the channel matched filter \mathbf{H}^H from the receiver to the transmitter. Then the precoding matrix is $\mathbf{P} = \mathbf{H}^H$ and the receive signal vector \mathbf{y} is given by

$$\mathbf{y} = \mathbf{H}\mathbf{H}^H \mathbf{s} + \mathbf{n}, \quad (2-51)$$

and the received vector at user k in this case is given by

$$\mathbf{y}_k = \mathbf{H}_k \mathbf{H}_k^H \mathbf{s}_k + \sum_{j=1, j \neq k}^K \mathbf{H}_k \mathbf{H}_j^H \mathbf{s}_j + \mathbf{n}_k. \quad (2-52)$$

The MF maximize the signal-to-noise ratio at the receiver side but it can't remove the MUI, since $\mathbf{H}_k \mathbf{H}_j^H \neq 0$.

2.6.3

Zero Forcing (ZF)

With the CSI available at the transmit side, this method deals with the MUI forcing all interference terms to zero, $\mathbf{H}_k \mathbf{P}_j = 0, \forall k \neq j$. Considering the signal model in (2-49) the ZF precoder is designed in such a way that the transmission chain is forced to be the identity, i.e. $\mathbf{P}\mathbf{H} = \mathbf{I}_{KN_R}$. To derive the expression for the ZF precoder, we have to minimize the transmit power, that is

$$\begin{aligned} \mathbf{P}_{ZF} &= \arg \min_{\mathbf{P}} \mathbb{E} \{ \|\mathbf{P}\mathbf{s}\|^2 \} \\ \text{s.t.: } &\mathbf{H}\mathbf{P} = \mathbf{I} \end{aligned}$$

Using the Lagrange multipliers method [41], we get

$$\mathbf{P}_{ZF} = \mathbf{H}^H (\mathbf{H}\mathbf{H}^H)^{-1}. \quad (2-53)$$

Since the transmitted power is limited by E_T , the precoding matrix has to be designed to satisfy the transmit power constraint, that is

$$\mathbb{E} \{ \|\mathbf{P}\mathbf{s}\|^2 \} = E_T. \quad (2-54)$$

To deal with this problem, a scalar factor $\beta_{ZF} \in \mathbb{R}_+$ is introduced in [42], which scales the transmit filter, i.e. $\beta_{ZF} \mathbf{P}_{ZF}$ to make sure that the transmitted signal power after precoding will not be changed. The expression to compute the gain factor β is deduced in [43] and can be expressed as

$$\beta_{ZF} = \sqrt{\frac{E_T}{\text{Tr} \left((\mathbf{H}\mathbf{H}^H)^{-1} \mathbf{R}_s \right)}} \quad (2-55)$$

2.6.4

Minimum Mean Square Error (MMSE)

Despite the ZF completely remove the MUI, for low SNR the ZF is outperformed by the MF. In order to find an optimum tradeoff between the signal maximization and the interference elimination, the MMSE precoder arise as an optimal solution. The Wiener Filter can be found solving the following

optimization problem

$$\begin{aligned} \mathbf{P}_{\text{MMSE}} &= \arg \min_{\mathbf{P}, \beta_{\text{MMSE}}} \mathbb{E} \left\{ \|\mathbf{s} - \beta_{\text{MMSE}}^{-1} \mathbf{y}\|^2 \right\} \\ \text{s.t.: } &\mathbb{E} [\|\mathbf{P}\mathbf{s}\|^2] = E_T \end{aligned}$$

Note that the scalar factor $\beta_{\text{MMSE}} \in \mathbb{R}_+$ is included in the definition of mean square error (MSE), since the automatic gain control of the receiver will not only scale the desired portion but also the noise portion of the received signal with β_{MMSE}^{-1} [43]. Then by applying the Lagrangian multiplier method [41], it is possible to find the optimal solutions for \mathbf{P}_{MMSE} and β_{MMSE} , given by

$$\mathbf{P}_{\text{MMSE}} = \beta_{\text{MMSE}} \mathbf{H}^H \left(\mathbf{H}\mathbf{H}^H + \frac{\text{Tr}(\mathbf{R}_n)}{E_T} \mathbf{I} \right)^{-1} \quad (2-56)$$

$$\beta_{\text{MMSE}} = \sqrt{\frac{E_T}{\text{Tr} \left(\left(\mathbf{H}\mathbf{H}^H + \frac{\text{Tr}(\mathbf{R}_n)}{E_T} \mathbf{I} \right)^{-2} \mathbf{H}\mathbf{R}_s\mathbf{H}^H \right)}} \quad (2-57)$$

Note that the transmitter needs to know the noise power to perform the MMSE precoding. Therefore, this value has to be fed back from the receiver to the transmitter, since the transmitter can't measure this quantity.

2.6.5

Block Diagonalization (BD)

As a generalization of the ZF precoding algorithm, Block Diagonalization (BD) based precoding algorithms have been proposed in [44], for MU-MIMO systems specially for receivers with multiple antennas. In the BD method, the complete suppression of MUI is achieved without any consideration on the noise and its design is performed in two stages. The first one, seeks a precoding matrix which suppresses the other users interference. Applying this matrix, block channels are formulated for each user. In the second one, each block channel is decoupled into parallel sub-channels in order to allow a single symbol detection. Correspondingly, the precoding matrix \mathbf{P}_k^{BD} for the k th user can be written as

$$\mathbf{P}_k^{BD} = \mathbf{P}_k^1 \mathbf{P}_k^2 \quad (2-58)$$

where $\mathbf{P}_k^1 \in \mathbb{C}^{N_T \times N_R}$ and $\mathbf{P}_k^2 \in \mathbb{C}^{N_R \times N_R}$. Considering the model in (2-50) applying BD precoding

$$\mathbf{y}_k = \mathbf{H}_k \mathbf{P}_k^{BD} \mathbf{s}_k + \sum_{j=1, j \neq k}^K \mathbf{H}_k \mathbf{P}_j^{BD} \mathbf{s}_j + \mathbf{n}_k, \quad (2-59)$$

we can cancel the interference generated by user j when $\mathbf{H}_k \mathbf{P}_j^{BD} = \mathbf{0}_{N_R \times N_R}$; $\forall j \neq k$. To determine \mathbf{P}_k^1 we exclude the k th user's channel matrix and define $\tilde{\mathbf{H}}_k \in \mathbb{C}^{(K-1)N_R \times N_R}$ as

$$\tilde{\mathbf{H}}_k = [\mathbf{H}_1^T \quad \cdots \quad \mathbf{H}_{k-1}^T \quad \mathbf{H}_{k+1}^T \quad \cdots \quad \mathbf{H}_K^T]^T, \quad (2-60)$$

thus \mathbf{P}_k^1 should be in the null space of $\tilde{\mathbf{H}}_k$, that is

$$\tilde{\mathbf{H}}_k \mathbf{P}_k^1 = \mathbf{0}_{(K-1)N_R \times N_R} \quad (2-61)$$

Assuming that the rank of $\tilde{\mathbf{H}}_k$ is $\tilde{L}_k = (K-1)N_R$ by performing the SVD, we can obtain

$$\tilde{\mathbf{H}}_k = \tilde{\mathbf{U}}_k \tilde{\Sigma}_k \tilde{\mathbf{V}}_k^H = \tilde{\mathbf{U}}_k \tilde{\Sigma}_k [\tilde{\mathbf{V}}_k^{(1)} \quad \tilde{\mathbf{V}}_k^{(0)}]^H \quad (2-62)$$

where $\tilde{\mathbf{U}}_k \in \mathbb{C}^{\tilde{L}_k \times \tilde{L}_k}$ and $\tilde{\mathbf{V}}_k \in \mathbb{C}^{N_T \times N_T}$ are the unitary matrices and $\tilde{\Sigma}_k \in \mathbb{C}^{\tilde{L}_k \times N_T}$ contains the singular values of $\tilde{\mathbf{H}}_k$. The matrices $\tilde{\mathbf{V}}_k^{(1)} \in \mathbb{C}^{N_T \times \tilde{L}_k}$ and $\tilde{\mathbf{V}}_k^{(0)} \in \mathbb{C}^{N_T \times (N_T - \tilde{L}_k)}$ consist of the non-zero singular vectors and the zero singular vectors respectively. Thus, $\tilde{\mathbf{V}}_k^{(0)}$ forms an orthogonal basis for the null space of $\tilde{\mathbf{H}}_k$ and

$$\mathbf{P}_k^1 = \tilde{\mathbf{V}}_k^{(0')} \quad (2-63)$$

where $\tilde{\mathbf{V}}_k^{(0')}$ is composed by selecting any N_R columns of $\tilde{\mathbf{V}}_k^{(0)}$.

In order to find the second precoding filter \mathbf{P}_k^2 we found the non-interfering block channel matrix for the k th user $\mathbf{H}_{eff} = \mathbf{H}_k \mathbf{P}_k^1$. Then we perform the second SVD to decouple the channel into N_R parallel sub channels

$$\mathbf{H}_{eff} = \mathbf{U}_k \Sigma_k \mathbf{V}_k^H \quad (2-64)$$

Finally the BD precoding for each user is given by

$$\begin{aligned} \mathbf{P}_k^{BD} &= \mathbf{P}_k^1 \mathbf{P}_k^2 \\ &= \tilde{\mathbf{V}}_k^{(0')} \mathbf{V}_k \end{aligned} \quad (2-65)$$

The computational complexity of the BD precoding algorithms comes from the two SVD operations, which need be implemented K times each one, making the computational complexity to increase with the number of users K and the system dimensions.

3

Transmit Antennas Selection

The main advantage of MIMO systems is based on the better performance that can be achieved without using additional transmit power or bandwidth extension. By increasing the number of transmit and/or receive antennas more dramatic gains can be obtained. However, the main drawback for the implementation of this technology is the hardware complexity and cost, that scale with the number of antennas, since high-cost RF modules are required as multiple antennas are employed. In general, RF modules contain a low noise amplifier (LNA), frequency down-converter and ADC/DAC converters. In an effort to reduce the cost associated with the multiple RF modules, antenna selection techniques can be used. The basic idea is to employ a smaller number of RF chains than the number of antennas. This reduction in the number of active RF chains increases the energy efficiency and decreases the cost of the system.

In this chapter, we point out the basis of the antenna selection approach, presenting a general model to describe the transmit antennas selection for the downlink of a MU-MIMO system. Expressions that relate the energy spent in transmission with the energy available for detection at each user are derived. Transmit antenna selection strategies are proposed, aiming at the minimization of the detection error probability. An efficient search algorithm, ITES (Iterative Search), to be used with the proposed antenna selection strategies is addressed. Simulation results describing the BER performance of the system, employing ZF and MMSE precoding, are presented.

3.1

Energy Relations

We consider the downlink of a MU-MIMO system, described in Section 2.1.1.2, where the base station (BS) is equipped with N_T transmit antennas serving K user stations (UE_s), each one with N_R antennas, where $KN_R \leq N_T$. Assuming, perfect channel state information (CSI) at the transmitter, transmission over flat fading channels and detection in presence of additive noise, the received signal vector by all users $\mathbf{y} = [\mathbf{y}_1, \mathbf{y}_2, \dots, \mathbf{y}_K]^T$ is expressed as

$$\mathbf{y} = \mathbf{H}\mathbf{x} + \mathbf{n}, \quad (3-1)$$

where the transmit vector $\mathbf{x} \in \mathbb{C}^{N_T \times 1}$ is given by

$$\begin{aligned} \mathbf{x} &= \mathbf{P}\mathbf{s} = [\mathbf{P}_1, \mathbf{P}_2, \dots, \mathbf{P}_K][\mathbf{s}_1^T, \mathbf{s}_2^T, \dots, \mathbf{s}_K^T]^T \\ &= \sum_{k=1}^K \mathbf{P}_k \mathbf{s}_k. \end{aligned} \quad (3-2)$$

Conveniently for our analyses, each entry $\mathbf{s}_k \in \mathbb{C}^{N_R \times 1}, k = 1, 2, \dots, K$ containing the user k information vector, are represented by

$$\mathbf{s}_k = \sqrt{E_k} \tilde{\mathbf{s}}_k = \sqrt{E_s} \sqrt{\varepsilon_k} \tilde{\mathbf{s}}_k, \quad (3-3)$$

where E_k is the energy of the information symbols sent to user k , $E_s = 1/K \sum_{k=1}^K E_k$ is the average energy of all the transmitted information symbols, $\varepsilon_k = E_k/E_s$ and $\tilde{\mathbf{s}}_k \in \mathbb{C}^{N_R \times 1}$ contains statistically independent symbols with zero mean and variance 1 in all its entries, taken from the modulation constellation $\mathcal{C} = \{c_1, c_2, \dots, c_M\}$, where M is the order of the modulation. Then (3-2) can be written as

$$\mathbf{x} = \sqrt{E_s} \mathbf{P} \boldsymbol{\mathcal{E}}^{1/2} \tilde{\mathbf{s}}, \quad (3-4)$$

where $\boldsymbol{\mathcal{E}}$ is a diagonal matrix containing the vectors $\boldsymbol{\epsilon}_k = \varepsilon_k \mathbf{u}$, $k = 1, 2, \dots, K$, in its main diagonal, $\mathbf{u} = \mathbf{1}_{N_R \times 1}$ is a vector of ones and $\tilde{\mathbf{s}} = [\tilde{\mathbf{s}}_1^T, \tilde{\mathbf{s}}_2^T, \dots, \tilde{\mathbf{s}}_K^T]^T$, then $\mathbb{E}[\tilde{\mathbf{s}}] = 0$ and $\mathbb{E}[\tilde{\mathbf{s}}\tilde{\mathbf{s}}^H] = \mathbf{I}_{KN_R}$.

The mean energy expended by the BS at each transmission is

$$E_T = \mathbb{E} \{ \|\mathbf{x}\|^2 \} = \text{Tr} \{ \mathbb{E} [\mathbf{x}\mathbf{x}^H] \}, \quad (3-5)$$

from (3-4), we then have

$$\begin{aligned} E_T &= \text{Tr} \{ E_s \mathbf{P} \boldsymbol{\mathcal{E}}^{1/2} \mathbb{E} [\tilde{\mathbf{s}}\tilde{\mathbf{s}}^H] \boldsymbol{\mathcal{E}}^{1/2} \mathbf{P}^H \} \\ &= \text{Tr} \{ E_s \mathbf{P} \boldsymbol{\mathcal{E}}^{1/2} \mathbf{I}_{KN_R} \boldsymbol{\mathcal{E}}^{1/2} \mathbf{P}^H \} \\ &= \text{Tr} \{ E_s \boldsymbol{\mathcal{E}} \mathbf{P}^H \mathbf{P} \} \\ &= E_s \gamma, \end{aligned} \quad (3-6)$$

with γ given by

$$\gamma = \text{Tr} \{ \boldsymbol{\mathcal{E}} \mathbf{P}^H \mathbf{P} \} = \sum_{k=1}^K \varepsilon_k \mathbf{u}^T \mathbf{g}_k, \quad (3-7)$$

where the column vectors \mathbf{g}_k are defined as

$$[\mathbf{g}_1^T, \mathbf{g}_2^T, \dots, \mathbf{g}_K^T]^T = \mathbf{d}(\mathbf{P}^H \mathbf{P}), \quad (3-8)$$

with $\mathbf{d}(\mathbf{A})$ denoting the vector whose entries are the main diagonal elements of matrix \mathbf{A} . Considering (3-6), and since $E_k = E_s \varepsilon_k$, we can express the relation

between the energy of symbols conveyed to user k and E_T as

$$E_k = E_T \frac{\varepsilon_k}{\gamma}. \quad (3-9)$$

3.2

Signal Model

To model the transmit antenna selection, we assume that BS is equipped with N_{ta} RF chains ($N_{ta} \leq N_T$). Figure 3.1 depicts the system with a new processing stage at the BS, where an antenna selection algorithm should be performed to reduce the number of active transmitting antennas.

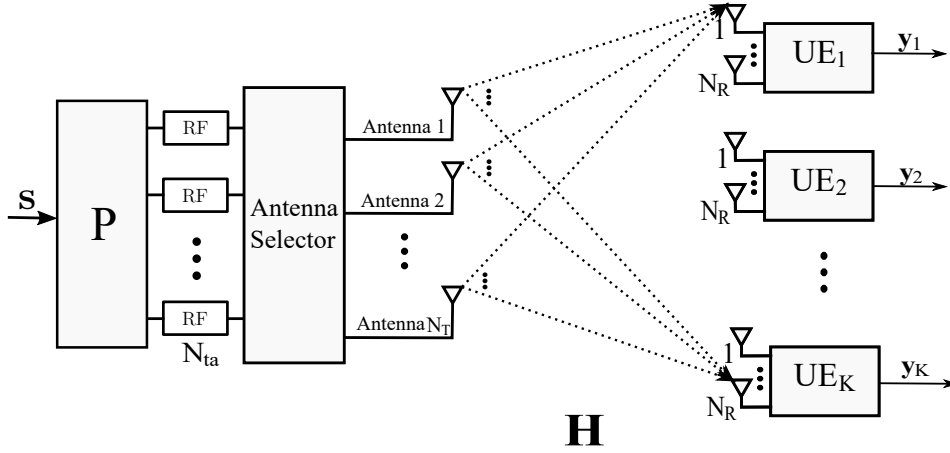


Figure 3.1: MU-MIMO system with antenna selector and N_{ta} RF chains.

Since N_{ta} antennas are used among N_T transmit antennas, the effective channel can now be represented by N_{ta} columns of $\mathbf{H} \in \mathbb{C}^{KN_R \times N_T}$. Let the column vector $\mathbf{p} \in \mathbb{R}^{N_T}$ denote a given set with N_{ta} active antennas, i.e. the elements of \mathbf{p} take the values 1 or 0, if the antenna is activated or not respectively. For instance, let $N_T = 5$ and $N_{ta} = 3$, pattern $\mathbf{p} = [11100]^T$ indicates that antennas 1, 2 and 3 are selected for transmission, while antennas 4 and 5 are deactivated. Then, the effective channel will be modeled by $\mathbf{H}_{(\mathbf{p})} \in \mathbb{C}^{KN_R \times N_{ta}}$ that represents the sub-channel matrix of \mathbf{H} obtained by selecting the columns indexed by \mathbf{p} . Consequently, $\mathbf{H}_{(\mathbf{p})}$ is given by

$$\mathbf{H}_{(\mathbf{p})} = \mathbf{H}\mathbf{U}_{(\mathbf{p})}, \quad (3-10)$$

where $\mathbf{U}_{(\mathbf{p})} \in \mathbb{C}^{N_T \times N_{ta}}$ is obtained from \mathbf{I}_{N_T} , suppressing its i th column, when the i th component of vector \mathbf{p} is zero. The matrix $\mathbf{U}_{(\mathbf{p})}$ fulfills the properties $\mathbf{U}_{(\mathbf{p})}^T \mathbf{U}_{(\mathbf{p})} = \mathbf{I}_{N_{ta}}$ and $\mathbf{U}_{(\mathbf{p})} \mathbf{U}_{(\mathbf{p})}^T = \mathbf{D}(\mathbf{p})$, where $\mathbf{D}(\mathbf{p})$ is a diagonal matrix with the elements of vector \mathbf{p} on its main diagonal. In this case, N_{ta} among N_T antennas, are selected to be active and the received signal \mathbf{y} can be written as

$$\mathbf{y} = \mathbf{H}_{(\mathbf{p})}\mathbf{x}_{\mathbf{p}} + \mathbf{n} \quad (3-11)$$

where $\mathbf{x}_{\mathbf{p}} \in \mathbb{C}^{N_{ta} \times 1}$ models the precoded signal, that will be transmitted by the active antennas indexed by \mathbf{p} . Considering equation (3-4), we have

$$\mathbf{y} = \sqrt{E_s}\mathbf{H}_{(\mathbf{p})}\mathbf{P}_{\mathbf{p}}\boldsymbol{\mathcal{E}}^{1/2}\tilde{\mathbf{s}} + \mathbf{n} \quad (3-12)$$

The channel capacity of the system in (3-12) will depend on which pattern \mathbf{p} is chosen and on the power distribution among all users $\boldsymbol{\mathcal{E}}$. It could be expressed as

$$C_{\mathbf{p}} = \log_2 \left[\det \left(\mathbf{I}_{KN_R} + \frac{E_s}{\sigma_n^2} \mathbf{H}_{(\mathbf{p})}\mathbf{P}_{\mathbf{p}}\boldsymbol{\mathcal{E}}\mathbf{P}_{\mathbf{p}}^H \mathbf{H}_{(\mathbf{p})}^H \right) \right] \text{ bps/Hz} \quad (3-13)$$

3.3

Antenna Selection Approach for ZF Precoding

At each transmission, the most suitable subset with N_{ta} active antennas should be selected, thus we have a total of S_t possibles combinations containing N_{ta} out of N_T antennas.

$$S_t = \binom{N_T}{N_{ta}} = \frac{N_T!}{(N_T - N_{ta})!N_{ta}!}. \quad (3-14)$$

Let $\boldsymbol{\Gamma}_t = \{\mathbf{p}_1, \mathbf{p}_2, \dots, \mathbf{p}_{S_t}\}$ denote the set of all possible transmit antenna configurations. The key question here is how to find the optimum subset of N_{ta} transmit antennas. In [45–47], the best solution is found through the channel capacity maximization, while in [10] and [13] a channel norm based selection is addressed. Based on the channel model described in the previous section we propose to find the optimum pattern \mathbf{p} , aiming at the maximization of the detection signal-to-noise ratio and consequent minimization of the detection error probability.

Considering the ZF precoding technique, addressed in Section 2.6.3, the expression of the precoding matrix for a given pattern \mathbf{p} is

$$\begin{aligned} \mathbf{P}_{\mathbf{p}ZF} &= \mathbf{H}_{(\mathbf{p})}^H [\mathbf{H}_{(\mathbf{p})}\mathbf{H}_{(\mathbf{p})}^H]^{-1} \\ &= \mathbf{U}_{(\mathbf{p})}^T \mathbf{H}^H [\mathbf{H}\mathbf{D}(\mathbf{p})\mathbf{H}^H]^{-1}. \end{aligned} \quad (3-15)$$

Applying (3-15) into the signal model described by (3-12) we have

$$\mathbf{y} = \mathbf{H}_{(\mathbf{p})}\mathbf{P}_{\mathbf{p}ZF}\mathbf{s} + \mathbf{n} = \mathbf{s} + \mathbf{n}, \quad (3-16)$$

and the signal received by user k is

$$\mathbf{y}_k = \sqrt{E_k}\tilde{\mathbf{s}}_k + \mathbf{n}_k. \quad (3-17)$$

From (3-9) and (3-17) it results evident that, for a fixed energy distribution $\varepsilon_k, k = 1, 2, \dots, K$ and a given energy E_T available at the transmitter, maximizing the detection energy E_k at the receivers is equivalent to minimize the factor γ given by (3-7) and (3-8). Hence the optimization problem can be written as

$$\mathbf{p}_o = \arg \min_{\mathbf{p} \in \Gamma_t} \gamma(\mathbf{p}), \quad (3-18)$$

where $\gamma(\mathbf{p})$ is given by

$$\gamma(\mathbf{p}) = \text{Tr} \left\{ \boldsymbol{\varepsilon} \left(\mathbf{P}_{\mathbf{p}ZF}^H \mathbf{P}_{\mathbf{p}ZF} \right) \right\} = \sum_{k=1}^K \varepsilon_k \mathbf{u}^T \mathbf{g}_k(\mathbf{p}), \quad (3-19)$$

with

$$\begin{aligned} [\mathbf{g}_1^T(\mathbf{p}), \mathbf{g}_2^T(\mathbf{p}), \dots, \mathbf{g}_K^T(\mathbf{p})]^T &= \mathbf{d} \left(\mathbf{P}_{\mathbf{p}ZF}^H \mathbf{P}_{\mathbf{p}ZF} \right) \\ &= \mathbf{d} \left([\mathbf{H}_{(\mathbf{p})} \mathbf{H}_{(\mathbf{p})}^H]^{-1} \right). \end{aligned} \quad (3-20)$$

The optimum subset of antennas \mathbf{p}_o that minimize $\gamma(\mathbf{p})$ is found by performing the exhaustive search, i.e. testing all possible patterns \mathbf{p} of the set Γ_t . For a fixed energy distribution, an expression for computing the capacity of the system can be found by substituting (3-15) in (3-13). Taken into account the energy relation given in (3-6), the capacity for a ZF precoded system with N_{ta} transmit antennas indexed by \mathbf{p} , when the total transmit power is limited by E_T is given by

$$C_{\mathbf{p}} = \log_2 \left[\det \left(\mathbf{I}_{KN_R} + \frac{E_T}{\gamma(\mathbf{p})\sigma_n^2} \boldsymbol{\varepsilon} \right) \right] \text{ bps/Hz} \quad (3-21)$$

Note that (3-21) is concave, thus by minimizing $\gamma(\mathbf{p})$, the capacity is also maximized. Then, to perform the antenna selection based on the proposed metric γ is optimum in the sense that minimize the detection error probability and maximize the capacity.

It is worth mentioning that the energy relations developed here satisfy the transmit energy constraint, then we don't need to include the scalar factor β_{ZF} in (3-15). Taken into account that

$$\begin{aligned} \mathbf{R}_s &= \mathbb{E} \{ \mathbf{s} \mathbf{s}^H \} = \mathbb{E} \left\{ \sqrt{E_s} \boldsymbol{\varepsilon}^{1/2} \tilde{\mathbf{s}} \tilde{\mathbf{s}}^H \boldsymbol{\varepsilon}^{1/2} \sqrt{E_s} \right\} \\ &= E_s \boldsymbol{\varepsilon} \mathbb{E} \{ \tilde{\mathbf{s}} \tilde{\mathbf{s}}^H \} \\ &= E_s \boldsymbol{\varepsilon} \end{aligned} \quad (3-22)$$

From (2-55) we know that

$$\beta_{ZF} = \sqrt{\frac{E_T}{\text{Tr} \left(\left(\mathbf{H}_{(\mathbf{p})} \mathbf{H}_{(\mathbf{p})}^H \right)^{-1} E_s \boldsymbol{\mathcal{E}} \right)}} \quad (3-23)$$

Using the relations in (3-6) and the expression for $\gamma(\mathbf{p})$ in (3-19), we get $\beta_{ZF} = \sqrt{\frac{E_T}{E_s \gamma}} = 1$.

3.3.1

Proposed Sub-optimum Search Algorithm ITES

Given the channel matrix \mathbf{H} and the normalized energy distribution $\varepsilon_k, k = 1, 2, \dots, K$, the subset of antennas that minimize $\gamma(\mathbf{p})$ can be obtained by exhaustive search. However, as the number of transmit antennas and available RF chains grow, the search complexity, that includes the inversion of large dimension matrices for each tested configuration pattern \mathbf{p} , increases dramatically. For that reason, we propose a sub-optimal search algorithm, described in Algorithm 1 [48]. ITES (Iterative Search) is based on a pilot-symbols allocation algorithm for OFDM systems proposed in [49].

It starts the algorithm by considering an initial pattern \mathbf{p}_{init} , randomly selected from the set $\mathbf{\Gamma}_t$, and its associated metric γ_{init} . The vectors $\boldsymbol{\alpha}_i$ and $\boldsymbol{\delta}_j$ index the able and unable antennas respectively. The algorithm generate new patterns by moving the active antennas positions independently, thus we have a new pattern for each possible position, i.e. each element $\mathbf{p}^{\alpha_i \rightarrow \delta_j}$ of de set Ω_i is generated by deactivating the i th antenna and activating the j th. The set Ω_i is composed by $N_d = N_T - N_{ta}$ new patterns and the algorithm finds the pattern in Ω_i that results in the best value of γ and saves it as \mathbf{p}_{otm} for the next cycle. Note that each iteration implies $N_{ta} \times N_d$ trials of antenna assignments. The process continues until no improvements in γ calculation are found, i.e. the algorithm stops when two consecutive iterations return the same pattern.

ITES can be implemented for different scenarios and precoding schemes. Moreover, as will be seen in the following, it reaches results near the optimal solution with significantly less implementation complexity.

Algorithm 1: Iterative Search Algorithm (ITES)

Input: $\mathbf{p}_{init}, \gamma_{init}$
Output: \mathbf{p}_{otm}

- 1 **Initialization:** $\mathbf{p}_{otm} = \mathbf{p}_{init}, \gamma^{in} = \gamma_{init}$
- 2 $\alpha_i \rightarrow$ index the N_{ta} active antennas
- 3 $\delta_j \rightarrow$ index the $N_d = (N_T - N_{ta})$ deactive antennas
- 4 **do**
- 5 $\gamma^{out} = \gamma^{in}$
- 6 **for** $i = 1$ **to** N_a **do**
- 7 $\mathbf{p} = \mathbf{p}_{otm}$
- 8 $\Omega_i = \left\{ \mathbf{p}^{\alpha_i \rightarrow \delta_j} \right\}_{j=1}^{N_d}$
- 9 $\mathbf{p} = \arg \min_{\mathbf{p} \in \Omega_i} \gamma(\mathbf{p})$
- 10 **if** $\gamma(\mathbf{p}) < \gamma^{in}$ **then**
- 11 $\gamma^{in} = \gamma(\mathbf{p})$
- 12 $\mathbf{p}_{otm} = \mathbf{p}$
- 13 **else**
- 14 **end**
- 15 update the vector δ_j for the next cycle
- 16 **end**
- 17 keep the best pattern \mathbf{p}_{otm} for the next iteration
- 18 **while** $(\gamma^{in} < \gamma^{out})$;

3.3.2**Maximum Likelihood (ML) detection**

Here we consider that the noise vector in (3-11) is a complex white Gaussian noise (AWGN). Considering the signal received by user k in (3-17), hence the optimal ML detection of the signal vector \mathbf{s}_k provides the estimate

$$\hat{\mathbf{s}}_k = \arg \min_{\tilde{\mathbf{s}}_k \in \mathcal{C}} \left\| \mathbf{y}_k - \sqrt{E_k} \tilde{\mathbf{s}}_k \right\|^2. \quad (3-24)$$

Since the symbols sent to each user are assumed statistically independent, decoupled detection may be employed, which treats the separate ML detection of the N_R modulated symbols. The advantage is that only $N_R \times M$ hypothesis need to be tested, instead of the M^{N_R} required if joint detection is implemented, thus the complexity reduction is noteworthy. We then have

$$\hat{\mathbf{s}}_k = \mathcal{Q} \left(\frac{\mathbf{y}_k}{\sqrt{E_k}} \right), \quad (3-25)$$

which in the case of PSK modulation (3-25), simplifies to

$$\hat{\mathbf{s}}_k = \mathcal{Q}(\mathbf{y}_k). \quad (3-26)$$

3.4

Antenna Selection Approach for MMSE precoding

We consider now that the BS uses the MMSE precoding technique, studied in section 2.6.4. Then the precoding matrix for each subset \mathbf{p} is given by

$$\mathbf{P}_{\mathbf{p}MMSE} = \mathbf{H}_{(\mathbf{p})}^H \left(\mathbf{H}_{(\mathbf{p})} \mathbf{H}_{(\mathbf{p})}^H + \frac{\text{Tr}(\mathbf{R}_{\mathbf{n}})}{E_T} \mathbf{I}_{KN_R} \right)^{-1} \quad (3-27)$$

Applying (2-56) into the signal model described by (3-11) we have

$$\mathbf{y} = \mathbf{H}_{(\mathbf{p})} \mathbf{P}_{\mathbf{p}MMSE} \mathbf{s} + \mathbf{n} \quad (3-28)$$

Taken into account that $\mathbf{P}_{\mathbf{p}MMSE} = [\mathbf{P}_{\mathbf{p}1}, \dots, \mathbf{P}_{\mathbf{p}K}]$, the signal received by user k can be expressed using equation (2-50) as

$$\mathbf{y}_k = \sqrt{E_k} \mathbf{H}_{(\mathbf{p})_k} \mathbf{P}_{\mathbf{p}k} \tilde{\mathbf{s}}_k + \sum_{j=1, j \neq k}^K \sqrt{E_j} \mathbf{H}_{(\mathbf{p})_k} \mathbf{P}_{\mathbf{p}j} \tilde{\mathbf{s}}_j + \mathbf{n}_k, \quad (3-29)$$

Unlike the ZF precoding, MMSE doesn't remove the MUI completely. For a fixed energy distribution $\varepsilon_k, k = 1, 2, \dots, K$ and a given energy E_T available for transmission, we know from (3-9) and (3-29) that minimizing the factor $\gamma(\mathbf{p})$ we maximize the desired detection energy E_k but also, the energy corresponding to the interference terms E_j . Then we can't guarantee that the minimization of $\gamma(\mathbf{p})$, given in equation (3-30) and (3-31), leads to the optimum subset of N_{ta} antennas.

$$\gamma(\mathbf{p}) = \text{Tr} \left\{ \mathcal{E} \left(\mathbf{P}_{\mathbf{p}MMSE}^H \mathbf{P}_{\mathbf{p}MMSE} \right) \right\} = \sum_{k=1}^K \varepsilon_k \mathbf{u}^T \mathbf{g}_k(\mathbf{p}), \quad (3-30)$$

with

$$\begin{aligned} [\mathbf{g}_1^T(\mathbf{p}), \mathbf{g}_2^T(\mathbf{p}), \dots, \mathbf{g}_K^T(\mathbf{p})]^T &= \mathbf{d}(\mathbf{P}_{\mathbf{p}MMSE}^H \mathbf{P}_{\mathbf{p}MMSE}) \\ &= \mathbf{d} \left(\left(\mathbf{H}_{(\mathbf{p})} \mathbf{H}_{(\mathbf{p})}^H + \frac{\text{Tr}(\mathbf{R}_{\mathbf{n}})}{E_T} \mathbf{I}_{KN_R} \right)^{-2} \mathbf{H}_{(\mathbf{p})} \mathbf{H}_{(\mathbf{p})}^H \right). \end{aligned} \quad (3-31)$$

The sum rate of the system can be expressed, using equation (2-34), as

$$R_{\mathbf{p}} = \sum_{k=1}^K \log_2 \left[\det \left(\mathbf{I}_{N_R} + \frac{E_T \varepsilon_k}{\gamma(\mathbf{p}) \sigma_n^2} \mathbf{P}_{\mathbf{p}k}^H \mathbf{H}_{(\mathbf{p})_k} \mathbf{R}_{\tilde{\mathbf{n}}_k}^{-1} \mathbf{H}_{(\mathbf{p})_k} \mathbf{P}_{\mathbf{p}k} \right) \right] \text{ bps/Hz} \quad (3-32)$$

where $\mathbf{R}_{\tilde{\mathbf{n}}_k}$ is given by

$$\mathbf{R}_{\tilde{\mathbf{n}}_k} = \mathbf{I}_{N_R} + \frac{E_T}{\gamma(\mathbf{p})\sigma_n^2} \sum_{j=1, j \neq k}^K \varepsilon_j \mathbf{H}_{(\mathbf{p})_j} \mathbf{P}_{\mathbf{p}_j} \mathbf{P}_{\mathbf{p}_j}^H \mathbf{H}_{(\mathbf{p})_j}^H \quad (3-33)$$

In a first tentative to find the most suitable transmit pattern, the expression of the sum rate was used as objective function, i.e. we select the subset \mathbf{p} aiming at the maximization of the sum rate in (3-32). The results, in term of BER performance, obtained by employing this metric to perform the transmit selection, were very poor. We conjectured, that this might be caused by numerical problems.

Looking for a more appropriated metric, we define the matrices $\mathbf{A}_{\mathbf{p}} = \mathbf{H}_{(\mathbf{p})} \mathbf{P}_{\mathbf{p}_{MMSE}}$, $\mathbf{D}(\mathbf{A}_{\mathbf{p}})$ which represent the diagonal matrix, containing the main diagonal elements of $\mathbf{A}_{\mathbf{p}}$ and $\bar{\mathbf{A}}_{\mathbf{p}} = \mathbf{A}_{\mathbf{p}} - \mathbf{D}(\mathbf{A}_{\mathbf{p}})$. Then the signal model in (3-28) can be rewritten as

$$\begin{aligned} \mathbf{y} &= \mathbf{A}_{\mathbf{p}} \mathbf{s} + \mathbf{n} \\ &= \mathbf{D}(\mathbf{A}_{\mathbf{p}}) \mathbf{s} + \bar{\mathbf{A}}_{\mathbf{p}} \mathbf{s} + \mathbf{n} \end{aligned} \quad (3-34)$$

where the first term contains the desired symbols and the second, the inter-symbol and interuser interferences. It can be verified that the elements in the diagonal of $\mathbf{D}(\mathbf{A}_{\mathbf{p}})$ are all real and positive. Now let $\mu(\mathbf{p})$ be the signal to interference-plus-noise ratio

$$\begin{aligned} \mu(\mathbf{p}) &= \frac{\text{Tr}\{\mathbf{D}(\mathbf{A}_{\mathbf{p}}) \mathbf{R}_s \mathbf{D}(\mathbf{A}_{\mathbf{p}})^H\}}{\text{Tr}\{\bar{\mathbf{A}}_{\mathbf{p}} \mathbf{R}_s \bar{\mathbf{A}}_{\mathbf{p}}^H\} + \text{Tr}\{\mathbf{R}_n\}} \\ &= \frac{E_s \text{Tr}\{\mathbf{D}(\mathbf{A}_{\mathbf{p}}) \mathcal{E} \mathbf{D}(\mathbf{A}_{\mathbf{p}})^H\}}{E_s \text{Tr}\{\bar{\mathbf{A}}_{\mathbf{p}} \mathcal{E} \bar{\mathbf{A}}_{\mathbf{p}}^H\} + \text{Tr}\{\mathbf{R}_n\}} \\ &= \frac{\text{Tr}\{\mathcal{E} \mathbf{D}(\mathbf{A}_{\mathbf{p}})^2\}}{\text{Tr}\{\mathcal{E} \bar{\mathbf{A}}_{\mathbf{p}}^H \bar{\mathbf{A}}_{\mathbf{p}}\} + \frac{\text{Tr}\{\mathbf{R}_n\}}{E_s}} \end{aligned} \quad (3-35)$$

By employing (3-9) and $\gamma(\mathbf{p})$ given in (3-30) we get

$$\mu(\mathbf{p}) = \frac{\text{Tr}\{\mathcal{E} \mathbf{D}(\mathbf{A}_{\mathbf{p}})^2\}}{\text{Tr}\{\mathcal{E} \bar{\mathbf{A}}_{\mathbf{p}}^H \bar{\mathbf{A}}_{\mathbf{p}}\} + \frac{\text{Tr}\{\mathbf{R}_n\} \gamma(\mathbf{p})}{E_T}} \quad (3-36)$$

We consider $\mu(\mathbf{p})$ the metric to perform the antenna selection approach, i.e. the strategy to find the best pattern \mathbf{p}_o is through the maximization of $\mu(\mathbf{p})$. Then, the optimization problem can be expressed as

$$\mathbf{p}_o = \arg \max_{\mathbf{p} \in \Gamma_t} \mu(\mathbf{p}), \quad (3-37)$$

The solution of this problem can be found by exhaustive search, considering a normalized energy distribution \mathcal{E} . However due to the combinatorial nature of

the problem, as we previously mentioned, it is unfeasible to solve it for large values of N_T . Then we employ the algorithm proposed in section 3.3.1 to find a near optimal solution.

To implement ITES, we use the algorithm described in **Algorithm 1**, by replacing γ by μ and modifying lines 10 and 18 by $\mu(\mathbf{p}) > \mu^{in}$ and $\mu^{in} > \mu^{out}$ respectively. With such changes a near optimum pattern can be found in systems where the MMSE precoding scheme is employed.

3.4.1 Detection

ML detection applied to the signal received by user k in (3-29) would require full knowledge of the statistics of the interuser interference. Here we consider suboptimal approaches to obtain $\hat{\mathbf{s}}_k$ requiring different levels of parameter knowledge (or estimation) by the receiver. Considering equation (3-29) and defining

$$\mathbf{A}_k = \sqrt{E_k} \mathbf{H}_{(\mathbf{p})_k} \mathbf{P}_{\mathbf{p}_k}, \quad (3-38)$$

we have

- Minimum Distance Detection (MDD)

$$\hat{\mathbf{s}}_k = \arg \min_{\tilde{\mathbf{s}}_k \in \mathcal{C}} \|\mathbf{y}_k - \mathbf{A}_k \tilde{\mathbf{s}}_k\|^2. \quad (3-39)$$

- Approximate MDD

$$\hat{\mathbf{s}}_k = \arg \min_{\tilde{\mathbf{s}}_k \in \mathcal{C}} \|\mathbf{y}_k - \mathbf{D}(\mathbf{A}_k) \tilde{\mathbf{s}}_k\|^2, \quad (3-40)$$

or equivalently,

$$\hat{\mathbf{s}}_k = \mathcal{Q}(\mathbf{D}^{-1}(\mathbf{A}_k) \mathbf{y}_k). \quad (3-41)$$

Since $\mathbf{D}(\mathbf{A}_k)$ is a diagonal matrix with positive elements in its main diagonal, then in the case of PSK modulation (3-40) simplifies to the element by element detection

$$\hat{\mathbf{s}}_k = \mathcal{Q}(\mathbf{y}_k), \quad (3-42)$$

that requires no parameter knowledge (or estimation).

3.5 Computational Complexity of ITES

To evaluate the computational complexity of the proposed antenna selection scheme, we count the number of floating-point operations (flops) required to carry it out, as a function of the dimensions of the matrices and vectors involved. A flop can be defined as one addition, subtraction, multiplication or division of two floating-point number [50], but for our complexity analyses we define a flop as one complex operation.

ITES leads to a significantly less implementation complexity because it implies $N_{ta}N_d$ trials of antennas pattern at each iteration, instead of the S_t trials required by performing the exhaustive search. The average number of iteration (N_{it}) executed can be found by simulations. Particularly, our simulations show that ITES perform between 2 and 3 iterations, that is a fairly good convergence speed.

In the case of ZF precoding, the calculation of $\gamma_{(\mathbf{p})}$, given by (3-19) and (3-20), involves the product of two $[KN_R \times N_{ta}]$ matrices, that making use of the Hermitian structure of the product, leads to $(N_{ta}(KN_R)^2 + N_{ta}KN_R - \frac{1}{2}(KN_R)^2 - \frac{1}{2}KN_R)$ flops and the inversion of a positive definite $[KN_R \times KN_R]$ matrix with $((KN_R)^3 + (KN_R)^2 + KN_R)$ flops [51]. Including the cost of multiplying by a diagonal matrix $((KN_R)^2)$ and the trace operation (KN_R) , we obtain a total of

$$N_{it}N_{ta}N_d \left[(KN_R)^3 + N_{ta}(KN_R)^2 + N_{ta}KN_R + \frac{3}{2}(KN_R)^2 - \frac{3}{2}KN_R \right] \text{ flops.} \quad (3-43)$$

On the other hand, when MMSE precoding is employed, the complexity is determinate by the computation of the factor $\mu(\mathbf{p})$, given in (3-36). We first consider that finding $\mathbf{A}_{\mathbf{p}}$ involves the inversion of the matrix $(\mathbf{H}_{(\mathbf{p})}\mathbf{H}_{(\mathbf{p})}^H + \frac{\text{Tr}(\mathbf{R}_n)}{E_T}\mathbf{I}_{KN_R})$ with a cost of $((KN_R)^3 + N_{ta}(KN_R)^2 + N_{ta}KN_R + \frac{1}{2}(KN_R)^2 + \frac{7}{2}KN_R + 1)$ flops and the multiplication of two square matrices with order KN_R . Then computing $\mathbf{A}_{\mathbf{p}}$ requires a total of $(3(KN_R)^3 + N_{ta}(KN_R)^2 + N_{ta}KN_R - \frac{1}{2}(KN_R)^2 + \frac{7}{2}KN_R + 1)$ flops. To compute the factor $\gamma_{(\mathbf{p})}$, defined in equations (3-30) and (3-31), it is considered $(3(KN_R)^3 + KN_R)$ flops additionally. Finally, the computation of $\mu(\mathbf{p})$ leads to a total of $(8(KN_R)^3 + N_{ta}(KN_R)^2 + N_{ta}KN_R - \frac{1}{2}(KN_R)^2 + \frac{21}{2}KN_R + 1)$ flops, consequently the computational complexity of ITES is given by

$$N_{it}N_{ta}N_d \left[8(KN_R)^3 + N_{ta}(KN_R)^2 + N_{ta}KN_R - \frac{1}{2}(KN_R)^2 + \frac{21}{2}KN_R + 5 \right] \text{ flops.} \quad (3-44)$$

Table 3.1, presented in the next Section, includes numerical examples of the number of complex operations associated with the different antenna selection approaches addressed in this Chapter.

3.6 Simulation Results

In this section, numerical results are presented to evaluate the bit-error-rate (BER) performance of the considered systems in different scenarios. The curves are obtained after N_{CR} independent realizations of the channel matrix

H. The entries of \mathbf{H} , are complex independent circularly symmetric gaussian random variables with zero mean and unity variance. The noise vector in (3-1) is a complex zero-mean gaussian vector with circularly symmetric components and covariance matrix $\mathbf{K}_n = \sigma_n^2 \mathbf{I}$. Results are expressed in terms of the signal-to-noise ratio

$$\text{SNR}_{\text{dB}} = 10 \log_{10} \left(\frac{E_T}{\sigma_n^2} \right), \quad (3-45)$$

and QPSK modulation is assumed. From (3-9) we have that the detection signal-to-noise ratio per receive antenna is

$$\frac{E_k}{\sigma_n^2} = \frac{E_T}{\sigma_n^2} \frac{\varepsilon_k}{\gamma} = \text{SNR} \frac{\varepsilon_k}{\gamma}. \quad (3-46)$$

ZF Precoding

With ML detection performed by the UE receivers it results that for a given channel realization and antenna pattern selection the user k conditional bit-error-rate, when ZF precoding is performed by the BS, is given by

$$\text{BER}_k(\gamma) = Q \left(\sqrt{\frac{E_k}{\sigma_n^2}} \right) = Q \left(\sqrt{\frac{\text{SNR}}{\gamma}} \varepsilon_k \right), \quad (3-47)$$

where $Q(\cdot)$ is the Q-function defined as

$$Q(x) = \frac{1}{\sqrt{2\pi}} \int_x^\infty \exp \left(-\frac{\beta^2}{2} \right) d\beta \quad (3-48)$$

and the user k BER performance is

$$\text{BER}_k = \mathbb{E} \left[Q \left(\sqrt{\frac{\text{SNR}}{\gamma}} \varepsilon_k \right) \right]. \quad (3-49)$$

In a semi-analytical approach we approximate (3-49) by

$$\text{BER}_k \cong \frac{1}{N_{CR}} \sum_{i=1}^{N_{CR}} Q \left(\sqrt{\frac{\text{SNR}}{\gamma_i}} \varepsilon_k \right). \quad (3-50)$$

We note that (3-47) and the approximation (3-50), with $\gamma_{(\mathbf{p})}$ given by (3-19) and (3-20), are only applicable to the case of transmit antenna selection with ZF precoding. The results in this section consider an uniform user energy allocation ($\varepsilon_k = 1$, for all k).

Figure 3.2 compares the BER performance obtained with Monte Carlo simulation and with the semi-analytical approximation (3-50), when the ZF precoding scheme is employed. In both cases the results are for $N_{CR} = 1000$ channel realizations, and in the Monte Carlo simulations a data frame of 1200 signal vectors are transmitted to each user per channel realization. Considering the coincidence of the BER results, the much less computation time consuming

approximation (3-50) was used to generate the results presented in Figures 3.3 and 3.4

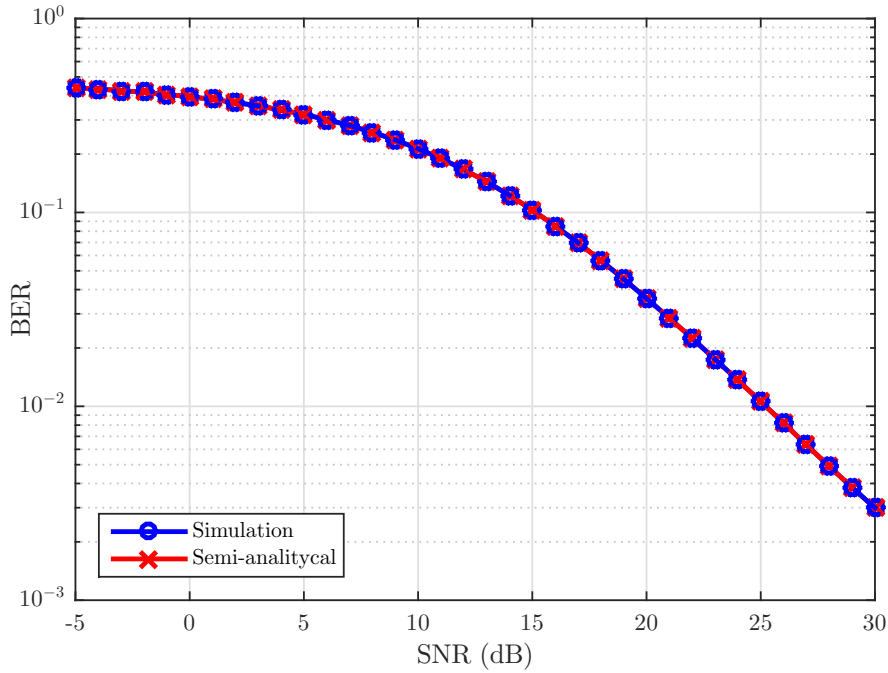


Figure 3.2: BER vs. SNR(dB) for $N_T = 8$, $N_R = 4$ and $K = 2$ in ZF precoded system.

The results in Figure 3.3 are for transmit antenna selection and illustrate the BER performance when the BS is equipped with different number of antennas and RF chains. It is easily observed that the case of no selection with 10 available antennas gives the best performance, but it requires a RF chain connected to each transmit antenna. However, if we have 6 RF chains available a notable improvement in BER performance is obtained when BS is equipped with 10 antennas and the most suitable set of 6 antennas is selected for transmission when compared to the case of 6 fixed antennas.

The results shown in Figure 3.4 correspond to a scenario with $N_T = 20$, $N_{ta} = 6$, $K = 2$ and $N_R = 3$ and illustrate the high gain in performance obtained with the proposed BER minimizing antenna selection approach when compared with a non-selective choice, where one of the possible S_t sets is randomly selected for each channel realization. Also in this figure are the BER results obtained with the use of the proposed suboptimal search algorithm (ITES) and with the Genetic Algorithm based search procedure proposed in [14]. The former resulted in a improvement in BER performance than the latter. To have a fair comparison, both algorithms use the same number of iterations to generate their results, i.e. we modify the stop condition of ITES so that it performs 3 iterations, same as GA. This change in the stop criteria

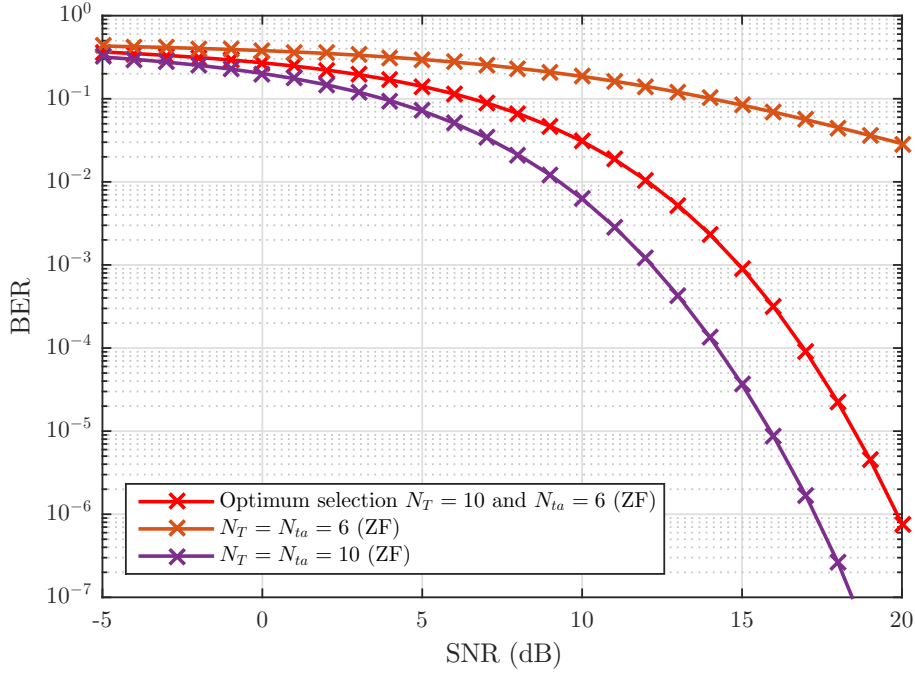


Figure 3.3: BER vs. SNR(dB) for transmit antenna selection considering different number of antennas and RF chains available at BS with ZF precoding, $N_R = 3$ and $K = 2$.

was made only for comparative purposes. Note that with only 3 iteration ITES achieves a BER performance close to that obtained with the optimum exhaustive search, with a very significant lower complexity. For the considered scenario, the exhaustive search tested all the $S_t = 38760$ possible antenna patterns, while the ITES and GA tested only $N_{it}N_aN_d = 252$ each.

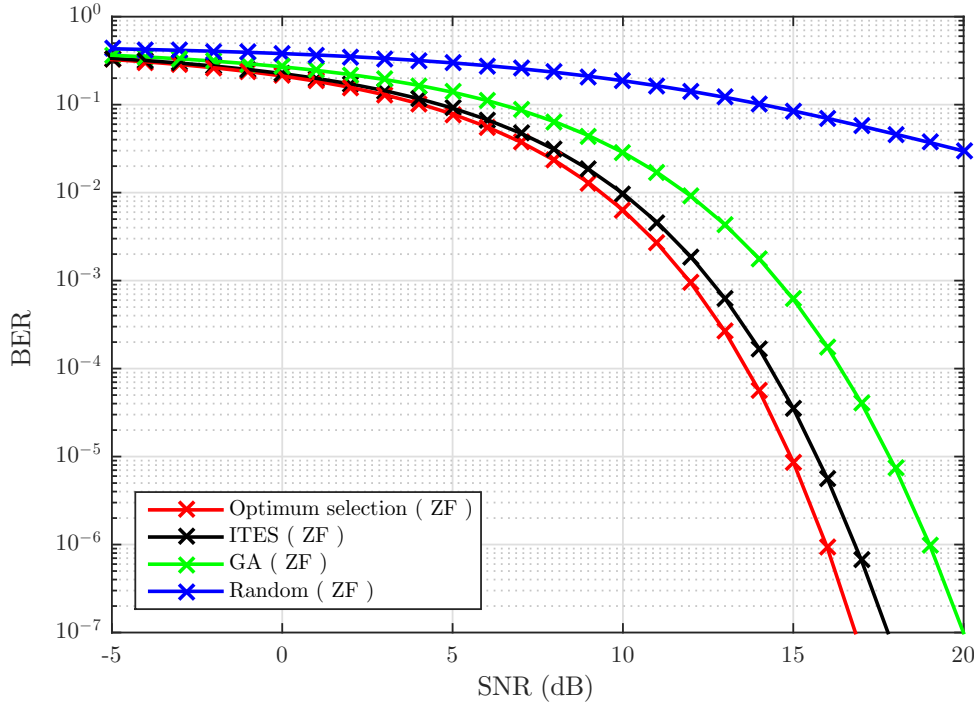


Figure 3.4: BER vs. SNR(dB) for transmit antenna selection with $N_T = 20$, $N_{ta} = 6$, $N_R = 3$ and $K = 2$ in ZF precoded system.

MMSE Precoding

Figure 3.5 depicts the BER performance when the BS implements the MMSE precoding scheme and it is equipped with different number of antennas and RF chains. The suboptimal detection procedure follows (3-42). It is observed the gain performance when the BS has 6 RF chains available and the proposed selection scheme to select 6 out of 10 antennas is implemented over the case when 6 fixed antennas are used.

In Figure 3.6 the results corresponding to a scenario with $N_T = 20$, $N_{ta} = 6$, $K = 2$ and $N_R = 3$ are plotted. We can appreciate the performance gap between the proposed BER minimizing antenna selection approach, based on the metric $\mu(\mathbf{p})$, and the case when a subset is randomly selected for each channel realization, between the possible S_t choices. We also illustrate the results obtained by using ITES when MMSE precoding technique is performed by the BS and how it outperforms the GA based search procedure, considering that both experience the same number of iterations.

In order to compare the system performance when ZF and MMSE precoding techniques are employed, we present the results for BER and Capacity in Figures 3.7 and 3.8 respectively, considering a scenario with

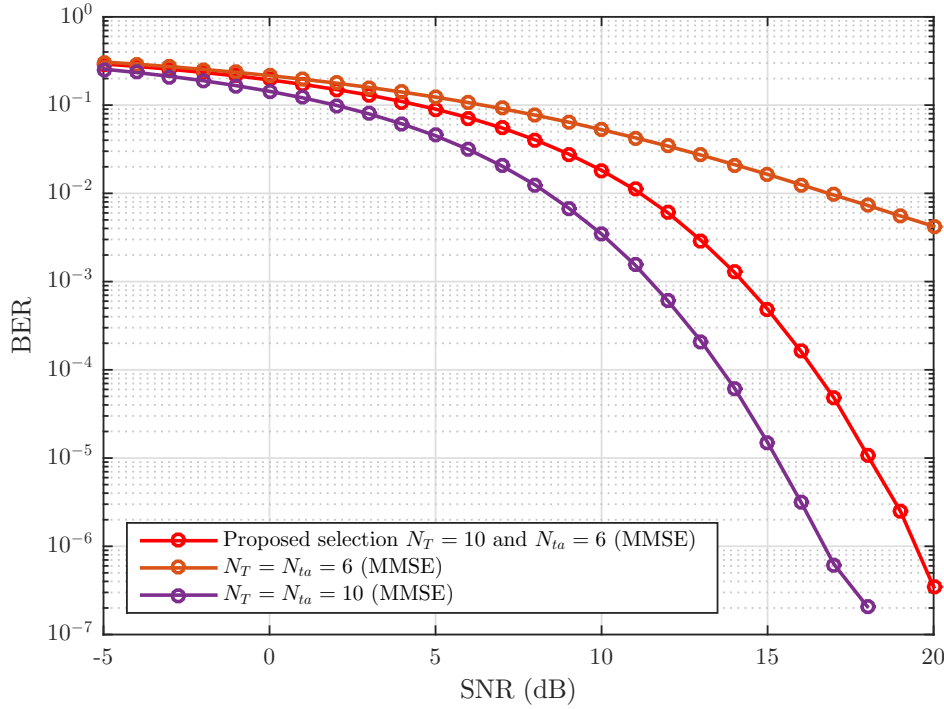


Figure 3.5: BER vs. SNR(dB) for transmit antenna selection considering different number of antennas and RF chains available at BS with MMSE precoding, $N_R = 3$ and $K = 2$.

$N_T = 10$, $N_{ta} = 6$, $K = 2$ and $N_R = 3$. In Figure 3.7 we can see how BER performance achieved by MMSE precoding slightly outperforms ZF, when the optimum and ITES selection procedures are executed. However, this gain of MMSE over ZF is higher in the random selection case. Based on this result we can conclude, that it is more suitable to employ the ZF precoding with the proposed transmit antennas selection approach since it achieves almost the same BER performance than MMSE, implying a lower computational complexity (see Table 3.1). Figure 3.8 depicts the capacity that can be achieved when the above mentioned selection techniques are employed, for each precoding scheme employing the expressions in (3-21) and (3-32). Note that for high SNR the capacity of the MMSE precoding converges to the ZF, as it is expected.

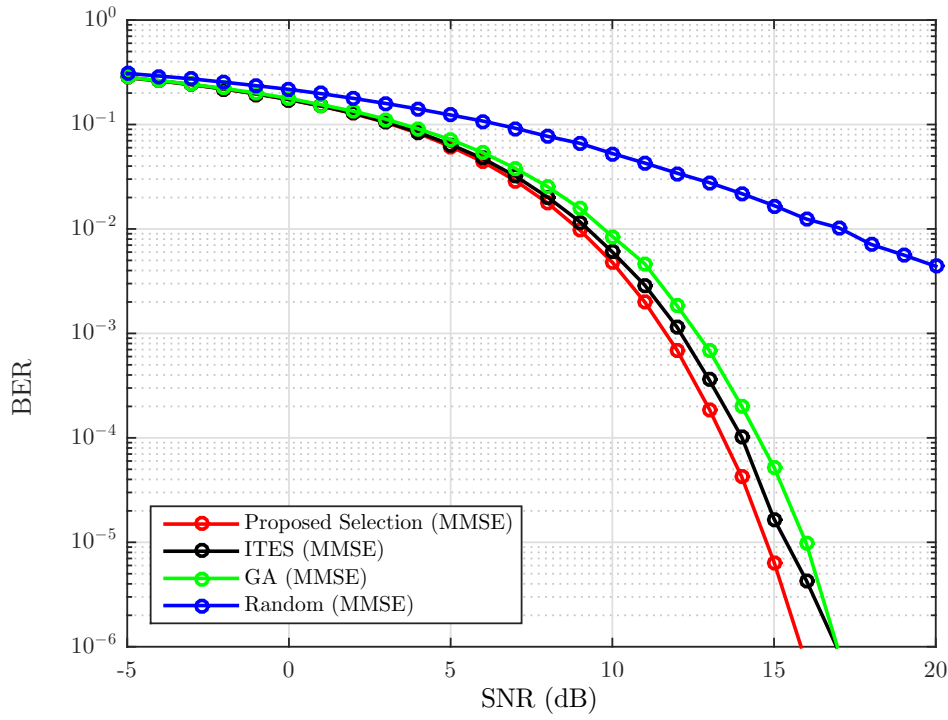


Figure 3.6: BER vs. SNR(dB) for transmit antenna selection with $N_T = 20$, $N_{ta} = 6$, $N_R = 3$ and $K = 2$ in MMSE precoded system.

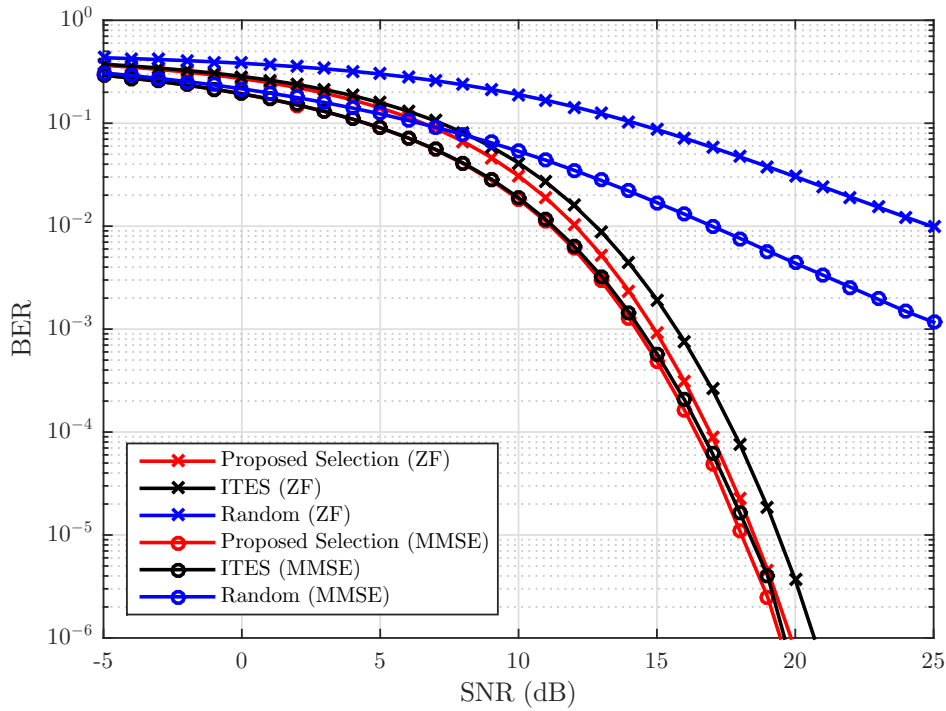


Figure 3.7: BER vs. SNR(dB) for transmit antenna selection with $N_T = 10$, $N_{ta} = 6$, $N_R = 3$ and $K = 2$.

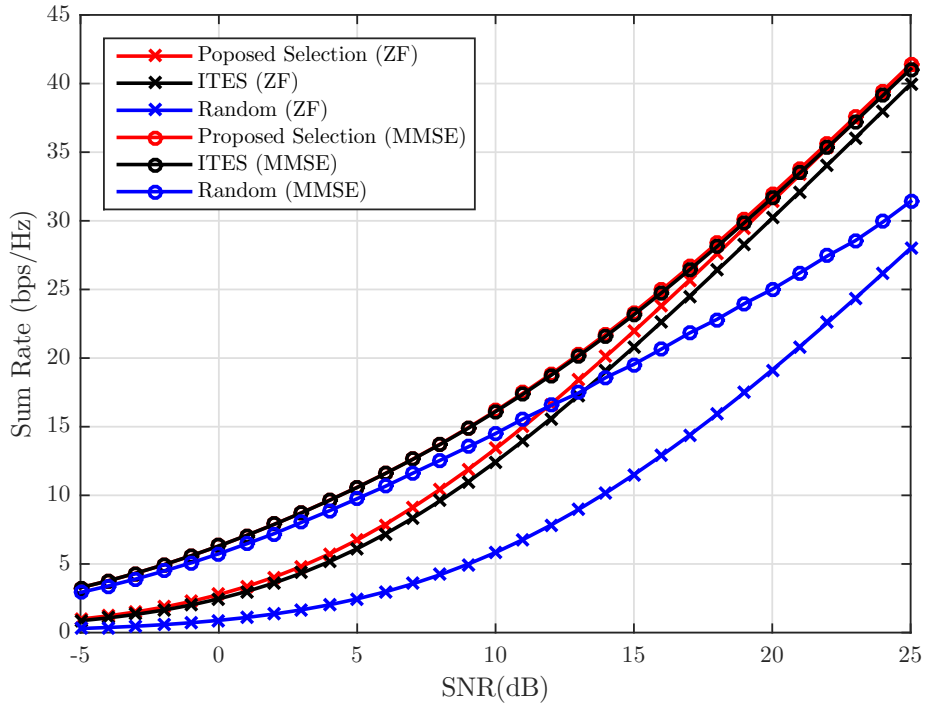


Figure 3.8: Sum Rate vs. SNR(dB) for transmit antenna selection with $N_T = 10$, $N_{ta} = 6$, $N_R = 3$ and $K = 2$.

Table 3.1: Computational complexity of the transmit antenna selection approaches

Scenario	Antenna Selection Approach	FLOPS
$N_T = 20$ $N_{ta} = 6$ $N_R = 3$ $K = 2$	Proposed Selection (ZF)	19883880
	Proposed Selection (MMSE)	78682800
	ITES (ZF)	86184
	ITES (MMSE)	341040
$N_T = 10$ $N_{ta} = 6$ $N_R = 3$ $K = 2$	Proposed Selection (ZF)	107730
	Proposed Selection (MMSE)	426300
	ITES (ZF)	24624
	ITES (MMSE)	97440

4

Receive Antennas Selection

In this chapter, we address the problem of the antenna selection at the receiver side. The downlink of a MU-MIMO system is also considered and the mathematical model for receive antennas selection is described. The proposed receive antenna selection scheme finds the most suitable subset of antennas for each UE, where the BS is responsible for carrying out the selection procedure, since it has a higher processing capacity. Consequently, the BS must inform to each user the antennas to which their RF chains should be connected, in this sense a frame notification procedure is proposed. Numerical results describing the system performance, employing ZF and MMSE precoding, are presented.

4.1

Signal Model

To evaluate the receive antenna selection, we consider that each UE is equipped with N_R receive antennas and only N_{ra} RF chains ($N_{ra} < N_R$), as it is depicted in Figure 4.1. The total number of combinations containing N_{ra} out of N_R antennas is given by

$$S_r = \binom{N_R}{N_{ra}} = \frac{N_R!}{(N_R - N_{ra})!N_{ra}!}. \quad (4-1)$$

The most appropriate set of N_{ra} antennas is selected by the transmitter to receive the transmitted information, i.e. the BS selects the set of antennas that should be activated and must notify the users which of the S_r possible patterns is chosen for transmission, in order to guarantee the correct signal detection. In the receiving antenna selection case, the signal vector conveyed to user k is expressed by

$$\mathbf{s}_k = \sqrt{E_k} \mathbf{U}'_{(\mathbf{q}_k)} \tilde{\mathbf{s}}_k = \sqrt{E_s} \sqrt{\varepsilon_k} \mathbf{U}'_{(\mathbf{q}_k)} \tilde{\mathbf{s}}_k, \quad (4-2)$$

where the N_R -dimensional vector \mathbf{q}_k has N_{ra} entries 1 and the remaining are zero. Its non-zero entries indicate the information bearing (IB) antennas to which the receiver N_{ra} RF chains are to be connected and $\mathbf{U}'_{(\mathbf{q}_k)} \in \mathbb{C}^{N_{ra} \times N_R}$ is obtained from \mathbf{I}_{N_R} , suppressing its i th row, when the i th component of vector \mathbf{q}_k is zero. The matrix $\mathbf{U}'_{(\mathbf{q}_k)}$ fulfills the properties $\mathbf{U}'_{(\mathbf{q}_k)} \mathbf{U}'_{(\mathbf{q}_k)}^T = \mathbf{I}_{N_{ra}}$ and $\mathbf{U}'_{(\mathbf{q}_k)}^T \mathbf{U}'_{(\mathbf{q}_k)} = \mathbf{D}(\mathbf{q}_k)$. Note that vector $\mathbf{s}_k \in \mathbb{C}^{N_{ra} \times 1}$, since only N_{ra} antennas

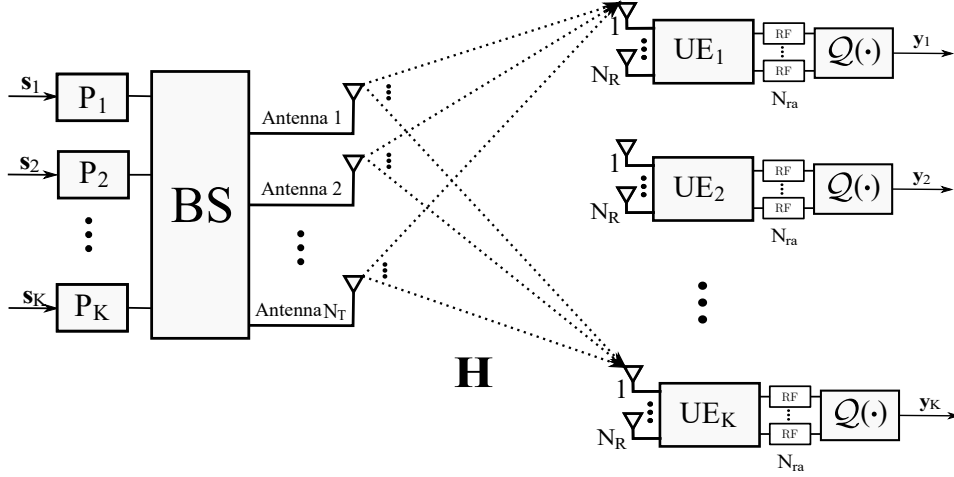


Figure 4.1: MU-MIMO system with N_{ra} RF chains available at each UE.

will be active for detection.

In this case, the effective channel will be modeled by $\mathbf{H}_{(\mathbf{q})} \in \mathbb{C}^{KN_{ra} \times N_T}$, that represents a sub-channel matrix of \mathbf{H} obtained by selecting the rows indexed by $\mathbf{q} = [\mathbf{q}_1^T, \mathbf{q}_2^T, \dots, \mathbf{q}_K^T]^T$. Consequently, $\mathbf{H}_{(\mathbf{q})}$ is given by

$$\mathbf{H}_{(\mathbf{q})} = \tilde{\mathbf{U}}_{(\mathbf{q})} \mathbf{H}, \quad (4-3)$$

where $\tilde{\mathbf{U}}_{(\mathbf{q})} \in \mathbb{C}^{KN_{ra} \times KN_R}$ is obtained from \mathbf{I}_{KN_R} , suppressing its i th row, when the i th component of vector \mathbf{q} is zero and can be expressed as

$$\tilde{\mathbf{U}}_{(\mathbf{q})} = \begin{bmatrix} \mathbf{U}'_{(\mathbf{q}_1)} & 0 & \cdots & 0 \\ 0 & \mathbf{U}'_{(\mathbf{q}_2)} & \cdots & 0 \\ \vdots & \vdots & \ddots & \vdots \\ 0 & 0 & 0 & \mathbf{U}'_{(\mathbf{q}_k)} \end{bmatrix}$$

When the set of N_{ra} antennas is selected by the BS to receive information at each user, the received signal $\mathbf{y} \in \mathbb{C}^{KN_{ra} \times 1}$ can be written as

$$\mathbf{y} = \mathbf{H}_{(\mathbf{q})} \mathbf{x} + \mathbf{n}, \quad (4-4)$$

where $\mathbf{x} \in \mathbb{C}^{N_T \times 1}$ models the precoded signal that will be transmitted to the K UEs. Then, we have

$$\mathbf{y} = \mathbf{H}_{(\mathbf{q})} \mathbf{P}_{\mathbf{q}} \mathbf{s} + \mathbf{n}, \quad (4-5)$$

where $\mathbf{P}_{\mathbf{q}} = [\mathbf{P}_{\mathbf{q}_1}, \mathbf{P}_{\mathbf{q}_2}, \dots, \mathbf{P}_{\mathbf{q}_K}] \in \mathbb{C}^{N_T \times KN_{ra}}$ and the received signal vector $\mathbf{y}_k \in \mathbb{C}^{KN_{ra} \times 1}$ for the k th UE is given by

$$\mathbf{y}_k = \sqrt{E_k} \mathbf{H}_{(\mathbf{q})_k} \mathbf{P}_{\mathbf{q}_k} \mathbf{U}'_{(\mathbf{q}_k)} \tilde{\mathbf{s}}_k + \sum_{j=1, j \neq k}^K \sqrt{E_j} \mathbf{H}_{(\mathbf{q})_k} \mathbf{P}_{\mathbf{q}_j} \mathbf{U}'_{(\mathbf{q}_j)} \tilde{\mathbf{s}}_j + \mathbf{n}_k. \quad (4-6)$$

4.2

Receive Antenna Selection Approach for ZF Precoding

Considering that the BS employs the ZF precoding to process the information symbols vectors that should be transmitted to each user, the expression of the precoding matrix is given by

$$\begin{aligned}\mathbf{P}_{\mathbf{q}_{ZF}} &= \mathbf{H}_{(\mathbf{q})}^H [\mathbf{H}_{(\mathbf{q})} \mathbf{H}_{(\mathbf{q})}^H]^{-1} \\ &= \mathbf{H}^H \tilde{\mathbf{U}}_{(\mathbf{q})}^T [\tilde{\mathbf{U}}_{(\mathbf{q})} \mathbf{H} \mathbf{H}^H \tilde{\mathbf{U}}_{(\mathbf{q})}^T]^{-1}.\end{aligned}\quad (4-7)$$

Applying (4-7) in (4-6) we get

$$\mathbf{y}_k = \sqrt{E_k} \mathbf{U}'_{(\mathbf{q}_k)} \tilde{\mathbf{s}}_k + \mathbf{n}_k. \quad (4-8)$$

At each transmission, the BS selects the most suitable subset of receiving antennas (\mathbf{q}_k) aiming at the maximization of the detection energy E_k for each user. Here the energy relation in (3-6) assumes the form

$$\begin{aligned}E_T &= E_s \text{Tr} \left\{ \boldsymbol{\mathcal{E}}_{\mathbf{q}} \mathbf{P}_{\mathbf{q}_{ZF}}^H \mathbf{P}_{\mathbf{q}_{ZF}} \right\} \\ &= E_s \gamma_r(\mathbf{q}),\end{aligned}\quad (4-9)$$

where the $\gamma_r(\mathbf{q})$ factor is given by

$$\gamma_r(\mathbf{q}) = \text{Tr} \left\{ \boldsymbol{\mathcal{E}}_{\mathbf{q}} \mathbf{P}_{\mathbf{q}_{ZF}}^H \mathbf{P}_{\mathbf{q}_{ZF}} \right\} = \sum_{k=1}^K \varepsilon_k \mathbf{u}^T \mathbf{g}_k(\mathbf{q}), \quad (4-10)$$

and vectors $\mathbf{g}_k, k = 1, \dots, K$ obtained according to (3-8) are given by

$$\begin{aligned}[\mathbf{g}_1^T(\mathbf{q}), \mathbf{g}_2^T(\mathbf{q}), \dots, \mathbf{g}_K^T(\mathbf{q})]^T &= \mathbf{d} \left(\mathbf{P}_{\mathbf{q}_{ZF}}^H \mathbf{P}_{\mathbf{q}_{ZF}} \right) \\ &= \mathbf{d} \left([\mathbf{H}_{(\mathbf{q})} \mathbf{H}_{(\mathbf{q})}^H]^{-1} \right).\end{aligned}\quad (4-11)$$

As was addressed in Chapter 3, for a fixed energy distribution $\varepsilon_k, k = 1, 2, \dots, K$ and energy E_T available for transmission, by minimizing γ_r the detection signal-to-noise ratio of all users is maximized. Let $\mathbf{\Gamma}_r$ denotes the set of all possible receive antennas configurations. Since each user has S_r possible patterns associated, the cardinality of $\mathbf{\Gamma}_r$ is $(S_r)^K$. The optimum subset of antennas \mathbf{q}_o that minimize $\gamma_r(\mathbf{q})$ is found by performing the exhaustive search, i.e. testing all possible patterns \mathbf{q} of the set $\mathbf{\Gamma}_r$.

$$\mathbf{q}_o = \arg \min_{\mathbf{q} \in \mathbf{\Gamma}_r} \gamma_r(\mathbf{q}), \quad (4-12)$$

Unlike the BS, UE are usually equipped with few antennas, therefore the exhaustive search could be performed when an small number of users are

involved. However the cardinality of the search space increases exponentially with K . Then we implement a sub-optimum selection approach that relax the problem in (4-12).

4.2.1

Sub-optimum Receive Antenna Selection

To model this suboptimal approach, we suppose that the signal vector conveyed to user k is given by

$$\mathbf{s}_k = \sqrt{E_k} \mathbf{D}(\mathbf{q}_k) \tilde{\mathbf{s}}_k = \sqrt{E_s \sqrt{\varepsilon_k}} \mathbf{D}(\mathbf{q}_k) \tilde{\mathbf{s}}_k, \quad (4-13)$$

where $\mathbf{s}_k \in \mathbb{C}^{N_R \times 1}$ has N_{ra} entries, indexed by \mathbf{q}_k , containing information symbols and the remaining entries are zero. Then the relation (3-6) assumes the form

$$E_T = E_s \text{Tr} \left\{ \mathbf{E} \mathbf{D}(\mathbf{q}) \mathbf{P}'_{ZF}{}^H \mathbf{P}'_{ZF} \right\} = E_s \gamma'_r, \quad (4-14)$$

where $\mathbf{P}'_{ZF} = \mathbf{H}^H [\mathbf{H} \mathbf{H}^H]^{-1}$ is the precoding matrix, supposing that no selection is implemented and the γ'_r factor is given by

$$\gamma'_r = \text{Tr} \left\{ \mathbf{E} \mathbf{D}(\mathbf{q}) \mathbf{P}'_{ZF}{}^H \mathbf{P}'_{ZF} \right\} = \sum_{k=1}^K \varepsilon_k \mathbf{q}_k^T \mathbf{g}_k, \quad (4-15)$$

where vectors $\mathbf{g}_k, k = 1, \dots, K$ obtained according to (3-8) are given by

$$[\mathbf{g}_1^T, \mathbf{g}_2^T, \dots, \mathbf{g}_K^T]^T = \mathbf{d} \left(\mathbf{P}'_{ZF}{}^H \mathbf{P}'_{ZF} \right) = \mathbf{d} \left([\mathbf{H} \mathbf{H}^H]^{-1} \right). \quad (4-16)$$

As pointed out previously, by minimizing γ'_r the detection signal-to-noise ratio of all users are maximized. In order to minimize γ'_r we consider the independent minimization of the terms in the summation (4-15), since they are all positive and each one is associated to a single user. Among the S_r possible choices of pattern \mathbf{q}_k , the one that results in minimal $\mathbf{q}_k^T \mathbf{g}_k$ is selected for user k . This is done by simply setting to one the elements of \mathbf{q}_k , in positions corresponding to the N_{ra} smaller values of \mathbf{g}_k entries.

It is important to be remarked here that the procedure described above is proposed only as a receive antenna selection. Once the antenna pattern \mathbf{q} is obtained, the precoding matrix is generated according to (4-7) and the received signal is characterized by (4-8)-(4-11).

As in (3-21), for a fixed energy distribution, the capacity of a ZF precoded system, when the total transmit power is limited by E_T is given by

$$C_{\mathbf{q}} = \log_2 \left[\det \left(\mathbf{I}_{KN_{ra}} + \frac{E_T}{\gamma_r(\mathbf{q}) \sigma_n^2} \mathbf{E}_{\mathbf{q}} \right) \right] \text{ bps/Hz} \quad (4-17)$$

4.3

Receive Antenna Selection Approach for MMSE Precoding

The precoding matrix, when the BS uses the MMSE precoding technique, is given by

$$\mathbf{P}_{\mathbf{q}_{MMSE}} = \mathbf{H}_{(\mathbf{q})}^H \left(\mathbf{H}_{(\mathbf{q})} \mathbf{H}_{(\mathbf{q})}^H + \frac{\text{Tr}(\mathbf{R}_{\mathbf{n}})}{E_T} \mathbf{I}_{KN_{ra}} \right)^{-1}. \quad (4-18)$$

Applying (4-18) into the signal model described in (4-5) we have

$$\mathbf{y} = \mathbf{H}_{(\mathbf{q})} \mathbf{P}_{\mathbf{q}_{MMSE}} \mathbf{s} + \mathbf{n}, \quad (4-19)$$

Considering $\mathbf{P}_{\mathbf{q}_{MMSE}} = [\mathbf{P}_{\mathbf{q}_1}, \dots, \mathbf{P}_{\mathbf{q}_K}]$, the signal received by user k can be expressed as

$$\mathbf{y}_k = \sqrt{E_k} \mathbf{H}_{(\mathbf{q})_k} \mathbf{P}_{\mathbf{q}_k} \mathbf{U}'_{(\mathbf{q}_k)} \tilde{\mathbf{s}}_k + \sum_{j=1, j \neq k}^K \sqrt{E_j} \mathbf{H}_{(\mathbf{q})_j} \mathbf{P}_{\mathbf{q}_j} \mathbf{U}'_{(\mathbf{q}_j)} \tilde{\mathbf{s}}_j + \mathbf{n}_k, \quad (4-20)$$

In order to maximize the detection signal-to-interference plus noise ratio of the sets of users in (4-19), we employ the metric introduced in Section 3.4 to select the most suitable subset of receiving antennas (\mathbf{q}_k) for each user. From equation (3-36), we define $\mu_r(\mathbf{q})$ as

$$\mu_r(\mathbf{q}) = \frac{\text{Tr}\{\mathcal{E}_{\mathbf{q}} \mathbf{D}(\mathbf{A}_{\mathbf{q}})^H \mathbf{D}(\mathbf{A}_{\mathbf{q}})\}}{\text{Tr}\{\mathcal{E}_{\mathbf{q}} \bar{\mathbf{A}}_{\mathbf{q}}^H \bar{\mathbf{A}}_{\mathbf{q}}\} + \frac{\text{Tr}\{\mathbf{R}_{\mathbf{n}}\} \gamma_r(\mathbf{q})}{E_T}} \quad (4-21)$$

where $\mathbf{A}_{\mathbf{q}} = \mathbf{H}_{(\mathbf{q})} \mathbf{P}_{\mathbf{q}_{MMSE}}$ and $\gamma_r(\mathbf{q})$ is given by

$$\gamma_r(\mathbf{q}) = \text{Tr}\{\mathcal{E}_{\mathbf{q}} \mathbf{P}_{\mathbf{q}_{MMSE}}^H \mathbf{P}_{\mathbf{q}_{MMSE}}\} = \sum_{k=1}^K \varepsilon_k \mathbf{u}^T \mathbf{g}_k(\mathbf{q}), \quad (4-22)$$

with

$$\begin{aligned} [\mathbf{g}_1^T(\mathbf{q}), \mathbf{g}_2^T(\mathbf{q}), \dots, \mathbf{g}_K^T(\mathbf{q})]^T &= \mathbf{d}(\mathbf{P}_{\mathbf{q}_{MMSE}}^H \mathbf{P}_{\mathbf{q}_{MMSE}}) \\ &= \mathbf{d}\left(\left[\mathbf{H}_{(\mathbf{q})} \mathbf{H}_{(\mathbf{q})}^H + \frac{\text{Tr}\{\mathbf{R}_{\mathbf{n}}\}}{E_T} \mathbf{I}_{KN_{ra}}\right]^{-2} \mathbf{H}_{(\mathbf{q})} \mathbf{H}_{(\mathbf{q})}^H\right). \end{aligned} \quad (4-23)$$

By employing an optimization procedure similar to the one in Section 3.4, for a fixed energy distribution $\varepsilon_k, k = 1, 2, \dots, K$ and energy E_T available for transmission, the detection signal-to-interference plus noise ratio of the set of all users is maximized by solving the following optimization problem

$$\mathbf{q}_o = \arg \max_{\mathbf{q} \in \Gamma_r} \mu_r(\mathbf{q}), \quad (4-24)$$

The sum rate of the system can be computed similar to the expression (2-34)

$$C_{\mathbf{q}} = \sum_{k=1}^K \log_2 \left[\det \left(\mathbf{I}_{N_{ra}} + \frac{E_T \epsilon_k}{\gamma(\mathbf{q}) \sigma_n^2} \mathbf{P}_{\mathbf{q}_k}^H \mathbf{H}_{(\mathbf{q})_k}^H \mathbf{R}_{\tilde{\mathbf{n}}_k}^{-1} \mathbf{H}_{(\mathbf{q})_k} \mathbf{P}_{\mathbf{q}_k} \right) \right] \text{ bps/Hz} \quad (4-25)$$

where

$$\mathbf{R}_{\tilde{\mathbf{n}}_k} = \mathbf{I}_{N_{ra}} + \frac{E_T}{\gamma(\mathbf{q}) \sigma_n^2} \sum_{j=1, j \neq k}^K \varepsilon_j \mathbf{H}_{(\mathbf{q})_j} \mathbf{P}_{\mathbf{q}_j} \mathbf{P}_{\mathbf{q}_j}^H \mathbf{H}_{(\mathbf{q})_j}^H \quad (4-26)$$

4.4

Notification

As mentioned before, to guarantee correct detection the UE receiver must connect its N_{ra} RF chains to the correct set of N_{ra} IB antennas. Since the IB pattern selected by the BS may change according to the variations of the channel, information regarding the pattern selection has to be periodically sent to the UE receiver (UE notification) where a very reliable retrieval of this information has to be performed. To implement the UE notification we consider a frame transmission scheme, where signals informing the index of the selected pattern are sent to the users during the notification period, preceding the user data frame.

The antenna pattern used during the notification period is fixed and known a priori by the receivers. Moreover by sending the same notification information several times, it is possible to further reduce the notification error probability. The UE accumulates the signal vectors received during the notification period and performs detection using the resulting summation of the F_{not} signals. The received signal vector in the notification interval can be expressed as

$$\mathbf{y}^{not} = \sum_{t=1}^{F_{not}} \mathbf{y}_k(t) = F_{not} \sqrt{E_k} \mathbf{H}_{(\mathbf{p})} \mathbf{P}_{\mathbf{p}} \mathbf{s}_k^{not} + \sum_{t=1}^{F_{not}} \mathbf{n}_k(t) \quad (4-27)$$

where $\mathbf{y}_k(t)$ denote the vector received by the user k at each transmission, \mathbf{s}_k^{not} is the symbol vector employed to notify the pattern for the next data frame and $\mathbf{n}_k(t)$ vector represents the AWGN components at the transmission t . With this procedure, if F_{not} is the number of repeated transmissions adopted, a detection signal-to-noise ratio gain of $10 \log_{10}(F_{not})$ dB is obtained.

4.5

Simulation Results

In this section, numerical results are presented to evaluate the bit-error-rate (BER) performance of the systems when receive antenna selection is performed. The curves are obtained after $N_{CR} = 1000$ independent realizations of the channel matrix \mathbf{H} . The noise vector is a complex zero-mean gaussian vector with circularly symmetric components and covariance matrix $\mathbf{K}_{\mathbf{n}} = \sigma_n^2 \mathbf{I}$.

Results are expressed in terms of the signal-to-noise ratio, defined in Section 3.6.

ZF Precoding

Here the previously addressed ML detection is used. The semi-analytical approach, expressed by (3-47) to (3-50), is applicable to the case of receive antenna selection only if error free notification is assumed.

In receive antenna selection, the BS uses all its N_T antennas for transmission and, based on the minimization of γ_r , given in (4-10) and (4-11), selects the most suitable set of antennas to be activated at each UE. Figures 4.2 and 4.3 present BER performance curves for a scenario with $N_T = 10$, $N_R = 4$, $N_{ra} = 2$ and $K = 2$, thus yielding a set of $S_r = 6$ possible antenna patterns that can be selected.

Figure 4.2 shows the BER curves assuming error-free user notification and the proposed notification method, employing the receive selection approach addressed in Section 4.2. These curves were generated using Monte Carlo simulations, where for each of the $N_{CR} = 1000$ channel realizations, 1200 data signal vectors followed by $F_{not} = 10$ notification signal vectors are transmitted to each user. The coincidence of the BER performance curves evidences the effectiveness of the adopted notification method.

The results in Figure 4.3 were generated using the semi-analytical approach, since error free notification is assumed. The BER performance curves correspond to the cases when the optimum and sub-optimum antenna selection approaches, proposed in Section 4.2, are implemented. The former implies a total of $(S_r)^2 = 36$ trials to find the optimum pattern for each user. The results also evidence the performance gain that can be obtained with the proposed receive antenna selection methods when compared with a random selection.

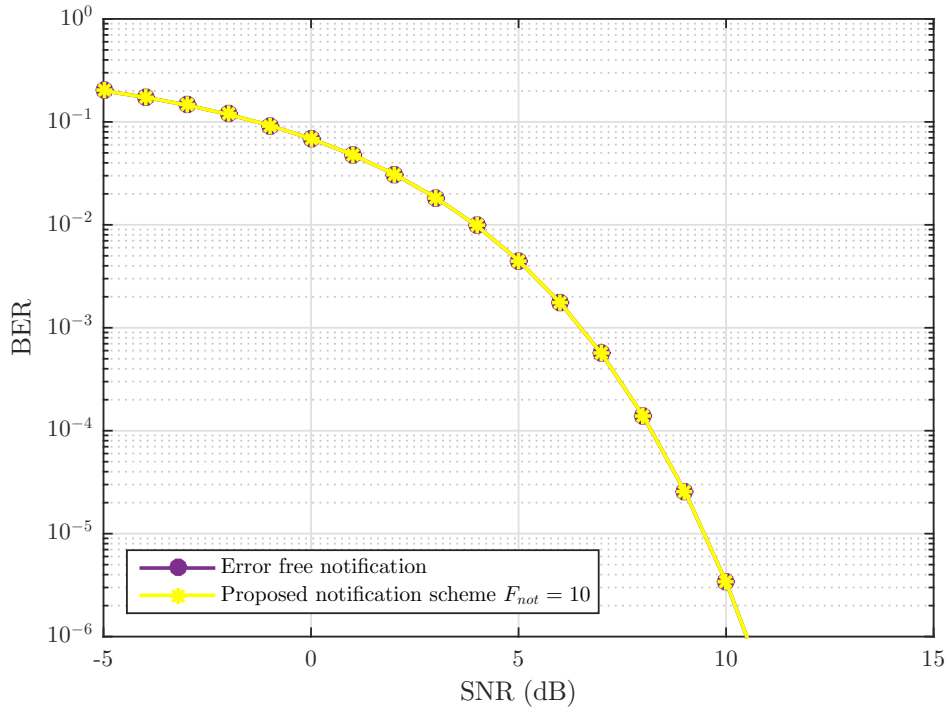


Figure 4.2: BER vs. SNR(dB) considering error free notification and the proposed notification scheme for $N_T = 10$, $N_R = 4$, $N_{ra} = 2$ and $K = 2$ in ZF precoded system.

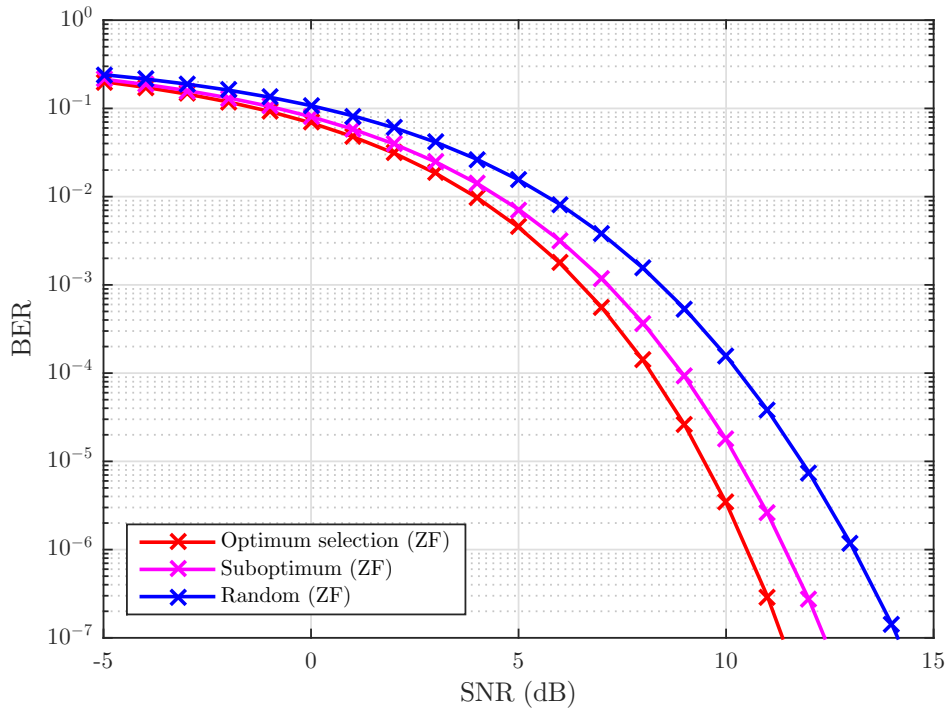


Figure 4.3: BER vs. SNR(dB) for receive antenna selection with $N_T = 10$, $N_{ra} = 2$, $N_R = 4$ and $K = 2$ employing ZF precoding.

MMSE Precoding

Considering the same scenario, Figure 4.4 shows BER performance curves, when the antenna selection procedure with MMSE precoding is implemented and detection is performed according to (3-42). It is notable the performance gain obtained with the proposed receive antenna selection technique.

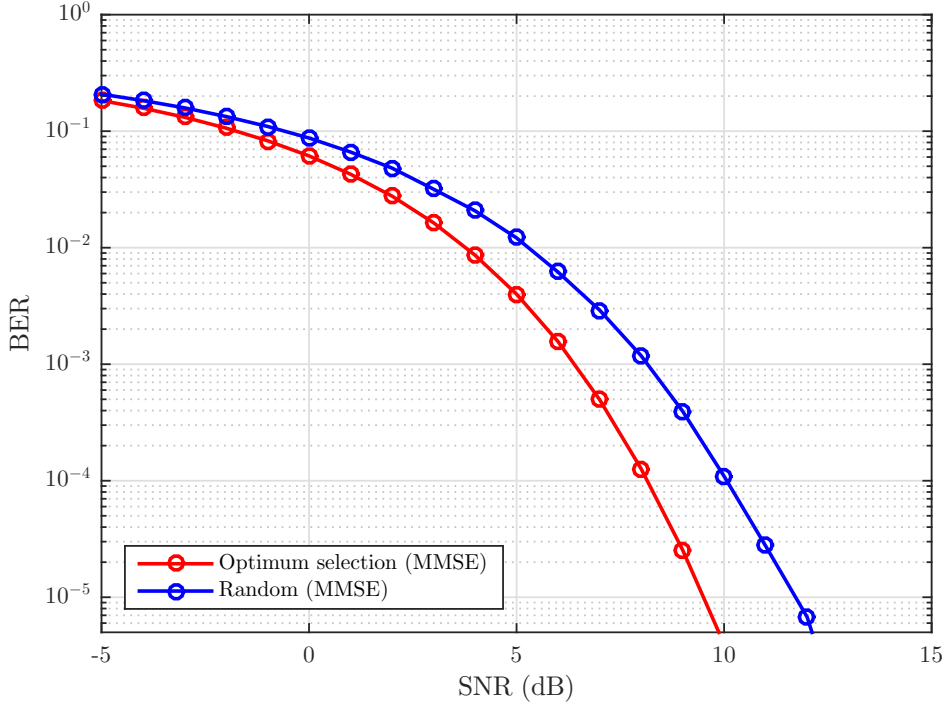


Figure 4.4: BER vs. SNR(dB) for receive antenna selection with $N_T = 10$, $N_{ra} = 2$, $N_R = 4$ and $K = 2$ employing MMSE precoding.

Figure 4.5 presents performance curves obtained with the proposed receive antenna selection approaches when ZF and MMSE precoding are employed. We consider a scenario where the BS is equipped with $N_T = 20$ and each UE with $N_R = 4$. We also consider a total of $K = 5$ users and different number of available RF chains at the receivers. In the case of no selection, i.e. when UE_s receive information through all its antennas ($N_{ra} = N_R$), the MMSE precoding experiences a high performance gain over the ZF. However, when the respective selection procedures are implemented this performance gap decrease dramatically. Note that when N_{ra} decreases the gain of MMSE over ZF also decreases and when a single antenna is used for detection both precoding techniques achieve virtually the same performance. The results indicate that when receive antenna selection is implemented in the MIMO

system, the use of ZF precoding might be more advantageous if the trade-off performance/complexity is considered.

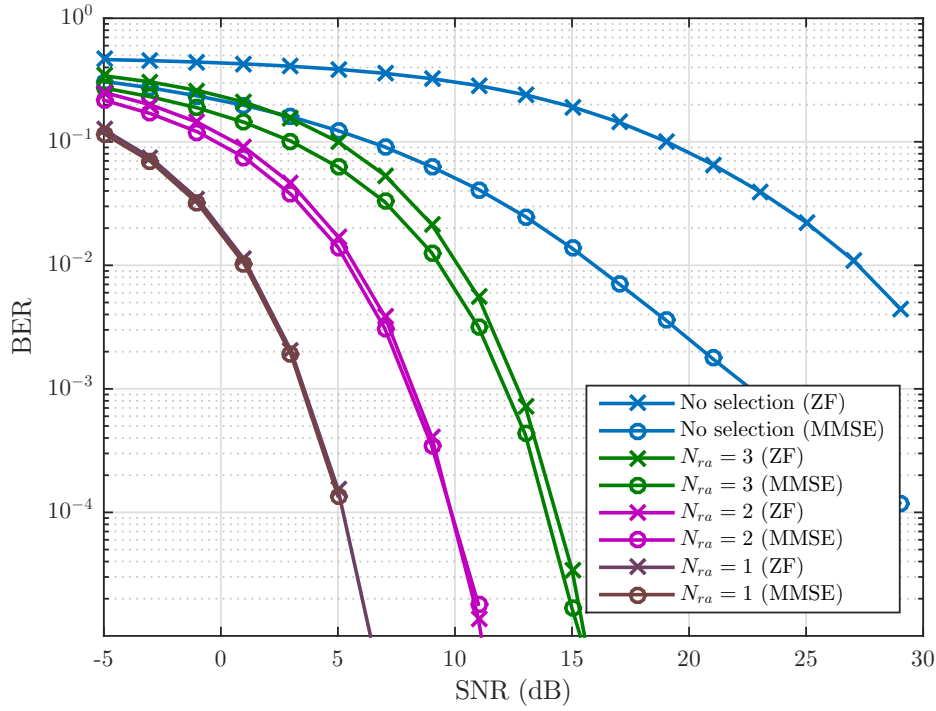


Figure 4.5: BER vs. SNR(dB) for receive antenna selection with $N_T = 20$, $N_R = 4$, $K = 5$ and different numbers of RF chains available at the UE.

5

Joint Transmit and Receive Antennas Selection

In this chapter, we address the general case of joint antenna selection at the transmitter and the receiver sides, through the adequate combination of the selection strategies examined in Chapters 3 and 4, leading to a hardware complexity reduction both in the BS and in the user terminals. The mathematical model for the joint antenna selection is presented, for the downlink of a MU-MIMO system when ZF precoding scheme is employed. We also introduce an alternative metric that can be used to perform the selection. Finally, numerical results to describe the BER performance achieved by the different selection approaches are presented.

5.1

Joint Selection Approach

To model the joint antenna selection, we consider that the BS selects the most suitable pair of subset (\mathbf{p}, \mathbf{q}) for transmitting and receiving information symbols. It's assumed that BS is equipped with N_{ta} RF chains ($N_{ta} \leq N_T$) and UE_s with N_{ra} ($N_{ra} \leq N_R$), as it's depicted in Figure 5.1.

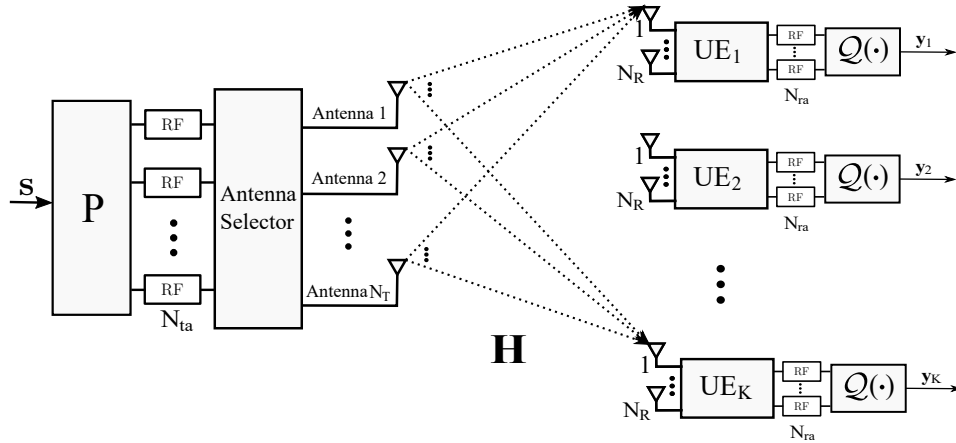


Figure 5.1: MU-MIMO system with N_{ta} and N_{ra} RF chains available at the BS and UE_s respectively.

The effective channel will be modeled by $\check{\mathbf{H}} \in \mathbb{C}^{KN_{ra} \times N_{ta}}$, that represents a sub-channel matrix of \mathbf{H} obtained by selecting the rows indexed by $\mathbf{q} = [\mathbf{q}_1^T, \mathbf{q}_2^T, \dots, \mathbf{q}_K^T]^T$ and the columns indexed by \mathbf{p} , and is given by

$$\check{\mathbf{H}} = \tilde{\mathbf{U}}_{(\mathbf{q})} \mathbf{H} \mathbf{U}_{(\mathbf{p})}, \quad (5-1)$$

where $\mathbf{U}_{(\mathbf{p})} \in \mathbb{C}^{N_T \times N_{ta}}$ and $\tilde{\mathbf{U}}_{(\mathbf{q})} \in \mathbb{C}^{KN_{ra} \times KN_R}$ are obtained from \mathbf{I}_{N_T} and \mathbf{I}_{KN_R} respectively, as was defined in the previous chapters. For implementing the joint selection, the ZF precoding scheme is considered, where the precoding matrix is expressed as

$$\begin{aligned} \check{\mathbf{P}}_{ZF} &= \check{\mathbf{H}}^H [\check{\mathbf{H}} \check{\mathbf{H}}^H]^{-1} \\ &= \mathbf{U}_{(\mathbf{p})}^T \mathbf{H} \tilde{\mathbf{U}}_{(\mathbf{q})}^T [\tilde{\mathbf{U}}_{(\mathbf{q})} \mathbf{H} \mathbf{D}(\mathbf{p}) \mathbf{H}^H \tilde{\mathbf{U}}_{(\mathbf{q})}^T]^{-1}. \end{aligned} \quad (5-2)$$

The received signal $\mathbf{y} \in \mathbb{C}^{KN_{ra} \times 1}$ can be written as

$$\begin{aligned} \mathbf{y} &= \check{\mathbf{H}} \check{\mathbf{P}}_{ZF} \mathbf{s} + \mathbf{n} \\ &= \sqrt{E_s} \mathcal{E}_{\mathbf{q}}^{1/2} \tilde{\mathbf{U}}_{(\mathbf{q})} \tilde{\mathbf{s}} + \mathbf{n}, \end{aligned} \quad (5-3)$$

where $\mathbf{s} \in \mathbb{C}^{KN_{ra} \times 1}$ is the vector containing the information symbols of the K users and $\tilde{\mathbf{s}} \in \mathbb{C}^{KN_R \times 1}$ contains statistical independent symbols, taken from the modulation constellation. The received signal vector $\mathbf{y}_k \in \mathbb{C}^{KN_{ra} \times 1}$ at user k is then

$$\mathbf{y}_k = \sqrt{E_k} \mathbf{U}'_{(\mathbf{q}_k)} \tilde{\mathbf{s}}_k + \mathbf{n}_k. \quad (5-4)$$

Aiming at the maximization of the detection energy E_k , the BS selects the most suitable subsets of transmit and receive antennas at each transmission. The energy relation deduced in equation (3-6) assumes the form

$$\begin{aligned} E_T &= E_s \text{Tr} \{ \mathcal{E}_{\mathbf{q}} \check{\mathbf{P}}_{ZF}^H \check{\mathbf{P}}_{ZF} \} \\ &= E_s \gamma(\mathbf{p}, \mathbf{q}), \end{aligned} \quad (5-5)$$

where $\gamma(\mathbf{p}, \mathbf{q})$ factor is given by

$$\gamma(\mathbf{p}, \mathbf{q}) = \text{Tr} \{ \mathcal{E}_{\mathbf{q}} \check{\mathbf{P}}_{ZF}^H \check{\mathbf{P}}_{ZF} \} = \sum_{k=1}^K \varepsilon_k \mathbf{u}^T \check{\mathbf{g}}_k, \quad (5-6)$$

and vectors $\check{\mathbf{g}}_k, k = 1, \dots, K$ obtained according to (3-8) are given by

$$\begin{aligned} [\check{\mathbf{g}}_1^T, \check{\mathbf{g}}_2^T, \dots, \check{\mathbf{g}}_K^T]^T &= \mathbf{d} \left(\check{\mathbf{P}}_{ZF}^H \check{\mathbf{P}}_{ZF} \right) \\ &= \mathbf{d} \left([\check{\mathbf{H}} \check{\mathbf{H}}^H]^{-1} \right). \end{aligned} \quad (5-7)$$

We know that, for a fixed energy distribution and energy E_T available for transmission, by minimizing $\gamma(\mathbf{p}, \mathbf{q})$ the detection signal-to-noise ratio of all users is maximized. To find the optimum pair (\mathbf{p}, \mathbf{q}) , the BS must test all possible receive patterns \mathbf{q} for each subset of transmit antennas \mathbf{p} . Let's

divide this problem in two steps. We first find the optimum receive subsets $\mathbf{q}_o = [\mathbf{q}_1^T, \mathbf{q}_2^T, \dots, \mathbf{q}_K^T]^T$ for a given transmit subset $\mathbf{p}' \in \Gamma_t$, that is

$$(\mathbf{p}', \mathbf{q}_o) = \arg \min_{\mathbf{q} \in \Gamma_r} \gamma(\mathbf{p}', \mathbf{q}), \quad (5-8)$$

where Γ_t and Γ_r were defined in sections 3.3 and 4.2 respectively. The problem in (5-8) should be solved for each possible transmit subset. Then, we have S_t pairs of $(\mathbf{p}, \mathbf{q}_o)$ and we choose the one that minimize $\gamma(\mathbf{p}, \mathbf{q}_o)$ by solving

$$(\mathbf{p}_o, \mathbf{q}_o) = \arg \min_{\mathbf{p} \in \Gamma_t} \gamma(\mathbf{p}, \mathbf{q}_o). \quad (5-9)$$

The cardinality of the search space Γ of the joint selection problem is given by

$$S_j = S_t(S_r)^K, \quad (5-10)$$

where S_t and $(S_r)^K$ are the cardinalities of Γ_t and Γ_r respectively. Due to the combinatorial nature of this problem, find the optimum subsets could be unfeasible for large dimension systems. Then we implement a sub-optimum joint selection approach that is presented in the next subsection.

The channel capacity of the system in equation (5-3) will depend on which patterns (\mathbf{p}, \mathbf{q}) are chosen and the power distribution among all users \mathcal{E} . It could be expressed as

$$C_{\mathbf{p}, \mathbf{q}} = \log_2 \left[\det \left(\mathbf{I}_{KN_{ra}} + \frac{E_T}{\sigma_n^2 \gamma(\mathbf{p}, \mathbf{q})} \check{\mathbf{H}} \check{\mathbf{P}}_{ZF} \mathcal{E} \check{\mathbf{P}}_{ZF}^H \check{\mathbf{H}}^H \right) \right] \text{ bps/Hz} \quad (5-11)$$

5.1.1

Sub-optimal Joint Selection Approaches

In order to relax the problem of the joint selection we consider the combination of the suboptimal approaches addressed in the previous chapters. In a first approximation, we suppose that BS employs the sub-optimum search algorithm ITES, proposed in Section 3.3.1, to find the patterns (\mathbf{p}, \mathbf{q}) . Then for each transmit subset \mathbf{p} tested at each iteration of the algorithm we should perform the optimization problem addressed in (5-8). The search space is then reduced to

$$S_{j'} = N_{it} N_a N_d (S_r)^K. \quad (5-12)$$

We obtain the pair $(\mathbf{p}_{o'}, \mathbf{q}_o)$, denoting the patterns provided by implementing ITES with the receive antenna selection approach, proposed in Section 4.2, which involves the exhaustive search.

In a second approximation, ITES is implemented by performing the sub-optimum receive selection procedure, proposed in Section 4.2.1, for each transmit subset \mathbf{p} tested at each iteration of the algorithm. Let's denote $(\mathbf{p}_{o'}, \mathbf{q}_{o'})$ the pair obtained with this version, where the cardinality of the search

space is given by

$$S_j'' = N_{it}N_aN_d. \quad (5-13)$$

It is notable the complexity reduction achieved with this suboptimal approaches. In Section 5.3 a BER performance comparison of the joint selection approaches addressed here is presented.

5.2

Alternative Joint Selection Approach

To perform the joint antennas selection, in ZF precoded systems, we have defined the metric $\gamma(\mathbf{p}, \mathbf{q})$ given in (5-6) and (5-7), that can be also expressed as

$$\begin{aligned} \gamma(\mathbf{p}, \mathbf{q}) &= \text{Tr} \left\{ \mathbf{E}_q \check{\mathbf{P}}_{ZF}^H \check{\mathbf{P}}_{ZF} \right\} \\ &= \text{Tr} \left\{ \mathbf{E}_q [\check{\mathbf{H}}\check{\mathbf{H}}^H]^{-1} \right\}, \end{aligned} \quad (5-14)$$

The calculation of γ involves the inversion of the matrix $[\check{\mathbf{H}}\check{\mathbf{H}}^H]^{-1}$, that can be computationally expensive for systems with large dimensions. In order to avoid the inversion operation, we consider an alternative selection approach, which is introduced below.

Let's define the symmetric non-negative definite matrix $\mathbf{B} \in \mathbb{C}^{KN_{ra} \times KN_{ra}}$, $\mathbf{B} = \check{\mathbf{H}}\check{\mathbf{H}}^H$ and considering an uniform distribution of users energy allocation ($\mathbf{E}_q = \mathbf{I}_{KN_{ra}}$), expression in (5-14) is given by

$$\gamma(\mathbf{p}, \mathbf{q}) = \text{Tr} \left\{ \mathbf{B}^{-1} \right\}, \quad (5-15)$$

If $\lambda_1, \lambda_2, \dots, \lambda_{KN_{ra}}$ are the eigenvalues of \mathbf{B} , where $\lambda_1 = \lambda_{min}$ and $\lambda_{KN_{ra}} = \lambda_{max}$ are its smallest and largest eigenvalues, respectively, we know that

$$\text{Tr} \left\{ \mathbf{B} \right\} = \lambda_1 + \lambda_2 + \dots + \lambda_{KN_{ra}} \quad (5-16)$$

$$\text{Tr} \left\{ \mathbf{B}^{-1} \right\} = \frac{1}{\lambda_{KN_{ra}}} + \dots + \frac{1}{\lambda_2} + \frac{1}{\lambda_1}, \quad (5-17)$$

where $\frac{1}{\lambda_1} = \frac{1}{\lambda_{min}}$ is the largest eigenvalue of the inverse matrix. Then, the trace of the inverse matrix can be upper bounded by

$$\text{Tr} \left\{ \mathbf{B}^{-1} \right\} \leq KN_{ra} \left(\frac{1}{\lambda_{min}} \right), \quad (5-18)$$

from (5-15) and (5-18) we have

$$\gamma(\mathbf{p}, \mathbf{q}) \leq KN_{ra} \left(\frac{1}{\lambda_{min}} \right). \quad (5-19)$$

We know that by minimizing $\gamma(\mathbf{p}, \mathbf{q})$ the detection energy of the users is maximized, then using the result in (5-19), we present an alternative approach to perform the joint antennas selection, based on the maximization of the minimum eigenvalue of \mathbf{B} , i.e. we are going to find the pair (\mathbf{p}, \mathbf{q}) aiming at the maximization of λ_{min} in order to minimize the upper bound in (5-19). The most suitable pair of patterns is found by following the procedure presented in Section 5.1 with the new metric. Thus we first find the receive subsets $\mathbf{q}_o = [\mathbf{q}_1^T, \mathbf{q}_2^T, \dots, \mathbf{q}_K^T]^T$ for each transmit pattern $\mathbf{p}' \in \Gamma_t$, by solving

$$(\mathbf{p}', \mathbf{q}_o) = \arg \max_{\mathbf{q} \in \Gamma_r} \lambda_{min}(\mathbf{p}', \mathbf{q}), \quad (5-20)$$

and then we choose the pair $(\mathbf{p}_o, \mathbf{q}_o)$, given by the solution of the following optimization problem,

$$(\mathbf{p}_o, \mathbf{q}_o) = \arg \max_{\mathbf{p} \in \Gamma_t} \lambda_{min}(\mathbf{p}', \mathbf{q}_o). \quad (5-21)$$

This approach, avoids the inversion of the matrix \mathbf{B} , we only need to find its smallest eigenvalue, that can be found by doing a Singular Values Decomposition (SVD) of \mathbf{B} or employing a more efficient method, since we are not interested in the eigenvectors of \mathbf{B} and don't need all its eigenvalues, only the smallest one.

5.3

Simulation Results

In this section, numerical results are presented to evaluate the performance of the system when joint antennas selection is considered. The curves are generated after $N_{CR} = 1000$ independents realizations of the channel matrix and applying the semi-analytical approach, expressed by (3-47) to (3-50), since error free notification is assumed. Results are expressed in terms of the signal-to-noise ratio (SNR), given by (3-46).

Figure 5.2 shows BER performance results when the joint transmit and receive antenna selection is implemented. It is considered a scenario with $N_T = 10$, $N_{ta} = 8$, $N_R = 4$, $N_{ra} = 2$ and $K = 2$. The optimum selection procedure slightly outperforms this suboptimal approach. The former is obtained by executing the exhaustive search, which involves the evaluation of $S_j = S_t(S_r)^K = 1620$ pairs of patterns, while the latter find the pair (\mathbf{p}, \mathbf{q}) employing the suboptimal procedure proposed in Section 4.2.1 for each transmit subset \mathbf{p} , evaluating only $S_t = 45$ pairs. Both experience a considerable performance gain over the random selection.

Considering the same scenario, the BER performance results achieved by the suboptimal approximations, proposed in Section 5.1.1, are plotted in

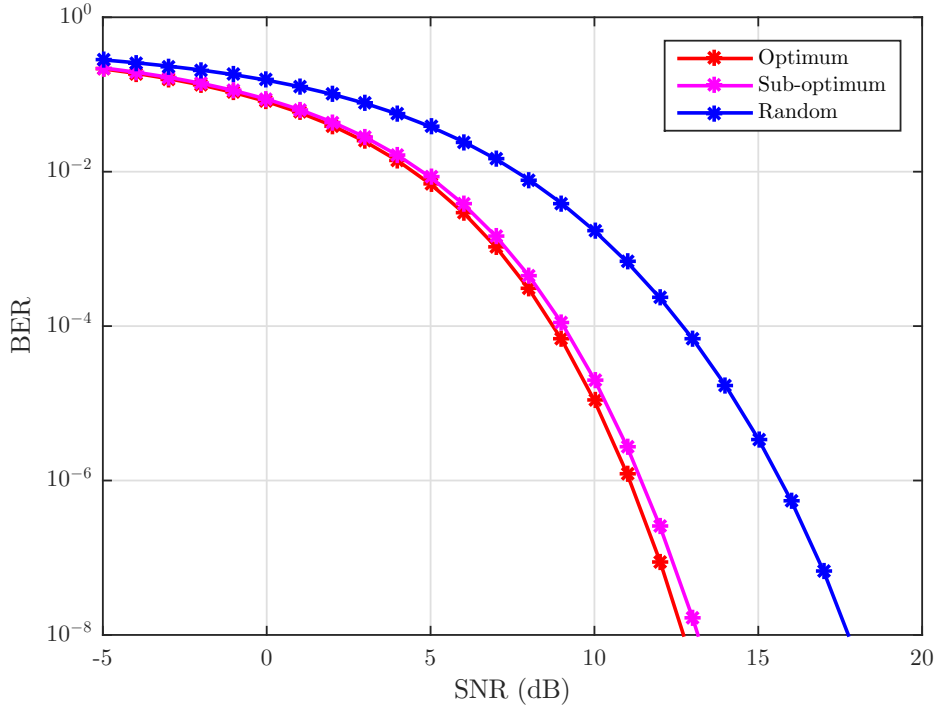


Figure 5.2: BER vs. SNR(dB) for the joint antenna selection with $N_T = 10$, $N_{ta} = 8$, $N_R = 4$, $N_{ra} = 2$ and $K = 2$.

Figure 5.3. With the first approximation is possible to achieve almost the same performance resulting from the exhaustive search, requiring a total of $S_{j'} = N_{it}N_aN_d(S_r)^K = 1152$, considering that ITES performs two iterations. In the second approximation case, where ITES is used with the suboptimal receive selection procedure, a little performance loss can be observed, but the complexity reduction is significant, since only $S_{j''} = N_{it}N_aN_d = 32$ pairs of patterns should be tested.

In Figure 5.4 we compare the BER performance achieved when the joint antenna selection is based on the alternative metric λ_{min} described in Section 5.2, with the result obtained using the proposed metric $\gamma(\mathbf{p}, \mathbf{q})$. The latter achieves a better performance but can be computationally more expensive, since the computation of γ involves a matrix inversion. In both cases the patterns $(\mathbf{p}_o, \mathbf{q}_o)$ are found by performing exhaustive searches, i.e. testing all the $S_j = 1620$ possible patterns.

Figure 5.5 illustrates the BER performance and system Capacity, considering a scenario with $N_T = 10$, $N_{ta} = 8$, $N_R = 4$, $N_{ra} = 2$ and $K = 2$. The curves show performance results when transmit only, receive only, joint selection and no selection are implemented. In the receive only selection case we consider that $N_{ta} = 8$ fixed antennas are used for transmission, while in the transmit only selection case we fixed $N_{ra} = 2$ antennas for receiving infor-

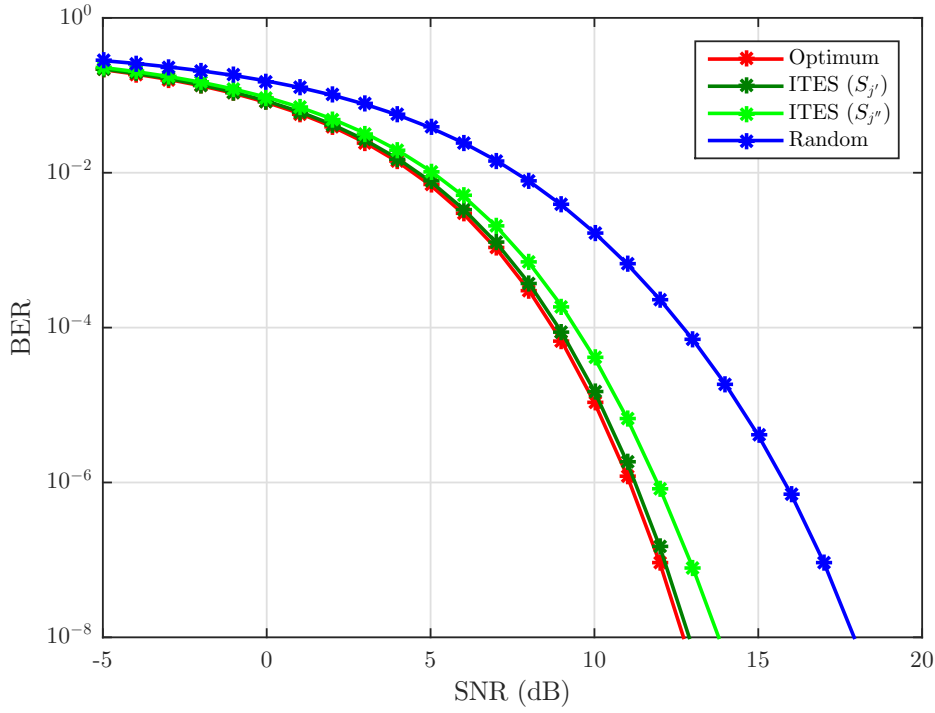


Figure 5.3: BER vs. SNR(dB) considering the suboptimal joint antenna selection with $N_T = 10$, $N_{ta} = 8$, $N_R = 4$, $N_{ra} = 2$ and $K = 2$.

mation symbols at each user. In the no selection case, $N_{ta} = 8$ and $N_{ra} = 2$ fixed antennas are used for transmitting and receiving information symbols, respectively. We can see that joint selection can achieve a better performance than when transmit and receive selection are implemented separately. Moreover, the introduction of antenna selection procedures can deliver a substantial performance gain when compared to the no selection case.

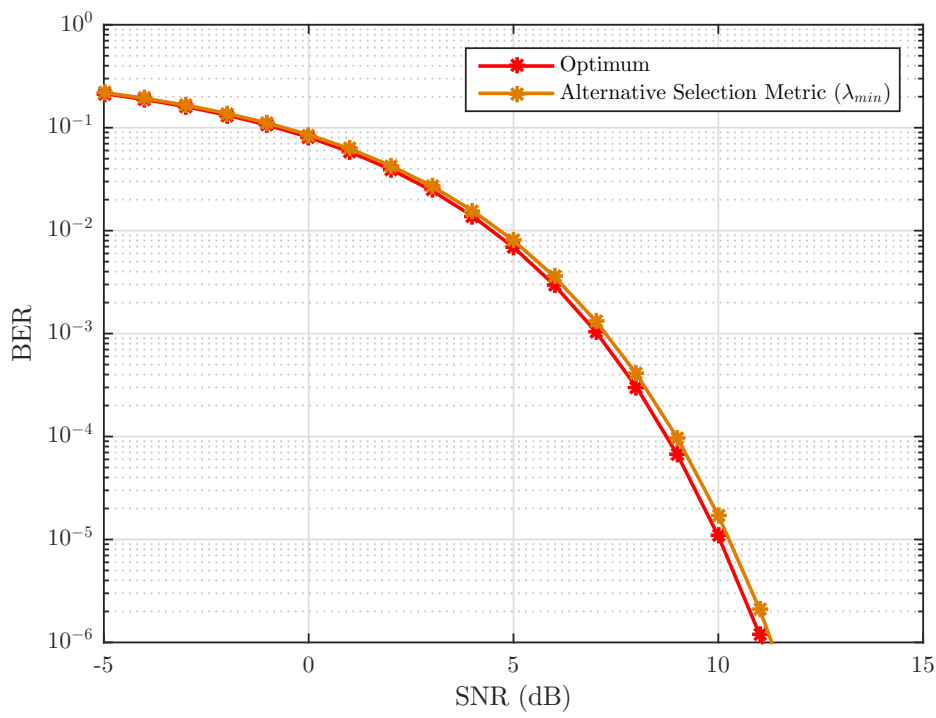
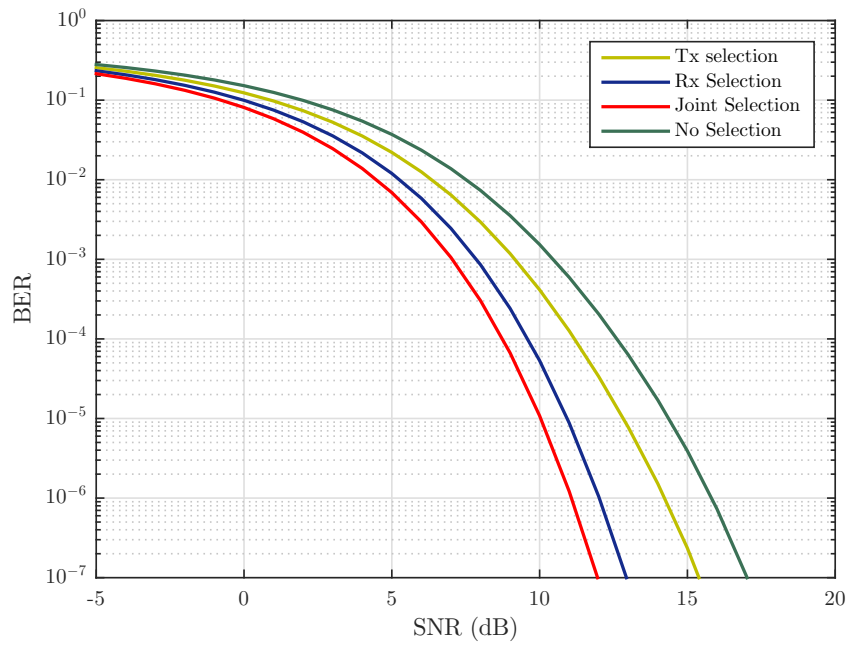
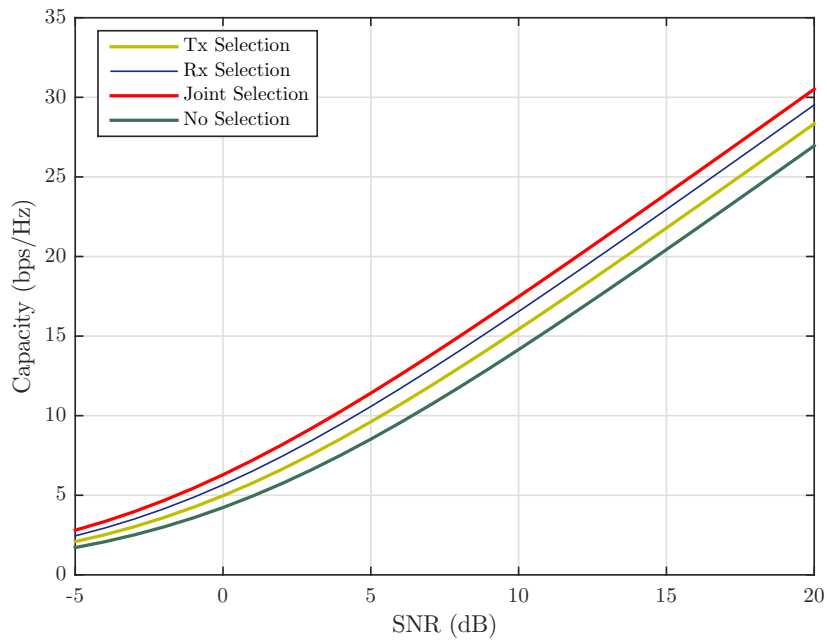


Figure 5.4: BER vs. SNR(dB) considering the exhaustive search with $N_T = 10$, $N_{ta} = 8$, $N_R = 4$, $N_{ra} = 2$ and $K = 2$.



(a): BER vs. SNR(dB)



(b): Capacity vs. SNR(dB)

Figure 5.5: Performance comparison between joint, transmit and receive selection for $N_T = 10$, $N_{ta} = 8$, $N_R = 4$, $N_{ra} = 2$ and $K = 2$.

This thesis focused on the antenna selection problem in the downlink of MU-MIMO systems. We have developed new procedures to perform the antenna selection when a reduced number of RF chains is available at the BS and/or UE_s.

An overview of the general principles involved in the design and implementation of MIMO communication systems have been studied in Chapter 2. The mathematical model for different MIMO systems were presented, deducing the expressions of the capacity, when the channel is known and unknown at the transmitter side and considering both deterministic and random channels. A review of the channel characterization and estimation schemes were also included. The most important linear and non-linear detection techniques, existing in the literature, have been presented, as well as the linear precoding methods employed at the base station for mitigating the MUI.

In Chapter 3, we have developed a procedure to perform the transmit antenna selection, aiming at the maximization of the energy available for detection at each UE. Consequently, appropriated metrics on which the selection is based have been proposed for both cases, when ZF and MMSE precoding techniques are employed in the BS. We have also introduced the ITES algorithm, that significantly reduces the search space and it is able to achieve a BER performance close to the optimum exhaustive search selection. Moreover, its computational complexity has been analyzed in terms of the number of complex operations, that it involves.

An extension of the procedure proposed for the receive antenna selection case was presented in Chapter 4, where it was assumed that the BS is in charge of selecting the most suitable set of antennas employed for detection at each user. A notification scheme to inform the BS selections to the users' receivers was explored. It has shown a high effectiveness, yielding essentially the same BER performance achieved when error-free notification was assumed. A sub-optimum receive antenna selection approach was also addressed that significantly reduces the problem complexity and shows fairly good BER performance results.

The general case of the joint antenna selection, at the transmitter and

receiver, that contemplates the combination of both strategies was examined in Chapter 5 for the ZF precoding case. It was shown that this approach leads to a reduction of the hardware complexity and achieves better results in term of BER performance and capacity than executing the transmit and receive selection separately. We have also proposed suboptimal joint selection approaches that reduce the search space and are able to achieve near optimal BER performance. Simulation results, showing the performance of the proposed selection approaches, have been presented.

Some suggestions for possible future works:

- The selection techniques presented here have been evaluated considering perfect channel state information (CSI) available at the transmitter. The performance of the proposed schemes could be analyzed for partial CSI knowledge, obtained by employing channel estimation algorithms.
- To employ "water-filling" algorithm to find the optimum user energy allocation. It can be considered the optimization of matrix \mathcal{E} for a given antenna pattern, obtained supposing uniform energy distribution ($\mathcal{E} = \mathbf{I}$).
- To evaluate the BER performance and convergence rate of ITES, in Massive MIMO scenarios, where BS is equipped with a substantially high number of transmit antennas.
- The proposed selection schemes could be extended to systems where non-linear precoding techniques, as Dirty Paper Coding (DPC) and Tomlinson-Harashima Precoding (THP), are employed.
- A new search algorithm to find the optimum subset of antennas could be developed using the Branch-and-Bound optimization method, which have been employed to solve different problems, especially in combinatorial optimization.

Bibliography

- [1] *Ericsson Mobility Report. On the pulse of the networked society. June 2016*, Ericsson. [Online]. Available: https://www.abc.es/gestordocumental/uploads/internacional/EMR_June_2016_D5%201.pdf
- [2] *Measuring the Information Society Report 2017*, UIT. [Online]. Available: <https://www.itu.int/en/ITU-D/Statistics/Pages/publications/mis2017.aspx>
- [3] M. N. S. Swamy and K.-L. Du, *Wireless Communication Systems: From RF Subsystems to 4G Enabling Technologies*. Cambridge University Press, 2010.
- [4] J. Govil and J. Govil, "4g mobile communication systems: Turns, trends and transition," in *2007 International Conference on Convergence Information Technology (ICCIT 2007)*, Nov 2007, pp. 13–18.
- [5] T. E. Bogale and L. B. Le, "Massive mimo and mmwave for 5g wireless hetnet: Potential benefits and challenges," *IEEE Vehicular Technology Magazine*, vol. 11, no. 1, pp. 64–75, March 2016.
- [6] N. Bhushan, J. Li, D. Malladi, R. Gilmore, D. Brenner, A. Damnjanovic, R. T. Sukhavasi, C. Patel, and S. Geirhofer, "Network densification: the dominant theme for wireless evolution into 5g," *IEEE Communications Magazine*, vol. 52, no. 2, pp. 82–89, February 2014.
- [7] X. Ge, J. Ye, Y. Yang, and Q. Li, "User mobility evaluation for 5g small cell networks based on individual mobility model," *IEEE Journal on Selected Areas in Communications*, vol. 34, no. 3, pp. 528–541, March 2016.
- [8] E. G. Larsson, O. Edfors, F. Tufvesson, and T. L. Marzetta, "Massive mimo for next generation wireless systems," *IEEE Communications Magazine*, vol. 52, no. 2, pp. 186–195, February 2014.
- [9] L. Lu, G. Y. Li, A. L. Swindlehurst, A. Ashikhmin, and R. Zhang, "An overview of massive mimo: Benefits and challenges," *IEEE Journal of Selected Topics in Signal Processing*, vol. 8, no. 5, pp. 742–758, Oct 2014.
- [10] S. Sanayei and A. Nosratinia, "Antenna selection in mimo systems," *IEEE Communications Magazine*, vol. 42, no. 10, pp. 68–73, Oct 2004.

- [11] R. W. Heath and A. Paulraj, "Antenna selection for spatial multiplexing systems based on minimum error rate," in *ICC 2001. IEEE International Conference on Communications. Conference Record (Cat. No.01CH37240)*, vol. 7, June 2001, pp. 2276–2280 vol.7.
- [12] R. W. Heath, S. Sandhu, and A. Paulraj, "Antenna selection for spatial multiplexing systems with linear receivers," *IEEE Communications Letters*, vol. 5, no. 4, pp. 142–144, April 2001.
- [13] T. Tai, H. Chen, W. Chung, and T. Lee, "Energy efficient norm-and-correlation-based antenna selection algorithm in spatially correlated massive multi-user mimo systems," in *2017 IEEE International Workshop on Signal Processing Systems (SiPS)*, Oct 2017, pp. 1–5.
- [14] B. Makki, A. Ide, T. Svensson, T. Eriksson, and M. Alouini, "A genetic algorithm-based antenna selection approach for large-but-finite mimo networks," *IEEE Transactions on Vehicular Technology*, vol. 66, no. 7, pp. 6591–6595, July 2017.
- [15] A. Dua, K. Medepalli, and A. J. Paulraj, "Receive antenna selection in mimo systems using convex optimization," *IEEE Transactions on Wireless Communications*, vol. 5, no. 9, pp. 2353–2357, September 2006.
- [16] A. Duarte and R. Sampaio-Neto, "Precoding and spatial modulation in the downlink of mu-mimo systems," in *Proceedings of the XXXV Brazilian Communications and Signal Processing Symposium*, September 2017.
- [17] J. Lain, "Joint transmit/receive antenna selection for mimo systems: A real-valued genetic approach," *IEEE Communications Letters*, vol. 15, no. 1, pp. 58–60, January 2011.
- [18] J. Wang, A. I. Pérez-Neira, and M. Gao, "A concise joint transmit/receive antenna selection algorithm," *China Communications*, vol. 10, no. 3, pp. 91–99, March 2013.
- [19] Q. H. Spencer, C. B. Peel, A. L. Swindlehurst, and M. Haardt, "An introduction to the multi-user mimo downlink," *IEEE Communications Magazine*, vol. 42, pp. 60–67, October 2004.
- [20] D. Gesbert, M. Kountouris, R. W. Heath, C. byoung Chae, and T. Salzer, "Shifting the mimo paradigm," *IEEE Signal Processing Magazine*, vol. 24, pp. 36–46, October 2007.

- [21] J. Kim, C. G. Kang, W.-Y. Yang, and Y. S. Cho, *MIMO-OFDM Wireless Communications with MATLAB*. John Wiley and Sons, 2010.
- [22] F. Gross, *Smart Antennas for Wireless Communication with Matlab*. McGraw-Hill Professional, 2005.
- [23] M. Jankiraman, *Space-Time Codes and MIMO Systems*. Artech House, 2004.
- [24] J. Proakis and M. Salehi, *Digital Communications*. McGraw-Hill, 2007.
- [25] D. Tse and P. Viswanath, *Fundamentals of Wireless Communications*. Cambridge University Press, 2005.
- [26] M. Biguesh and A. B. Gershman, "Training-based mimo channel estimation: A study of estimator tradeoffs and optimal training signals," *IEEE Transactions on Signal Processing*, vol. 54, no. 3, pp. 884–893, March 2006.
- [27] R.S.Ganesh, D. J.Jayakumari, and A. I.P, "Channel estimation analysis in mimo-ofdm wireless systems," in *International Conference on Signal Processing, Communication, Computing and Networking Technologies*, July 2011, pp. 399–403.
- [28] S. M. Kay, *Fundamentals of Statistical Signal Processing: Estimation Theory*. PRENTICE HALL, 1993.
- [29] I. E. Telatar, "Capacity of multi-antenna gaussian channels," *Eur. Trans. Telecommun.*, vol. 10, no. 6, pp. 585–595, 1999.
- [30] M. A. Khalighi, J. M. Brossier, G. V. Jourdain, and K. Raoof, "Water filling capacity of rayleigh mimo channels," in *12th IEEE International Symposium on Personal, Indoor and Mobile Radio Communications. PIMRC 2001. Proceedings (Cat. No.01TH8598)*, vol. 1, Sep 2001, pp. A–155–A–158.
- [31] H. Boche and E. A. Jorswieck, "Sum capacity optimization of the mimo gaussian mac," in *The 5th International Symposium on Wireless Personal Multimedia Communications*, vol. 1, Oct 2002, pp. 130–134 vol.1.
- [32] W. Yu, W. Rhee, S. Boyd, and J. M. Cioffi, "Iterative water-filling for gaussian vector multiple-access channels," *IEEE Transactions on Information Theory*, vol. 50, no. 1, pp. 145–152, Jan 2004.
- [33] S. Vishwanath, N. Jindal, and A. Goldsmith, "On the capacity of multiple input multiple output broadcast channels," in *2002 IEEE International*

- Conference on Communications. Conference Proceedings. ICC 2002 (Cat. No.02CH37333)*, vol. 3, 2002, pp. 1444–1450 vol.3.
- [34] H. Boche, M. Schubert, and E. A. Jorswieck, “Throughput maximization for the multiuser mimo broadcast channel,” in *Acoustics, Speech, and Signal Processing, 2003. Proceedings. (ICASSP '03). 2003 IEEE International Conference on*, vol. 4, April 2003, pp. IV–808–11 vol.4.
- [35] S. S. Christensen, R. Agarwal, E. de Carvalho, and J. M. Cioffi, “Weighted sum-rate maximization using weighted mmse for mimo-bc beamforming design,” in *2009 IEEE International Conference on Communications*, June 2009, pp. 1–6.
- [36] A. Paulraj, D. Gore, and R. Nabar, *Introduction to Space-Time Wireless Communications*. Cambridge University Press, 2003.
- [37] J. L. A. García, “Interference mitigation schemes for the uplink of massive mimo in 5g heterogeneous cellular networks,” Brazil, March, 2016.
- [38] P. Li, “Low-complexity iterative detection algorithms for multi-antenna systems,” UK, December, 2011.
- [39] R. C. D. Lamare, R. Sampaio-Neto, and A. Hjørungnes, “Joint iterative interference cancellation and parameter estimation for cdma systems,” *IEEE Communications Letters*, vol. 11, no. 12, pp. 916–918, December 2007.
- [40] R. Esmailzadeh and M. Nakagawa, “Pre-rake diversity combination for direct sequence spread spectrum communications systems,” in *Communications, 1993. ICC '93 Geneva. Technical Program, Conference Record, IEEE International Conference on*, vol. 1, May 1993, pp. 463–467 vol.1.
- [41] R. Fletcher, *Practical Methods of Optimization*. New York: Wiley, 1987.
- [42] B. R. Vojcic and W. M. Jang, “Transmitter precoding in synchronous multiuser communications,” *IEEE Transactions on Communications*, vol. 46, no. 10, pp. 1346–1355, Oct 1998.
- [43] M. Joham, W. Utschick, and J. A. Nossek, “Linear transmit processing in mimo communications systems,” *IEEE Transactions on Signal Processing*, vol. 53, no. 8, pp. 2700–2712, Aug 2005.
- [44] Q. H. Spencer, A. L. Swindlehurst, and M. Haardt, “Zero-forcing methods for downlink spatial multiplexing in multiuser mimo channels,” *IEEE Transactions on Signal Processing*, vol. 52, no. 2, pp. 461–471, Feb 2004.

- [45] X. Gao, O. Edfors, J. Liu, and F. Tufvesson, "Antenna selection in measured massive mimo channels using convex optimization," in *2013 IEEE Globecom Workshops (GC Wkshps)*, Dec 2013, pp. 129–134.
- [46] S. Mahboob, R. Ruby, and V. C. M. Leung, "Transmit antenna selection for downlink transmission in a massively distributed antenna system using convex optimization," in *2012 Seventh International Conference on Broadband, Wireless Computing, Communication and Applications*, Nov 2012, pp. 228–233.
- [47] D. A. Gore, R. U. Nabar, and A. Paulraj, "Selecting an optimal set of transmit antennas for a low rank matrix channel," in *2000 IEEE International Conference on Acoustics, Speech, and Signal Processing. Proceedings (Cat. No.00CH37100)*, vol. 5, June 2000, pp. 2785–2788 vol.5.
- [48] D. A. Pérez and R. Sampaio-Neto, "Bit error rate minimizing antenna selection in zero-forcing precoded mu-mimo systems," in *XXXVI Brazilian Communications and Signal Processing Symposium, Campina Grande*, September 2018.
- [49] R. B. Moraes and R. Sampaio-Neto, "Bit error rate minimizing pilot symbol arrangement in closed-loop orthogonal frequency division multiplexing systems," *IET Communications*, vol. 5, no. 14, pp. 1999–2008, Sept 2011.
- [50] S. Boyd and L. Vandenberghe, *Convex Optimization*. Cambridge University Press, 2004.
- [51] R. Hunger, *Floating Point Operations in Matrix-Vector Calculus*, Technische Universität München, Associate Institute for Signal Processing. [Online]. Available: <https://mediatum.ub.tum.de/doc/625604>